



POSS related polymer nanocomposites

Shiao-Wei Kuo^{a,*}, Feng-Chih Chang^{b,1}

^a Department of Materials and Optoelectronic Science, Center for Nanoscience and Nanotechnology, National Sun Yat-Sen University, Kaohsiung 804, Taiwan

^b Institute of Applied Chemistry, National Chiao-Tung University, Hsin-Chu 30050, Taiwan

ARTICLE INFO

Article history:

Received 22 June 2010

Received in revised form 5 May 2011

Accepted 6 May 2011

Available online 25 May 2011

Keywords:

POSS

Nanocomposites

Structure–property relationship

ABSTRACT

This review describes the syntheses of polyhedral oligomeric silsesquioxane (T₈-POSS) compounds, the miscibility of POSS derivatives and polymers, the preparation of both multifunctional and monofunctional monomers and polymers containing POSS including styryl-POSS, methacrylate-POSS, norbornyl-POSS, vinyl-POSS, epoxy-POSS, phenolic-POSS, benzoxazine-POSS, amine-POSS, and hydroxyl-POSS. The thermal, dynamic mechanical, electrical, and surface properties of POSS-related polymeric nanocomposites prepared from both monofunctional and multifunctional POSS monomers are discussed. In addition, we describe the applications of several high-performance POSS nanocomposites in such systems as light emitting diodes, liquid crystals, photoresist materials, low-dielectric constant materials, self-assembled block copolymers, and nanoparticles.

© 2011 Elsevier Ltd. All rights reserved.

Contents

1. Introduction	1651
2. General approaches in the syntheses of polyhedral oligomeric silsesquioxanes	1651
2.1. Monofunctional POSS	1652
2.2. Multifunctional POSS	1652
3. Hydrogen bonding and miscibility behavior of polymer/POSS nanocomposites	1652
3.1. Hydrogen bonding interactions between polymers and POSS	1652
3.2. Miscibility between polymers and POSS derivatives	1654
4. POSS-containing polymers and copolymers	1657
4.1. Polyolefin/POSS and norbornyl/POSS copolymers	1657
4.1.1. Polyethylene and norbornyl/POSS copolymers	1657
4.1.2. Polypropylene/POSS nanocomposites	1659
4.1.3. Other polyolefin POSS nanocomposites	1660
4.2. Polystyrene/POSS nanocomposites	1660
4.3. Poly(acrylate)/POSS copolymers	1662
4.4. Poly(ethylene oxide)/POSS nanocomposites	1664
4.5. Polyester/POSS nanocomposites	1665
4.5.1. PCL/POSS nanocomposites	1665
4.5.2. Other polyester/POSS nanocomposites	1666

* Corresponding author. Tel.: +886 7 5252000x4079; fax: +886 7 5254099.

E-mail addresses: kuosw@faculty.nsysu.edu.tw (S.-W. Kuo), changfc@mail.nctu.edu.tw (F.-C. Chang).

¹ Fax: +886 3 5131512.

4.6.	Polyamide/POSS nanocomposites	1667
4.6.1.	Nylon/POSS nanocomposites	1667
4.6.2.	PNIPAM/POSS nanocomposites	1667
4.6.3.	PVP/POSS nanocomposites	1667
4.6.4.	Other polyamide/POSS nanocomposites	1668
4.7.	Polyimide/POSS nanocomposites	1670
4.8.	Polyurethane/POSS nanocomposites	1672
4.9.	Phenolic/POSS nanocomposites	1673
4.10.	Epoxy/POSS nanocomposites	1674
4.10.1.	Multifunctional epoxy-POSS nanocomposites	1674
4.10.2.	Multifunctional NH ₂ -POSS and OH-POSS nanocomposites	1676
4.10.3.	Monofunctional epoxy-POSS and NH ₂ -POSS nanocomposites	1677
4.10.4.	Other epoxy/POSS systems	1678
4.11.	Polybenzoxazine/POSS nanocomposites	1679
5.	POSS-containing functional materials	1680
5.1.	Polymer light emitting diodes (PLEDs) incorporating POSS hybrid polymers	1680
5.2.	Liquid crystal polymers (LCPs) incorporating POSS hybrid polymers	1681
5.3.	Lithographic applications of POSS-containing photoresists	1681
5.4.	Low-k applications of POSS-containing materials	1683
5.5.	Self-assembly behavior of POSS-containing block copolymer materials	1684
5.6.	Nanoparticle with POSS-containing materials	1686
5.6.1.	POSS modified clay nanocomposites	1686
5.6.2.	POSS modified gold nanoparticles	1687
6.	Conclusions	1689
	Acknowledgments	1689
	References	1689

Nomenclature

AFM	atomic force microscopy
AM-POSS	aminopropylisobutyl POSS
ATRP	atom transfer radical polymerization
iBu-POSS	isobutyl-POSS
CD	cyclodextrins
Cp-POSS	cyclopentyl-POSS
Cy-POSS	cyclohexyl-POSS
DDM	4,4'-diaminodiphenyl methane
DDS	4,4'-diaminodiphenyl sulfone
DMA	dynamic mechanic analysis
DSC	differential scanning calorimetry
DOP	dioctyl phthalate
DGEBA	diglycidyl ether bisphenol A
IR	infrared spectroscopy
LiClO ₄	lithium perchlorate
MAiBu-POSS	methacrylo isobutyl-POSS
NMR	nuclear magnetic resonance
MALDI-TOF	matrix-assisted laser desorption ionization-time of flight
OA-POSS	octakis(dimethyl(4-acetoxy phenethyl)siloxy)-POSS
OAM-POSS	octa(aminopropyl)-POSS
OAP-POSS	octakis(aminophenyl)-POSS
OiBu-POSS	octaisobutyl-POSS
ODA	4,4'-diaminodiphenyl ether
ODADS	4,4'-diaminodiphenyl ether-2,2'-disulfonic acid
OEC-POSS	octaepoxycyclohexyldimethylsilyl-POSS
OF-POSS	octakis(dimethylsiloxyhexafluoropropyl ether)-POSS

OG-POSS	octaglycidyl dimethylsilyl-POSS
OH-POSS	octakis(3-hydroxypropyldimethylsilyl)- POSS
OMA-POSS	octamethacryl-POSS
OM-POSS	octa-methyl-POSS
OP-POSS	octakis(dimethyl(4- hydroxyphenethyl)siloxy)-POSS
OV-POSS	octa-vinyl POSS
OPE-POSS	octa-phenethyl-POSS
OS-POS	octakis(dimethyl(phenethyl)siloxy)-POSS
PA	polyamide
PAA	poly(amic acid)
PAMAM	poly(amidoamine)
PAS	poly(acetoxystyrene)
PBD	poly(butadiene)
PBLG	poly(γ -benzyl-L-glutamate)
PBT	poly(butylene terephthalate)
PC	poly(carbonate)
PCL	poly(ϵ -caprolactone)
PDIB-POSS	1,2-propanediolisobutyl-POSS
PE	poly(ethylene)
PEEK	poly(ether ether ketone)
PEI	poly(ethylene-imine)
PET	poly(ethylene terephthalate)
PLGA	poly(lactide-co-glycolide)
POSS	polyhedral oligomeric silsesquioxane
PP	poly(propylene)
PPO	poly(dimethyl phenylene oxide)
PP-g-MA	PP-grafted maleic anhydride
PS	poly(styrene)
PSMA	poly(styrene-co-maleic anhydride)

PU	polyurethane
PVC	poly(vinyl chloride)
PVP	poly(vinyl pyrrolidone)
P4VP	poly(4-vinyl pyridine)
PVPh	poly(vinyl phenol)
$Q_8M_8^H$	octakis(dimethylsiloxy)silsesquioxane
SAXS	small-angle X-ray scattering
SEM	scanning electron microscopy
SH-POSS	mercaptopropyl-isobutyl-POSS
TEM	transmission electron microscopy
TGA	thermal gravity analysis
WAXD	wide-angle X-ray diffraction

1. Introduction

Relative to metals and ceramics, polymeric materials generally have lower moduli and strength. One way to effectively improve the mechanical properties of polymers is to reinforce them with nano-sized inorganic particles (defined herein as having at least one dimension in the range 1–100 nm). Using this approach, the polymer properties can be efficiently improved while maintaining its inherently low density and high ductility. Improvements in mechanical properties are often found even at relatively low filler content. The nanofillers may have spherical (metal or semi-conductive nanoparticles (NPs)), layered (clay), or fibrous (nanofibers and carbon nanotubes) shapes. Such polymer nanocomposites are diverse and versatile functional materials, with applications in systems ranging from electronic devices to biosensors and catalysts. The field of polymer nanocomposite materials has attracted great attention from polymer scientists and engineers in recent years. The simple premise involves using building blocks of nanosize dimensions to create new polymeric materials exhibiting improved physical properties.

Silsesquioxanes are nanostructures having the empirical formula $RSiO_{1.5}$, where R is a hydrogen atom or an organic functional group such as an alkyl, alkylene, acrylate, hydroxyl, or epoxide unit. Based on images in the first review of POSS polymers and resins published by the Pittman group, Fig. 1 illustrates that silsesquioxanes can be formed as random, ladder, cage, or partial cage structures [1,2]. Scott [3] discovered the first oligomeric organosilsesquioxane, $(CH_3SiO_{1.5})_n$, along with other volatile compounds through the thermolysis of polymeric products prepared from co-hydrolysis of methyl trichlorosilane and dimethyl chlorosilane.

Although silsesquioxane chemistry has been studied for more than half a century, interest in this field has increased dramatically in recent years. Baney et al. [4] reviewed the preparation, properties, structures, and applications of silsesquioxanes, especially those of ladder-like polysilsesquioxanes (Fig. 1(b)). More recently, attention has been concentrated on silsesquioxanes possessing the specific cage structures displayed in Figs. 1(c)–(f). These polyhedral oligomeric silsesquioxanes are commonly referred to by the acronym “POSS”. Derivatives of

POSS are true hybrid inorganic/organic chemical composites that possess an inner inorganic silicon and oxygen core $(SiO_{1.5})_n$ and external organic substituents that can feature a range of polar or nonpolar functional groups. POSS nanostructures having diameters ranging from 1 to 3 nm can be considered as the smallest possible particles of silica, i.e., molecular silica. Unlike most silicones or fillers, POSS molecules contain organic substituents on their outer surfaces, making them compatible or miscible with most polymers. In addition, these functional groups can be specifically designed as either non-reactive (e.g., for polymer blending) or reactive (for copolymerization). POSS derivatives can be prepared with one or more covalently bonded reactive functionalities suitable for polymerization, grafting, blending, or other transformations. Unlike traditional organic compounds, POSS derivatives are nonvolatile, odorless and environmentally friendly materials. The incorporation of POSS moieties into a polymeric material can dramatically improve its mechanical properties (e.g., strength, modulus, rigidity) as well as reduce its flammability, heat evolution, and viscosity during processing. These enhancements apply to a wide range of commercial thermoplastic polymers, high-performance thermoplastic polymers, and thermosetting polymers [1,2]. It is especially convenient to incorporate POSS moieties into polymers through simple blending or copolymerization. In addition, when POSS monomers are soluble in monomer mixtures, they can be incorporated as true molecular dispersions in the resulting polymer matrix. The macrophase separation that usually occurs through the aggregation of POSS units can be avoided through copolymerization (i.e., covalent bond formation between the POSS units and the polymers)—a significant advantage over the traditional filler technologies. POSS nanostructures also have significant promise for use in catalyst supports and biomedical applications, such as scaffolds for drug delivery, imaging reagents, and combinatorial drug development [5,6].

In this review, we describe methods for synthesizing POSS compounds and preparing monomers and polymers containing POSS derivatives. We discuss both mono- and multifunctional POSS monomers that have been used to develop thermoplastic and thermosetting polymers. In addition, we compare the miscibility, phase behavior, thermal, dynamic mechanical, electrical, and surface properties of polymers containing POSS units.

2. General approaches in the syntheses of polyhedral oligomeric silsesquioxanes

POSS derivatives featuring Si–O linkages in the form of a cage present a silicon atom at each vertex, with substituents coordinating around the tetrahedral silicon vertices. The nature of the exo cage substituents in such compounds determines the mechanical, thermal, and other physical properties. The number of $RSiO_3$ units determines the shape of the frame, which is uniquely unstrained for 6–12 units. Voronkov et al. [7] have reviewed the known methods of synthesizing POSS compounds. Many substituents appended to the silicon/oxygen cages $(RSiO_{1.5})_n$, (where R is an organic or inorganic group) allow the poly-

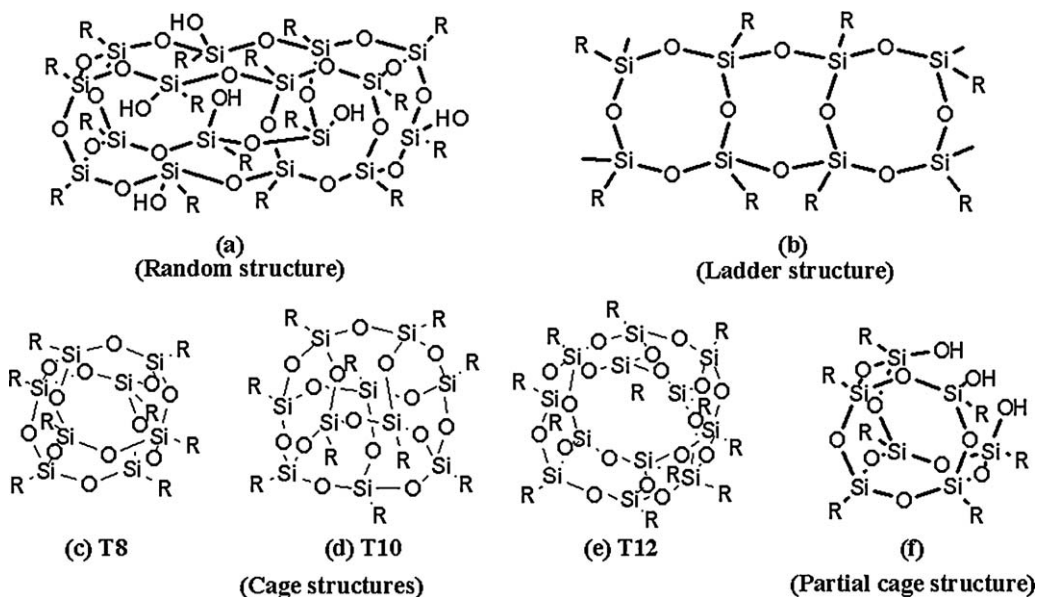


Fig. 1. Structures of silsesquioxanes.

merization of POSS units or the copolymerization of specific POSS derivatives with other monomers.

2.1. Monofunctional POSS

Monofunctional POSS derivatives are among the most useful compounds for polymerization or copolymerization with other monomers. Fig. 2 summarizes the three general approaches to synthesize monofunctional POSS derivatives of the form $R'R_7Si_8O_{12}$ [10].

Route I. Coadhydrolysis of trifunctional organo- or hydrosilanes: Polycondensation of monomers is the classical method of synthesizing silsesquioxanes [8–10]. When this reaction is performed in the presence of monomers possessing various R groups, mixtures of heterosubstituted compounds are obtained, including the desired monosubstituted products (ca. 48% overall yield).

Route II. Substitution reactions with retention of the siloxane cage: Fig. 2 presents a selection of substitution reactions using octahydro-silsesquioxanes as the starting materials (IIa–c) that have been applied successfully to prepare monosubstituted silsesquioxanes [11–13]. By adjusting the ratio of the reactants, it is possible to obtain a considerable yield (18.6–43.6%) of the desired monosubstituted product.

Route III. Corner-capping reactions: Feher and coworkers [14–17] developed this approach starting from incompletely condensed $R_7Si_7O_9(OH)_3$ molecules (T_7). The three silanol groups are very reactive toward $R'SiCl_3$, giving the fully condensed products. Variation of the R' group on the silane enables the syntheses of a variety of monofunctionalized siloxane cages [18]. Subsequent transformations can be performed until the desired functionality is obtained. Moreover, incompletely condensed silsesquioxanes offer a route for the generation of hetero- and metalla-siloxanes, in which a hetero main group or a transition metal element is introduced into the Si–O framework [19–21].

2.2. Multifunctional POSS

POSS $(RSiO_{1.5})_n$ derivatives have values of n of 4, 6, 8, 10, or 12, with the R groups being hydrogen, alkyl, aryl, or inorganic units. Unique POSS structures ($R=H$) can be formed through the hydrolysis and condensation of trialkoxysilanes $[HSi(OR)_3]$ or trichlorosilanes $(HSiCl_3)$ [7]. The hydrolysis of trimethoxysilane in a cyclohexane/acetic acid mixtures in the presence of concentrated hydrochloric acid provides the octamer in low yield (13%) [22]. Another synthetic approach to generate multifunctional POSS derivatives is the functionalization of preformed POSS cages; e.g., through Pt-catalyzed hydrosilylation of alkenes or alkynes with $(HSiO_{1.5})_8$ and octakis(dimethylsiloxy)silsesquioxane $((HMe_2SiOSiO_{1.5})_8, Q_8M_8^H)$ cages (Fig. 3) [23–25].

3. Hydrogen bonding and miscibility behavior of polymer/POSS nanocomposites

3.1. Hydrogen bonding interactions between polymers and POSS

Most inorganic silicas or ceramics are immiscible in most organic polymer systems because of poor specific interactions within these organic/inorganic hybrids and the negligibly small combined entropy contribution to the free energy of mixing. Specific intermolecular interactions are generally required to enhance the miscibility of polymers and inorganic particles. Such interactions include hydrogen bonding, dipole–dipole interactions and acid/base complexation [26]. Determining the types and strengths of the interactions between the POSS derivatives and polymers is an important challenge. For convenience, our group has prepared a phenolic/POSS hybrid from a mixture of phenolic resin and an octakisobutyl-POSS

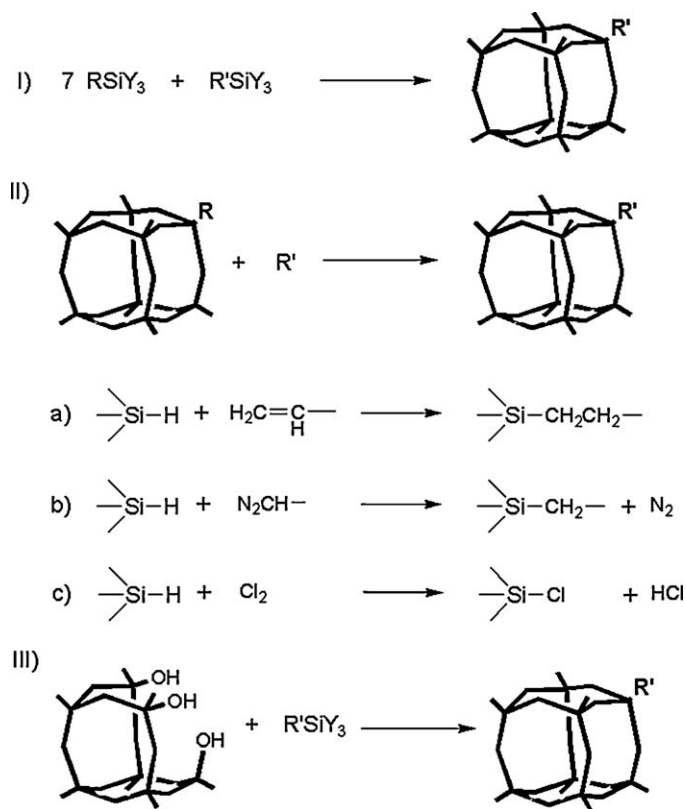


Fig. 2. Three general ways to synthesize monosubstituted octasilsesquioxane.

(OiBu-POSS) to investigate the miscibility, specific interactions, and microstructural behavior [27]. The nature of the hydrogen bonding sites in the phenolic/POSS hybrid was investigated, using 2D-IR correlation spectroscopy [28,29]. Fig. 4 presents the synchronous and asynchronous 2D correlation maps in the range from 1000 to 1250 cm^{-1} [27]. The absorption bands of the OiBu-POSS derivative at

1100 and 1223 cm^{-1} correspond to siloxane Si–O–Si and Si–C stretching vibrations, respectively, and the peak at 1223 cm^{-1} is due to the phenyl–OH stretching vibration of the phenolic. Two positive cross-peaks in the synchronous 2D map in Fig. 4(a) indicate the existence of hydrogen bonds between the siloxane group of the POSS derivative (1100 cm^{-1}) and the phenyl–OH group (1223 cm^{-1})

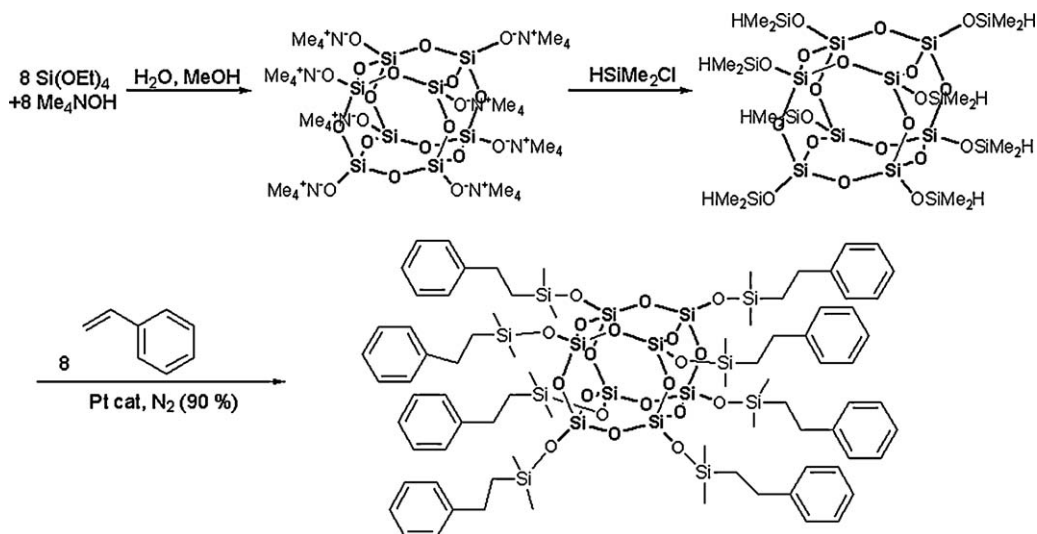


Fig. 3. An example of the synthesis of a multifunctional POSS, (octakis[dimethyl(phenethyl)siloxy] silsesquioxane, OS-POSS).

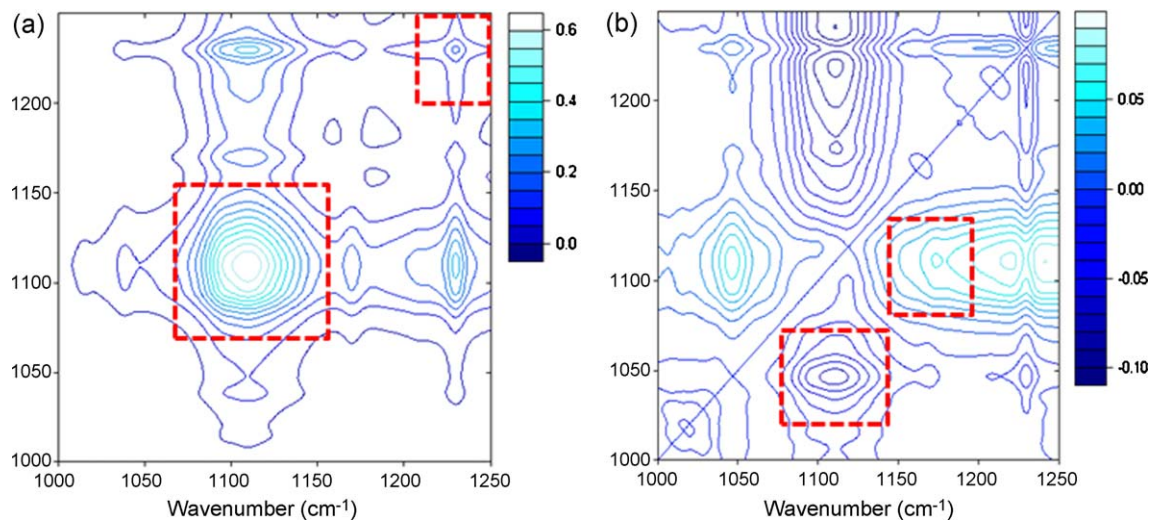


Fig. 4. The synchronous version (a) and asynchronous version (b) of 2D correlation map at 1000–1250 cm^{-1} region for phenolic/OiBu-POSS blends under compositions perturbation.

Reprinted with permission from Ref. [27]. Copyright 2004, Wiley-VCH, Germany.

of the phenolic. In the asynchronous 2D correlation map in Fig. 4(b), the 1100 cm^{-1} absorption splits into two separate bands located at ca. 1105 and 1160 cm^{-1} for the POSS units, suggesting two different types of siloxane (Si–O–Si) sites in the POSS cage. One (at higher wavenumber) undergoes hydrogen bonding with the OH groups of the phenolic, while the other (at lower wavenumber) is free. The positive crosspeaks at 1105 and 1220 cm^{-1} also reveals the presence of hydrogen bonding between the siloxane (Si–O–Si) groups of the POSS and the phenyl–OH groups of the phenolic resin.

3.2. Miscibility between polymers and POSS derivatives

Painter and Coleman [26] suggested that adding an additional term to the simple Flory–Huggins expression to account for the free energy of hydrogen bond formation upon mixing two polymers, as formulated in Eq. (1):

$$\frac{\Delta G_m}{RT} = \frac{\phi_A}{M_A} \ln \phi_A + \frac{\phi_B}{M_B} \ln \phi_B + \phi_A \phi_B \chi_{AB} + \frac{\Delta G_H}{RT} \quad (1)$$

where ΔG_H denotes the free energy change contributed by the hydrogen bonding between the two components. The combinatorial entropy expressed in the first two logarithmic terms contributes a very small, but nonetheless favorable, amount to the free energy of mixing. ϕ_A and ϕ_B are the volume fractions of polymers A and B in the blend, respectively, and M_A and M_B are the corresponding degrees of polymerization. According to the Painter–Coleman association model (PCAM) [30,31], the equilibrium constant for the association of a non carbonyl group component with a hydrogen bond-donating component can be calculated using the classical Coggeshall and Saier (C&S) equation (2) [32]:

$$Ka = \frac{1 - f_m^{\text{OH}}}{f_m^{\text{OH}}(C_A - (1 - f_m^{\text{OH}})C_B)} \quad (2)$$

where C_A and C_B are the concentrations (in mol L^{-1}) of OiBu-POSS and 2,4-dimethylphenol (a model compound for phenolic) and f_m^{OH} is the fraction of free hydroxyl group of 2,4-dimethylphenol. Fig. 5 displays the OH group absorption of 2,4-dimethylphenol in cyclohexane solutions containing various concentrations of OiBu-POSS;

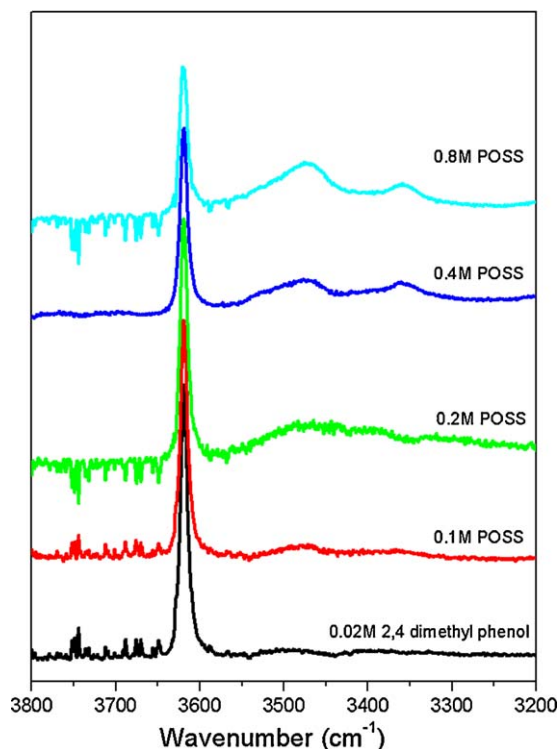


Fig. 5. FT-IR spectra of 2,4-dimethylphenol (xylene) with various OiBu-POSS concentrations.

Reprinted with permission from Ref. [27]. Copyright 2004, Wiley-VCH, Germany.

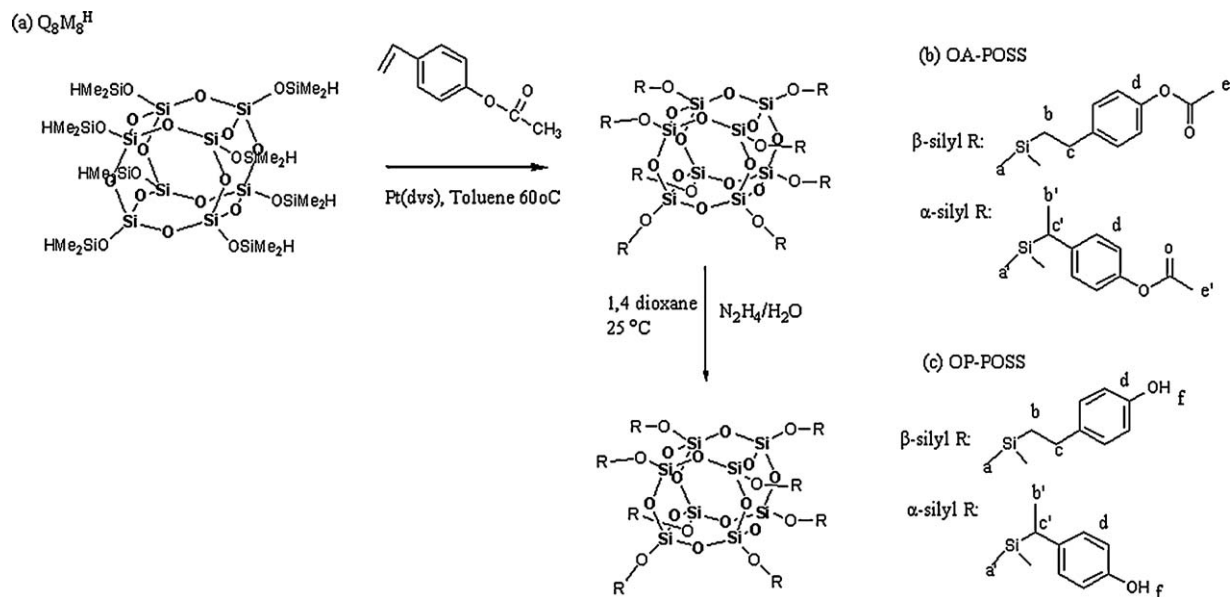


Fig. 6. Chemical Structures of octakis[dimethyl(4-acetoxy phenethyl)siloxy]-POSS (OA-POSS) and octakis[dimethyl(4-hydroxyphenethyl)siloxy]-POSS (OP-POSS).

the intensity of the free OH absorption at 3620 cm^{-1} decreases upon increasing the OiBu-POSS content. The absolute intensity of the free OH group at 3620 cm^{-1} is an indication of the content of free OH groups in the mixture [33,34]. The value of K_A of 38.67 was obtained by using C&S equation. The equilibrium constant for self-association of the Novalac type phenolic resin is 52.3 [33]. Since the equilibrium constant for the association between phenolic/OiBu-POSS is smaller than that for the self-association of pure phenolic, the phenolic/OiBu-POSS hybrid should be partially miscible or immiscible. For this reason, functionalization of POSS derivatives with pendent hydrogen bond-acceptor groups should improve their miscibility with phenolic resin. Functionalization of $Q_8M_8^H$ can be achieved through hydrosilylation of its Si-H groups with acetoxystyrene [35] in the presence of a Pt catalyst to form octakis[dimethyl(4-acetoxy phenethyl)siloxy] silsesquioxane [OA-POSS; Fig. 6(b)].

Fig. 7 presents scaled room temperature IR spectra of pure phenolic and various phenolic/OA-POSS nanocomposites [35]. Fig. 7a reveals that the intensity of the free OH absorption (3525 cm^{-1}) decreases gradually as the OA-POSS content of the blend is increased from 5 to 90 wt%. The band for the hydrogen-bonded OH units in the phenolic shifted to higher frequency (toward 3465 cm^{-1}) upon increasing the OA-POSS content. This change is due to the switch from hydroxyl-hydroxyl interactions to the formation of hydroxyl-carbonyl and/or hydroxyl-siloxane hydrogen bonds. Fig. 7b displays the room temperature IR spectra ($1680\text{--}1820\text{ cm}^{-1}$) of various phenolic/OA-POSS blend composites. The C=O stretching frequency is split into bands at 1763 and 1735 cm^{-1} , corresponding to free and hydrogen-bonded C=O groups, respectively [36–39]. Fig. 8 indicates that the experimental values of K_A are generally lower than the predicted values when using the value of K_A of 64.6 obtained from the pheno-

lic/PAS blends [34]. This result reveals that the OH groups of phenolic interact with the C=O groups of the acetoxystyrene units as well as the siloxane groups of the POSS core. The equilibrium constants K_A for the association of phenolic/OA-POSS and the phenolic/PAS blend blends are 26.0 and 64.6. Therefore, the value of K_A for the interaction between the OH group of phenolic and the siloxane groups of the POSS derivative is equal to 38.6 (i.e., $64.6 - 26.0 = 38.6$), consistent with the value reported based on the classical C&S methodology [32]. Our group also synthesized a new POSS derivative containing eight phenol groups (octakis[dimethyl(4-hydroxyphenethyl)siloxy] silsesquioxane, OP-POSS, Fig. 6(b)) and copolymerized it with phenol and formaldehyde to form covalently linked novolac-type phenolic/OP-POSS nanocomposites that exhibited higher thermal stabilities and lower surface energies [40]. Differential scanning calorimetry (DSC) and thermogravimetric analysis (TGA) of the phenolic/OP-POSS nanocomposites at various weight ratios revealed that each of these hybrids possessed essentially a single value of T_g , suggesting that they each featured a single phase [40]. The values of T_g of these nanocomposites were significantly enhanced after incorporation of OP-POSS units, presumably because of the restricted motion of the polymer chains caused by physical crosslinking through hydrogen bonds with the evenly distributed POSS units within the phenolic matrix.

In addition, our group has synthesized three amorphous POSS derivatives: OS-POSS (Fig. 3), OA-POSS and OP-POSS (Fig. 6). Fig. 9 displays MALDI-TOF mass spectra of these compounds. Monodisperse mass distributions of the sodiated molecular ions appear at 1873 g/mol for $[\text{OS-POSS} + \text{Na}]^+$, 2337 g/mol for $[\text{OA-POSS} + \text{Na}]^+$, and 2001 g/mol for $[\text{OP-POSS} + \text{Na}]^+$, the good agreement between the experimental and calculated molecular masses confirms the well-defined structures of OS-POSS,

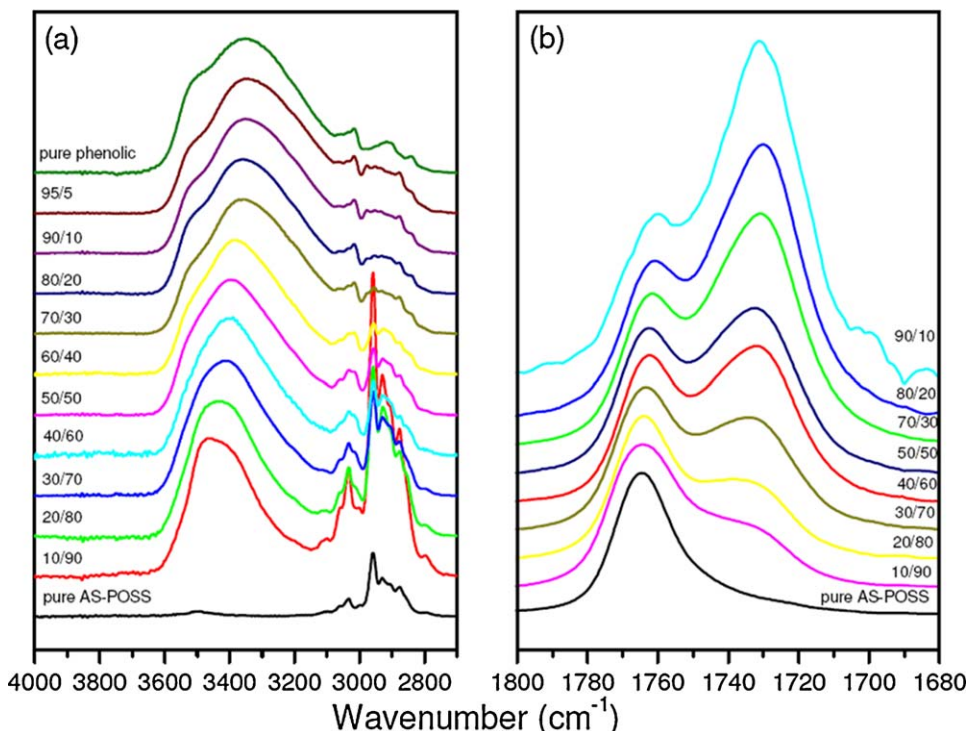


Fig. 7. IR spectra for phenolic/AS-POSS blends: (a) hydroxyl and (b) carbonyl.

Reprinted with permission from Ref. [35]. Copyright 2006, Wiley-VCH, Germany.

OA-POSS, and OP-POSS [25]. Blending OS-POSS, and OP-POSS with polystyrene PS, PAS, or P4VP facilitated investigation of the effects of intermolecular interactions on the dispersion of these POSS derivatives in the polymer matrices [hydrophobic interactions between aromatic rings (OS-POSS/PS), dipole–dipole interactions between ester groups (OA-POSS/PAS), and hydrogen bonding between phenol and pyridine units (OP-POSS/P4VP)]. Fig. 10 displays transmission electron microscopy (TEM) images and schematic representations of the microstructures of these POSS-based polymer nanocomposites [25].

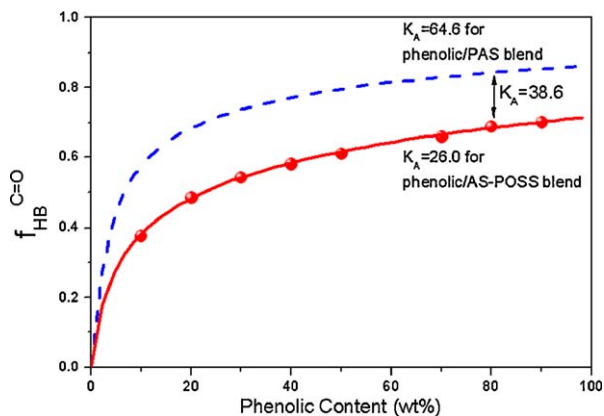


Fig. 8. Fraction of hydrogen-bonded carbonyl groups versus phenolic contents.

Reprinted with permission from Ref. [27]. Copyright 2006, Wiley-VCH, Germany.

Our octakis-functionalized amorphous POSS derivatives were dispersed through physical intermolecular interactions between their outer organic units and the organic polymer matrices. Thus, the size and distribution of the POSS aggregates depend strongly on the type and strength of the intermolecular interactions. Clearly, the weak aromatic hydrophobic interactions between OS-POSS and

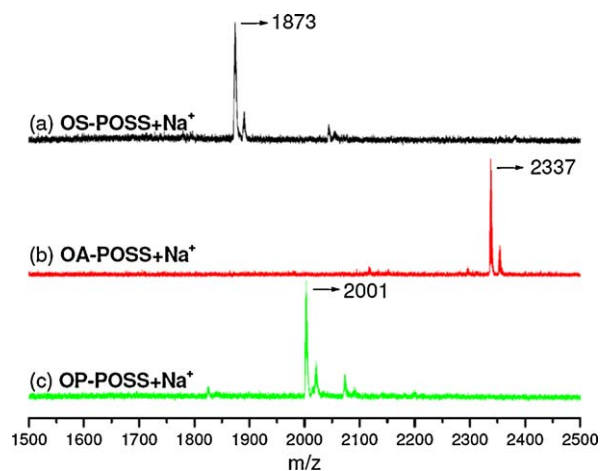


Fig. 9. MALDI-TOF mass spectra of (a) octakis[dimethyl(phenethyl)siloxy] silsesquioxane, (OS-POSS), (b) octakis[dimethyl(4-acetoxyphenethyl)siloxy]-POSS (OA-POSS) and octakis[dimethyl(4-hydroxyphenethyl)siloxy]-POSS (OP-POSS).

Reprinted with permission from Ref. [25]. Copyright 2008, Elsevier Science Ltd., UK.

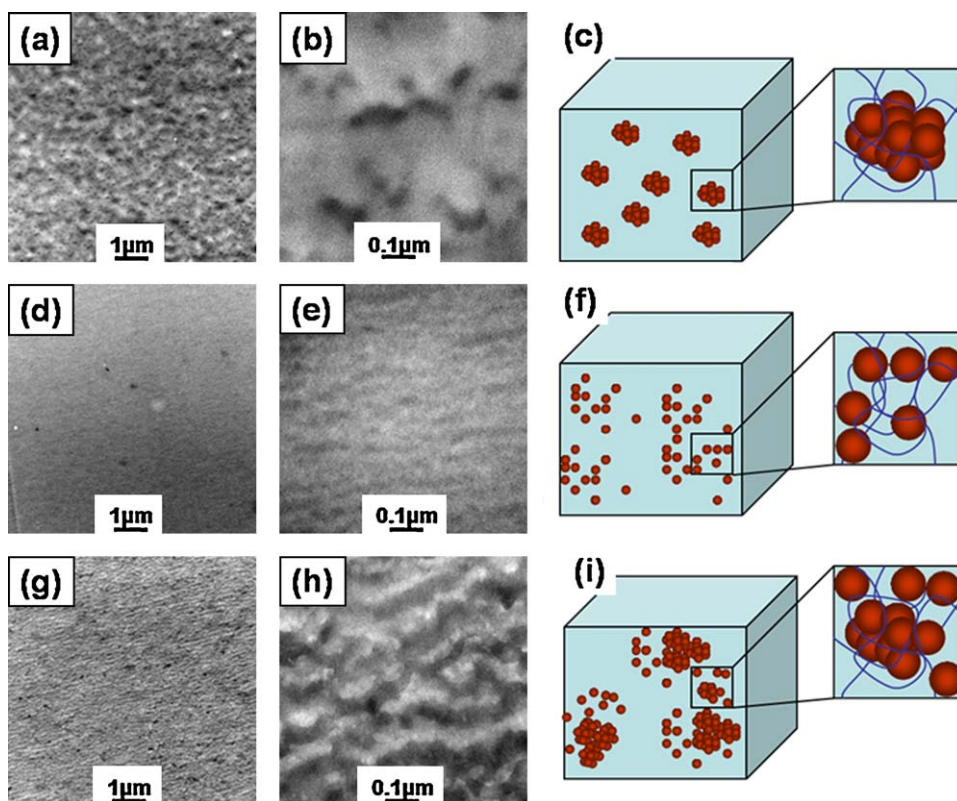


Fig. 10. TEM images and schematic microstructures of POSS-based polymer nanocomposites (a–c) OS-POSS/PS, (d–f) OA-POSS/PAS, and (g–i) OP-POSS/P4VP. Reprinted with permission from Ref. [25]. Copyright 2008, Elsevier Science Ltd., UK.

PS were unable to overcome the attraction force among of the POSS cores, even though premixing did promote uniform dispersion of the POSS derivatives. With their stronger intermolecular dipole–dipole interactions, we do not observe any dark regions representing OA-POSS aggregates. The polar P4VP is also miscible in OP-POSS because of hydrogen bonding between hydroxyl and pyridine units.

4. POSS-containing polymers and copolymers

POSS feedstocks functionalized with various reactive organic groups can be incorporated into virtually any existing polymer system through grafting, copolymerization or blending. The incorporation of POSS nanocluster cages into a polymeric material can result in dramatic improvements in the polymer's properties including greater temperature and oxidation resistance, surface hardening, and reduction in flammability. Therefore, research in POSS-related polymers and copolymers has accelerated in recent years. Depending on the number of POSS functional groups, various architectures of polymer/POSS nanocomposites can be obtained (Fig. 11) [41]. Some representative systems are discussed below.

4.1. Polyolefin/POSS and norbornyl/POSS copolymers

4.1.1. Polyethylene and norbornyl/POSS copolymers

A number of interesting design strategies for the preparation of polyolefin/POSS hybrid materials have evolved

over the past decade [42–50]. Coughlin and coworkers [42] synthesized PE hybrid containing POSS through ring-opening metathesis copolymerization (Fig. 12). From studies of nanostructured PE-POSS copolymers through controlled crystallization and aggregation, they found that two distinctly different crystallizing components were present in these copolymers and the final structure depended on the respective crystallization kinetics under different crystallization conditions [42]. Fig. 13 presents TEM micrographs of polybutadiene-POSS (PBD-POSS) random copolymers with POSS contents of 12 and 43 wt% [51]. In Fig. 13(a), POSS aggregates are clearly observed as short randomly oriented lamellae having lateral dimensions of ca. 50 nm. The thickness of the lamellae ca. 3–5 nm, roughly corresponds to twice the diameter of a POSS NP. Increasing the incorporation ratio of POSS to 43 wt% resulted in the formation of continuous lamellae having lateral lengths on the order of microns (Fig. 13(c)). The irregular lamellar spacing observed in this image possibly arose from a combination of both twisting of the POSS lamella and the random nature of the copolymers. The morphology bears similarity to the lamellar morphology formed by precise diblock copolymers [51]. Furthermore, Coughlin and coworkers [42,52] and Mather et al. [53] reported polyolefin copolymers containing norbornyl-POSS macromonomers. Polyolefin-POSS copolymers incorporating norbornylene-POSS macromonomer have been prepared using a metallocene/methyl aluminoxane (MAO) co-catalyst system [52]. Using a Pd-diimine catalyst, Ye and

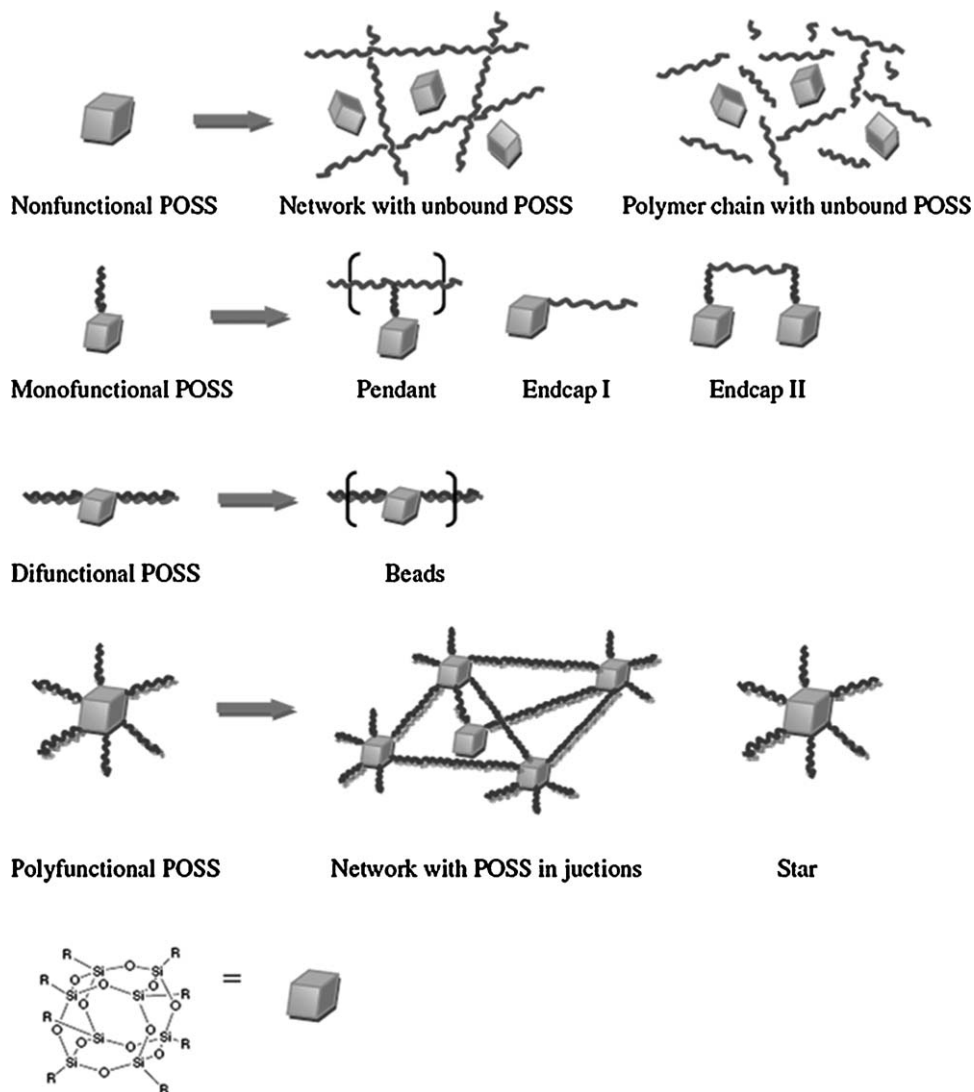


Fig. 11. Polymer/POSS architectures.

coworkers [54] synthesized hyperbranched PE containing covalently tethered POSS NPs through chain-walking ethylene copolymerization with a POSS macromonomer bearing a polar acryloisobutyl-POSS unit. The covalent incorporation of the high-mass POSS NPs significantly reduced the intrinsic viscosity of the copolymers relative

to the pure PE of the same molecular weight, owing to the highly compact spherical cage structure of the POSS NPs. Thermal studies confirm that the incorporation of POSS units significantly enhanced the thermal oxidative stability of the polymers in air, with the value of T_g of the copolymer increasing upon increasing the POSS contents.

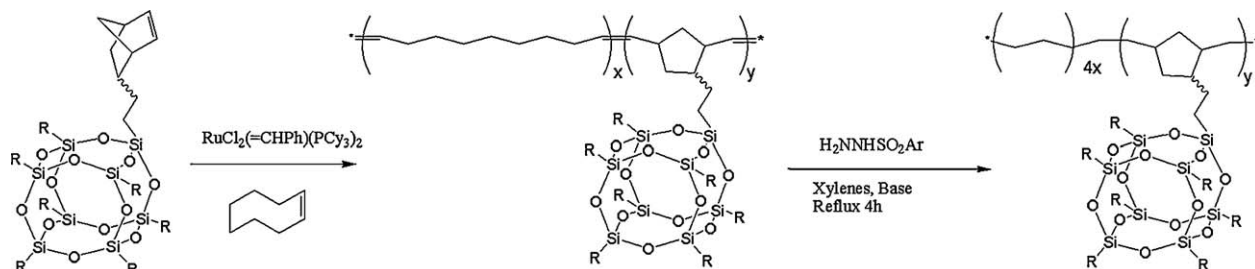


Fig. 12. Copolymerization of cyclooctene and norbornene-POSS.

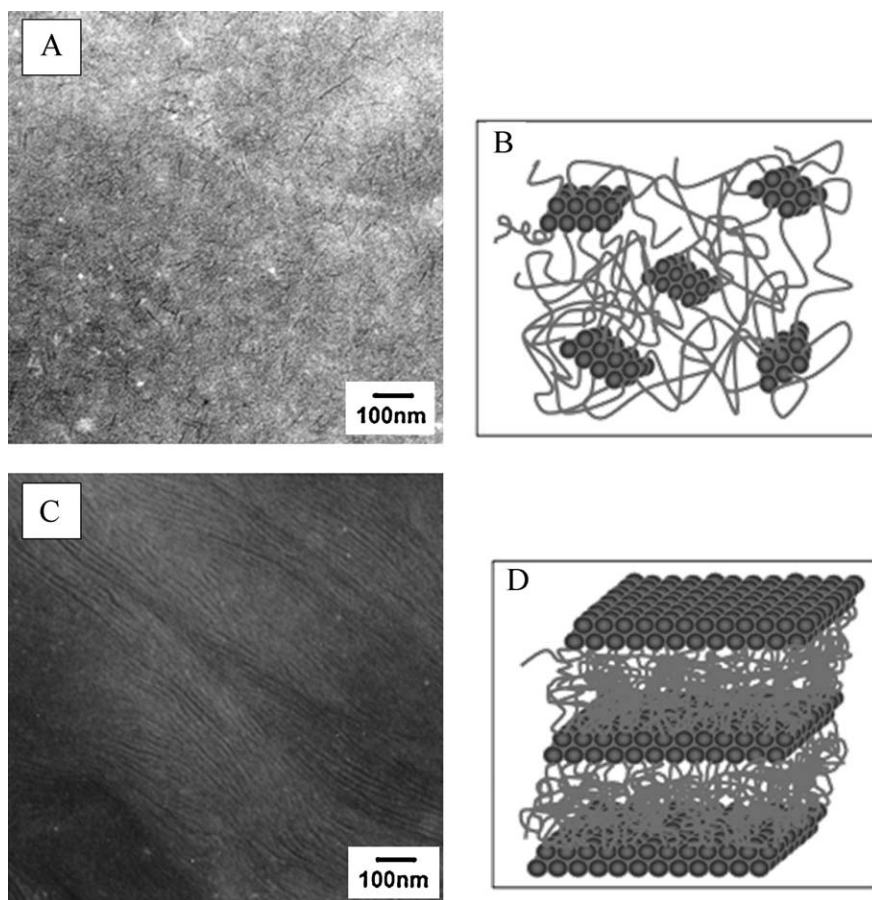


Fig. 13. (a) TEM of polybutadiene-POSS (PBD-POSS) copolymer with 12 wt% of Cp-POSS. (b) Schematic drawing of PBD-POSS assembly at low POSS concentration. (c) TEM of PBD-POSS copolymer with 43 wt% of Cp-POSS. (d) Schematic drawing of PBD-POSS assembly at high POSS concentration. Reprinted with permission from Ref. [51]. Copyright 2001, American Chemical Society, USA.

Joshi et al. [47] used a melt mixture route to prepare high-density PE/octamethyl-POSS (OM-POSS) nanocomposites. The rheological results revealed that, at lower filler contents (0.25–0.5 wt%) the POSS particles acted as a lubricant to reduce the complex viscosity of the nanocomposites. At higher POSS concentrations, the viscosities of the nanocomposites increased. The POSS derivatives remained miscible with HDPE at lower concentrations and lower temperatures, but they tended to aggregate at higher concentrations and higher temperatures. From studies of non-isothermal crystallization of the HDPE/OM-POSS nanocomposites using the Kissinger method [49], they also found that the presence of the POSS units did not have any significant effect on the activation energy for the transport of the polymer segments to the growing surface. They observed that only those POSS units dispersed at the molecular level could act as nucleating agents while the POSS nanocrystals did not affect the crystallization process.

4.1.2. Polypropylene/POSS nanocomposites

Zhang et al. [55] prepared polypropylene-POSS nanocomposites using a C_2 symmetric ansa-metallocene catalyst in conjunction with a modified MAO. Their PP/POSS copolymers exhibited improved thermal sta-

bilities with higher degradation temperature and char yields, revealing that inclusion of the inorganic POSS NPs made the organic polymer matrix more thermally robust. Hsiao and coworkers [56] used DSC to investigate a series of isotactic polypropylene (iPP) melt-blended with nanostructured OM-POSS molecules to study the quiescent melt crystallization behavior and shear-induced crystallization behavior. They observed that the addition of OM-POSS molecules increased the crystallization rate of iPP under both isothermal and non-isothermal conditions, implying that POSS crystals acted as nucleating agents, a finding that is similar to that with PE systems. Tabuani and coworkers [57–61] reported the influence of the POSS substituent on the morphological and thermal characteristics of melt-blended PP/POSS composites [57–61]. By varying the amount of filler, they investigated the effects of three different alkyl substituents (R=ethyl, isobutyl, iso-octyl) in the POSS structure on the morphological characteristics, crystallization and melting behavior of PP/POSS composites. They found that the lengths of the alkyl groups of the POSS molecules played a fundamental role affecting the degrees of dispersion and interactions with the PP matrix during the cooling process from the melt.

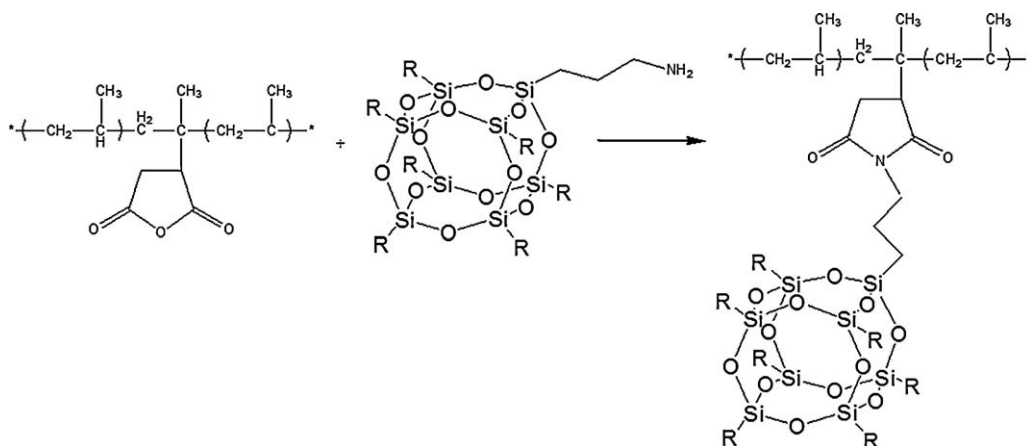


Fig. 14. Reaction between PP-g-MA and NH₂-POSS producing imide bond.

Two metal-POSS (M-POSS) systems, Ti(IV)- and Al(III)-isobutyl-POSS were blended with PP to study the morphological, crystallization, and thermal behavior of these M-POSS/PP composites [61]. Ti- and Al-POSS had different effects on the thermoxidative behavior of the polypropylene matrix in the M-POSS/PP composites, revealing the clear specificity of the metal center on the PP degradation pathway. In particular, Ti-POSS significantly stabilized PP when heated in air, whereas Al-POSS had only limited effects. Moreover, Ti-POSS affected the crystallization of PP, driving the crystallization process along specific crystallographic directions.

Fina et al. [62] reported the maleic anhydride-grafted polypropylene (PP-g-MA)/POSS hybrids prepared through grafting of aminoethylaminopropyl heptaisobutyl POSS (AM-POSS) in a one-step reactive blending process (Fig. 14). Morphological analyses revealed the dispersion of POSS units on the nanoscale because of the high chemical reactivity between POSS and PP-gMA. The presence of grafted POSS moieties improved the thermoxidative stability of PP-g-MA, in terms of delaying mass loss during thermal degradation under air, relative to pure PP-g-MA and PP-g-MA containing comparable amount of the non-reactive OiBu-POSS.

Chen and coworkers [63,64] studied the isothermal crystallization kinetics and morphological development of iPP blended with small loadings of OM-POSS. The predominantly nanocrystalline POSS acted as an effective nucleating agent to promote the nucleation rate of iPP. In contrast, the minor amount of those slightly miscible and dispersed POSS molecules retarded the nucleation and growth rates of iPP in the remaining bulk region. Zhou et al. [65–68] studied the crystallization behavior of PP/octavinyl-POSS (OV-POSS) prepared using two different processing methods: reactive blending and physical blending. Crystallization in the PP/POSS composites was strongly influenced by the processing method. POSS particles can act as effective nucleating agents to accelerate the crystallization of PP. The crystallization rate increased more dramatically for the reactive blending composite because of the stronger nucleating effect of PP-grafted POSS. The surface energy of chain folding of the physical-blend and

reactive-blend composites changed from 156.5 mJ/m² for pure PP to 81.2 and 24.5 mJ/m², respectively [62].

Misra et al. [69] used melt blending to study the surface energy and mechanical behavior of PP/OiBu-POSS nanocomposites. Incorporation of 10% POSS resulted in a 3% reduction in the surface energy (to 24 mN/m), and a 27% increase in the water contact angle (to 99°). The increased water contact angle reveals the hydrophobic nature of the PP/POSS nanocomposite surface. The observed increases in surface hydrophobicity by increasing POSS concentration can be related to surface roughness through AFM roughness analysis [69]. Tang and Lewin [70] studied the migration and surface modification of PP/POSS nanocomposites by annealing the melt and by heating the solid blend in a microwave oven. Their static contact angle measurements revealed very high hydrophobicity as well as low surface free energy of the surface of the annealed sample, close to Teflon or pristine POSS. The migration of POSS was due to its lower surface tension and lower cohesive energy with the matrix chains relative to the cohesion energy between polymer chains, and the density and temperature fluctuations of the matrix chains upon relaxation repulse. As a result, the POSS units were propelled to the surfaces [70].

4.1.3. Other polyolefin POSS nanocomposites

Cohen and coworkers [71,72] found that octamethacryl-POSS (OMA-POSS) has the ability to plasticize PVC better than organic plasticizers such as dioctyl phthalate (DOP). They found that the value of T_g of ternary blends of PVC/POSS/DOP could be reduced to near room temperature. Zheng et al. [73] reported that the inclusions of octaglycidyl dimethylsilyl POSS (OG-POSS) into PEI resulted in higher values of T_g and enhanced thermal stabilities relative to those of pure PEI. In addition, PEI containing hepta(3,3,3-trifluoropropyl) glycidylether-propyl POSS exhibited typical amphiphilicity as evidenced by increased surface hydrophobicity.

4.2. Polystyrene/POSS nanocomposites

Linear thermoplastic hybrid materials containing an organic PS backbone and large inorganic silsesquioxane

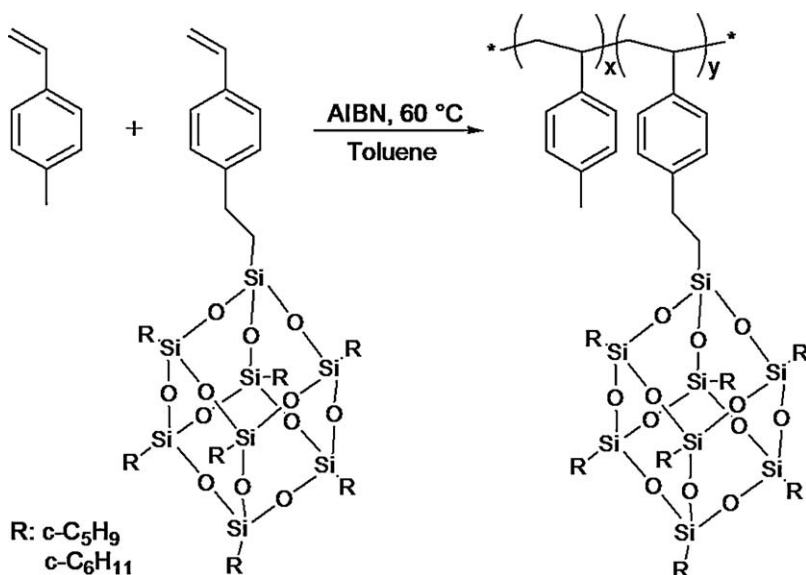


Fig. 15. Polymerization of PS–POSS copolymers.

groups pendent to the polymer backbone have been prepared through free radical copolymerization (Fig. 15) [74]. The pendent inorganic groups drastically modify the thermal properties of the PS, interchain and/or intrachain POSS–POSS interactions affect the solubility and thermal properties. Haddad and coworkers [75] reported the viscoelastic behavior of poly(4-methylstyrene) (P4MS)-POSS nanocomposites in which the POSS units possessed various R groups such as cyclopentyl (Cp) and cyclohexyl (Cy) moieties. Rheological measurements revealed that the polymer dynamics were profoundly affected by the POSS contents. In addition, the glass transition and decomposition temperatures increased upon increasing POSS content. Mather and coworkers [76] reported the linear viscoelastic properties of PS-iBu-POSS nanocomposites. Fig. 16(a) shows a TEM image of PS-POSS incorporating 6 wt% iBu-POSS where the domain size ranging from 1.5 to 3 nm was close to the dimensions of a single POSS molecule [76]. Further increase in the iBu-POSS concentration led to an increase in the dispersed particle density (Fig. 16(b)), whereas the particle size remained nearly unchanged, indicating that the iBu-

POSS groups grafted on the PS chain were well dispersed in the PS matrix almost at the molecular level. iBu-POSS was found to have a plasticizer-like effect, yielding a monotonic decrease in T_g upon increasing the iBu-POSS contents.

Mather and coworkers [77] also studied the linear viscoelastic behavior of PS-POSS nanocomposites featuring three different functional groups: i-Bu, Cp, and Cy. The T_g was strongly dependent on the POSS vertex group, i-Bu played a plasticizer-like role while Cp and Cy enhanced T_g . The rubbery plateau modulus decreased upon increasing the POSS contents which was also strongly dependent on the nature of vertex groups following the order i-Bu-POSS > Cp-POSS > Cy-POSS. They reported two distinct effects of POSS incorporation: influencing the microscopic topology of the polymer chains and the intermolecular interaction between PS and POSS.

Patel et al. [78] performed molecular dynamic simulations of PS-POSS nanocomposites featuring various R groups to identify the origin of the property changes imparted upon the chemical incorporations of POSS. When the POSS substituents were phenyl groups, the increase in

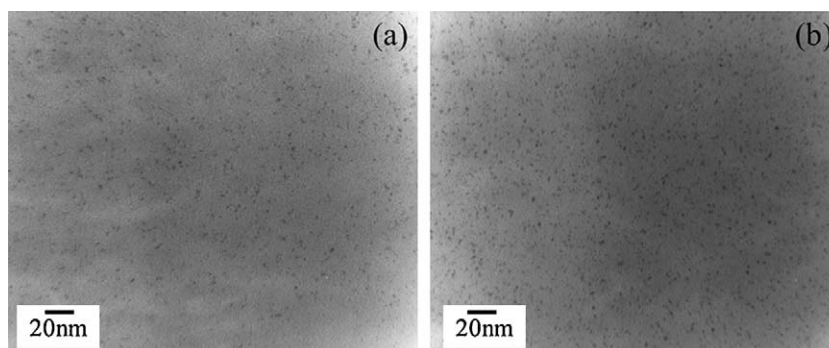


Fig. 16. TEM images of PS–POSS copolymers: (a) 6 and (b) 30 wt% i-Bu POSS. The samples were stained by RuO_4 vapor at ambient condition. Reprinted with permission from Ref. [76]. Copyright 2006, American Chemical Society, USA.

the T_g of the PS-POSS copolymer was significantly greater than that of alkyl groups. Such R group compatibility allows massive pendent POSS moieties to exert larger restrictions on segmental motion. When the R groups are alkyl functions, they are less compatible with the PS phenyl rings and pack less efficiently [78]. Monticelli et al. [79] reported the preparation of PSMA through one-step reactive blending with AM-POSS, similar to the PP-g-MA/POSS system described above [62]. The grafted POSS had no significant influence on the thermal and mechanical properties because of the competing effects of (i) the molecular constraints imparted by the presence of the bulky POSS cages and (ii) the increase in the free volume.

Couglin and coworkers [80] reported a synthetic protocol for preparing well-defined POSS-PS hemi-telechelic hybrids through anionic living polymerization. These model systems provided the opportunity to experimentally probe the ordering or aggregation behavior of inorganic NPs within polymeric matrices. Zheng et al. [81] employed a reversible addition-fragmentation transfer (RAFT) agent to prepare by AM-POSS. The POSS-containing RAFT agent was successively applied to the RAFT polymerization of styrene, producing the organic/inorganic hybrid homopolymer and block copolymers. The thermal properties of the hybrid PS derivatives were effectively enhanced by the presence of POSS molecules. Liu and coworkers [82] used a combination of atom transfer radical polymerization (ATRP) and click chemistry techniques to synthesize a quatrefoil-shaped star-cyclic PS derivative containing a POSS core, a new chain topology for nonlinearly shaped polymers. Ning et al. [83] reported PS/octa-phenethyl-POSS (OPE-POSS) nanocomposites prepared through simple solution blending, homogeneous transparent films were obtained at POSS contents from 0 to 40 wt% POSS as a result of interactions between the phenyl groups of POSS and PS. Rotello and coworkers [84] reported that multiple hydrogen bonding interactions in a between the PS and POSS using a random thymine PS copolymer (Fig. 17) increased the thermal stability through POSS-POSS crystalline packing. Couglin and coworkers [85] developed a synthetic route for preparing syndiotactic PS (sPS)/POSS copolymers. Copolymerizations of styrene and POSS afforded a novel nanocomposite of sPS and POSS [86]. The rate of copolymerization was much slower than that of radical polymerization, presumably because of a coordination polymerization mechanism.

Our group has used free radical polymerization to synthesize a series of poly(acetoxystyrene-co-isobutylstyryl-POSS) (PAS-POSS) hybrid systems [87,88]. At lower POSS contents, the POSS moieties mainly played a diluent role by reducing the degree of PAS self-interaction. At higher POSS contents in these hybrids, interactions between the siloxane units of the POSS moieties and the dipolar carbonyl groups of the PAS became dominant, resulting in of T_g . In addition, nanoscale physical aggregation of POSS was also partially responsible for these effects. Xu and coworkers [89,90] reported a series of network formed from PAS (or PS)/OV-POSS hybrid nanocomposites that had been prepared through free radical polymerization. Similar PAS networks were also formed from linear pendent POSS in a PAS matrix [87,88].

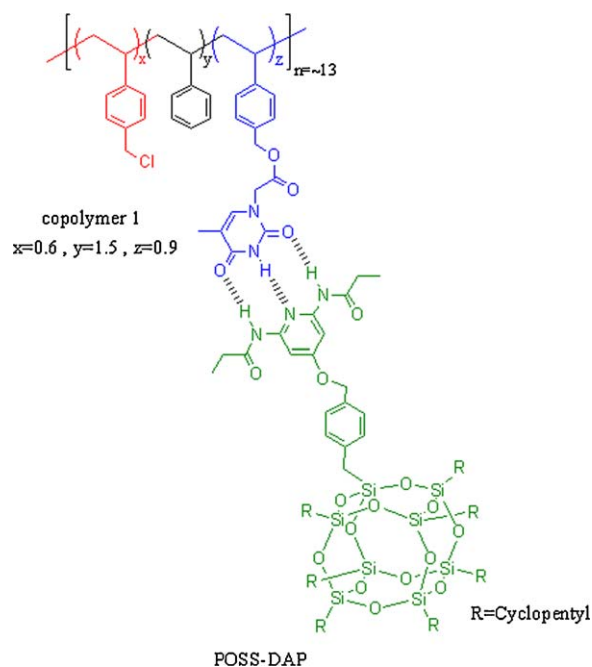


Fig. 17. The multiple hydrogen bonding interaction between POSS-DAP and PS random copolymers.

4.3. Poly(acrylate)/POSS copolymers

Poly(methyl methacrylate) (PMMA) is a transparent polymeric material possessing many desirable properties including light weight, high light transmittance, chemical resistance, colorlessness, resistance to weathering corrosion, and good insulating properties [91–94]. Methacrylate-substituted POSS macromers can be prepared containing one polymerizable functional group (Fig. 18) [95–100]. The resultant materials are generally transparent and brittle because the incorporation of the POSS group into linear polymers tends to prevent or reduce the segmental segregation or mobility. In general, glass transition and decomposition temperatures increase upon increasing the POSS contents. Kopesky et al. [96] reported PMMA containing both tethered and untethered POSS units, the presence of tethered-POSS in the entangled copolymers decreased the plateau modulus relative to that of the pure PMMA homopolymer. The untethered-POSS units induced a significant increase in the zero-shear viscosity due to the associations between the POSS moieties. Chen and coworkers [101] used living metallocene polymerization to prepare an interesting stereoregular methacrylate-POSS hybrid polymer possessing a high value of T_m (ca. 213 °C). Laine and coworkers [102] used the “core-first” method and ATRP to synthesize a star PMMA from an octafunctional silsesquioxane cube. PMMA polymers featuring chain-end-tethered POSS moieties have been widely reported [103–107]. For example, Fukuda and coworkers [103,104] used an incompletely condensed POSS derivative possessing a highly reactive trisodium silanolate group to synthesize several initiators for ATRP, thereby obtaining tadpole-shaped polymeric hybrids with a POSS unit

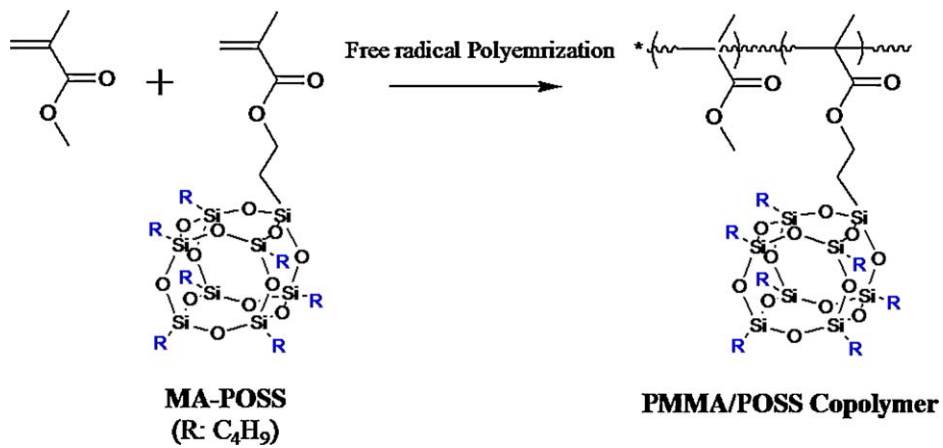


Fig. 18. Synthesis of PMMA–POSS copolymers.

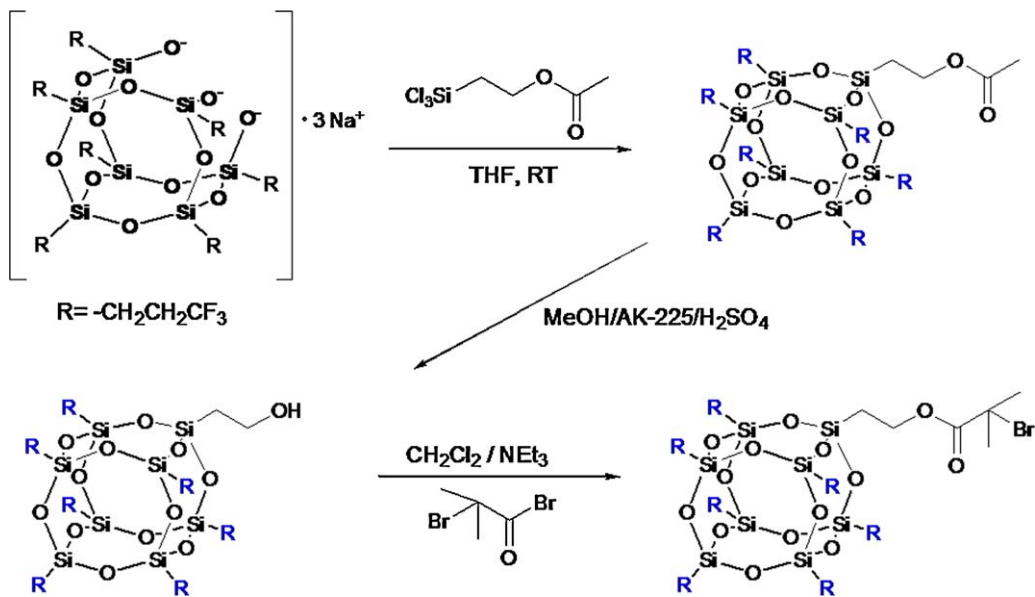


Fig. 19. Synthesis of fluorinated POSS initiator for ATRP.

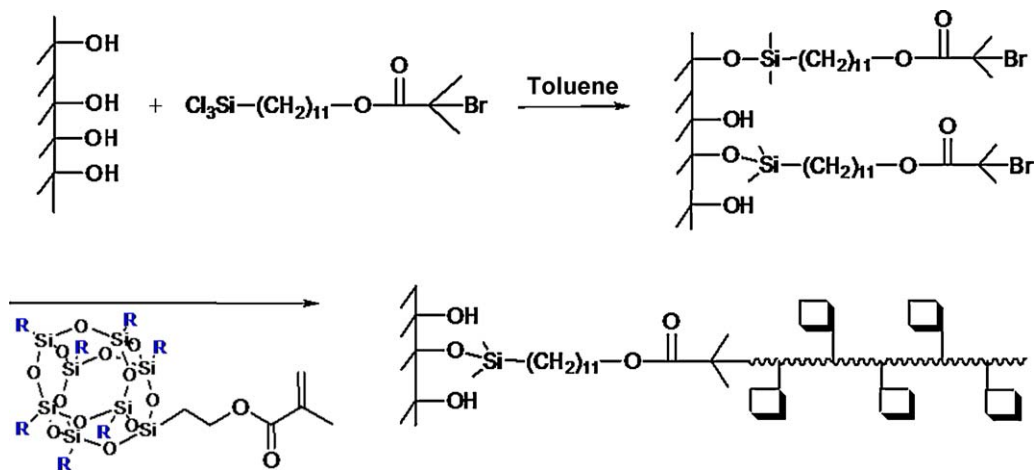


Fig. 20. Surface-initiated ATRP of MAiBu-POSS monomer to form poly(MAiBu-POSS) on Si wafer.

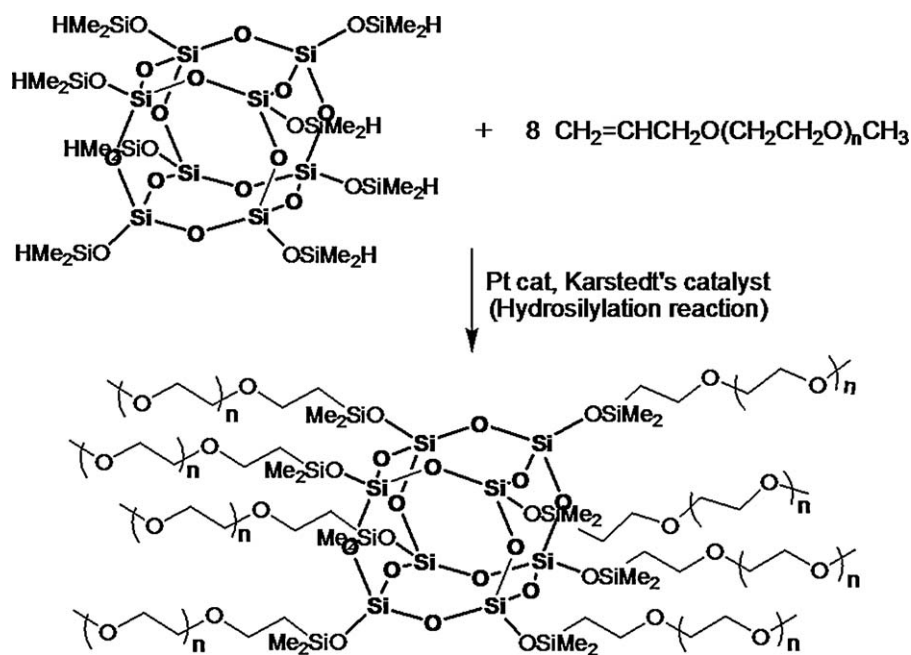


Fig. 21. Reaction scheme to prepare PEO-octafunctionalized silsesquioxanes.

at the end of the polymer chain (Fig. 19). Our group has used ATRP to synthesize PMMA hybrids having controllable molecular weights with a chain-end-tethered POSS moiety [105]. Similar structures have been reported by Kotal et al. [106] (thiol-mediated radical polymerization) and Liu et al. [107] (ATRP polymerization). Blending both PMMA-POSS and PMMA with phenolic resin revealed that the POSS terminus affected the thermal properties, miscibility behavior, and hydrogen bonding interactions [105]. Further investigation of specific association between the terminal siloxane units of the POSS moieties and the OH groups of the phenolic revealed an interesting screening effect [31] in these phenolic and low-molecular-weight PMMA-POSS blends (for PMMA molecular weight below its entanglement value) [105] that tends to significantly decrease the hydrogen bond formation of the hydroxyl-carbonyl inter-association. Chen et al. [108] reported the polymerization of a methacrylo isobutyl-POSS (MAiBu-POSS) monomer from a self-assembled monolayer of ATRP initiators covalently immobilized on Si wafers (Fig. 20). This simple and effective approach allows the preparation of well-defined POSS-containing polymer films from flat surfaces.

Network structures featuring pendent POSS groups have been synthesized using free radical polymerization [109–118]. The presence of POSS units in these systems did not increase T_g or improve the mechanical properties, it actually caused decreases in T_g and elastic moduli in both glassy and rubbery states. For example, Galy and coworkers [98] reported a dimethacrylate-based network with a multifunctional methacrylate-POSS (OMA-POSS) that exhibited improved miscibility with the dimethacrylate monomer and better dispersion in the network structure than did the corresponding monofunctional methacrylate-POSS. The rubbery modulus increased upon increasing the

POSS contents, but the T_g remained constant. Yang and coworkers [112] used free radical polymerization or solution blending to prepare a series of network hybrids of PMMA with OV-POSS. The increase in T_g strongly correlated with the degree of dipole–dipole interaction between the carbonyl groups of PMMA and POSS. The thermal stability was enhanced upon increasing the POSS content, mainly due to the uniform dispersion of the nanoscale inorganic POSS at the molecular level.

4.4. Poly(ethylene oxide)/POSS nanocomposites

Poly(ethylene oxide) (PEO) is used as an important polymeric electrolyte in lithium ion batteries because of its ability to solvate lithium ions [119–121]. One approach to increase the room temperature (RT) conductivity of PEO-based polymer electrolytes is to attach short-chain PEO (i) oligomers as side chains to form “comb-shaped” or “hairy rod”-like polymeric structures, or (ii) as “arms” from inorganic scaffolds. The grafting of oligomeric PEO chains onto $Q_8M_8^H$ to produce PEO-functionalized silsesquioxanes has been widely reported (Fig. 21) [122–128]. The grafting of PEO onto POSS results in a chain-length-dependent increase in T_g and suppression of crystallization because these dendrimers or star polymers feature high ratio of chain ends. In addition, PEO grafted with POSS have a lower melt viscosity and greater free volume than those of the linear PEO polymers having a similar molecular weight. Since these PEO-POSS hybrids do not crystallize and have relatively lower T_g than the corresponding PEO chains, they have potential to be used as low temperature solvents in lithium ion batteries. Wunder and coworkers [125] reported a strong self-supporting film prepared from 10% methyl cellulose and 90% PEO-POSS/ $LiClO_4$ that possessed an RT conductivity of 10^{-5} S/cm [125,126];

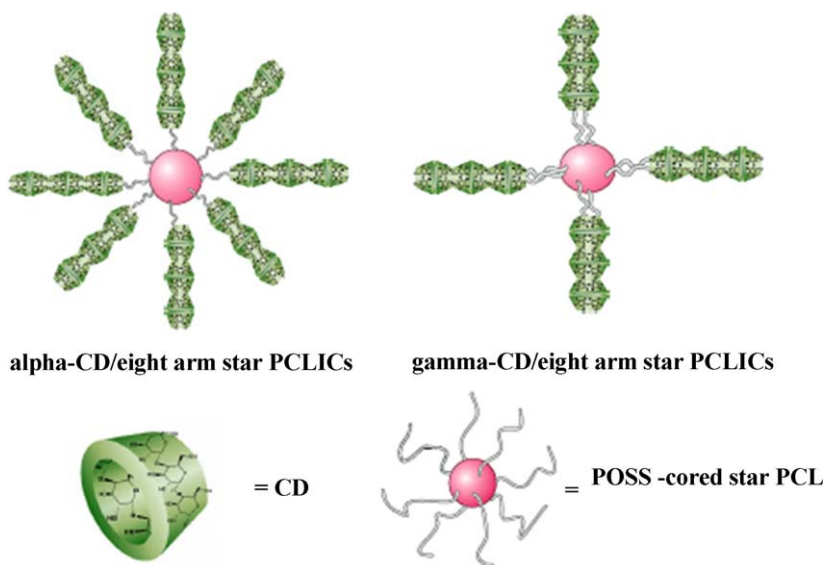


Fig. 22. Proposed structures of the α -CD/eight-arm star PCL ICs (left) and the γ -CD/eight-arm star PCL ICs (right).

higher conductivity of 10^{-4} S/cm was obtained from a PEO-POSS/LiN(CF₃CF₂SO₂)₂ hybrid.

Huang et al. [124] reported that similar to the linear PEO homopolymer, the star PEO formed inclusion complexes (ICs) with α - and γ -cyclodextrin (CD), but not with β -CD. CDs are among the most popular host molecules employed to construct molecular assemblies; they are cyclic oligosaccharides comprising six (α), seven (β), or eight (γ) glucose units linked through 1,4- α -glucosidic bonds [129,130]. A channel-type structure was found in the ICs, but the segments of PEO arms near the POSS cores were not covered by CD units [123]. Zheng et al. [131] reported an IC formed from N₃-POSS and a dialkene-terminated PEO with CD units. TGA analyses showed that the organic/inorganic hybrid polyrotaxanes exhibited enhanced thermal stability relative to that of polysulfurrotaxane. They also reported an interpenetrating polymer network (IPN) prepared via in situ crosslinking between OG-POSS and bisphenol A in the presence of PEO. FTIR spectroscopic analysis showed the presence of hydrogen bonding between the hydroxyl group of POSS and the ether groups of PEO. TGA revealed that the thermal stability of the INPs was dependent on the mass ratios of the POSS network to PEO [132].

Our group has investigated the effects of three different octuply functionalized POSS derivatives (OS-POSS, OA-POSS and OP-POSS) in PEO matrix nanocomposites [133]. The intermolecular interactions between these POSS derivatives and the PEO segments have a great effect on the thermal properties and miscibility behavior of their respective blends. The strongest hydrogen bonding interaction occurred between OP-POSS and PEO, as a result, its blend displayed superior thermal properties. The addition of an amorphous hydrogen-bonding POSS nanoparticle into PEO tends to depress the rates of crystallization and spherulite growth, the OP-POSS/PEO showed greater influence than OA-POSS/PEO, consistent with the relative intermolecular hydrogen bonding strengths.

Well-defined amphiphilic telechelic polymers incorporating POSS have been synthesized through direct urethane linkage between the OH end groups of a poly(ethylene glycol) (PEG) homopolymer and the monoisocyanate groups of a POSS macromer [134–136]. These amphiphilic telechelics exhibited a relatively narrow and unimodal molecular weight distribution ($M_w/M_n < 1.1$), with close to 2.0 end groups per PEG chain [134]. The crystallinity of the PEO segments in the amphiphilic telechelics decreased dramatically upon increasing the POSS content to 40.7%, becoming amorphous at values beyond ca. 50%.

4.5. Polyester/POSS nanocomposites

4.5.1. PCL/POSS nanocomposites

Our group has synthesized a series of the organic/inorganic hybrid star PCLs through coordinated ring-opening polymerization of ϵ -caprolactone using octakis(3-hydroxypropyl)dimethylsilyl-POSS (OH-POSS) as the initiator [137]. Similar to the linear PCL analogues reported previously, these star PCLs formed ICs with α - and γ -CD, but not with β -CD [137]. The stoichiometries of all of the ICs with α - and γ -CD were greater than those of the corresponding CD/linear PCL ICs because of steric hindrance around the bulky POSS core (i.e., some of the ϵ -caprolactone units near the core were unable to form ICs; Fig. 22) [137]. Another possible structure for the γ -CD/star PCL ICs would have two PCL chains simultaneously included within a single γ -CD channel. The inclusion of arms from two different star PCLs within the same γ -CD might occur as a result of unequal splaying of each arm of the star polymer. As a result, a gel-like physically crosslinked structure was formed. Zheng and coworkers [138] reported another approach for the preparation of octakis(3-hydroxypropyl)-POSS using an octafunctional initiator for the synthesis of eight-armed star-shaped PCLs. Organic/inorganic star PCLs possessing various

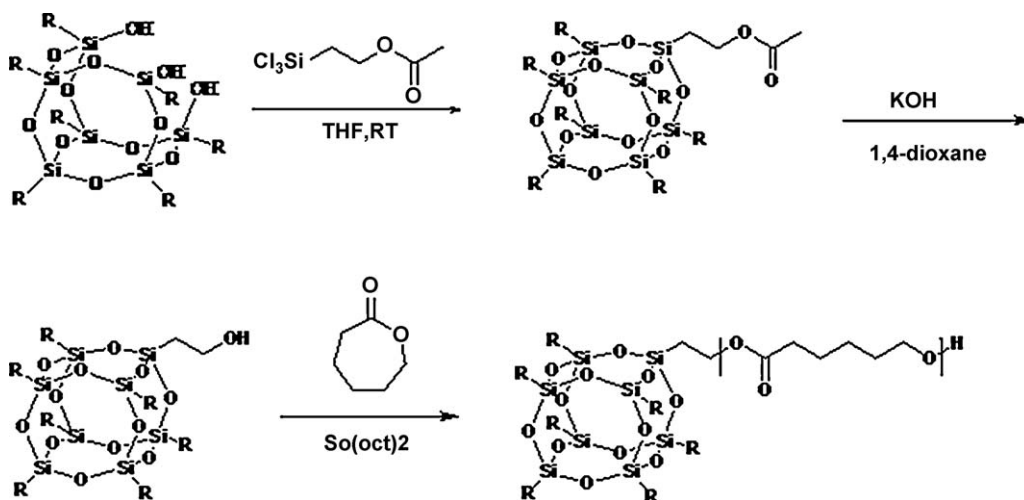


Fig. 23. Synthesis of the mono-POSS-end-capped PCL.

degrees of polymerization have been synthesized through ring opening polymerization catalyzed by stannous(II) octanoate [$\text{Sn}(\text{Oct})_2$] [138].

Our group has prepared a mono-POSS-end-capped PCL through ring-opening polymerization from hydroxyethylisobutyl-POSS (mono-OH-POSS; Fig. 23) [139]. Similar chemical structures have been prepared by other researchers using the ring-opening polymerization of caprolactone monomer [140–142]. From a study of the melting and crystallization behavior of POSS-end-capped PCL, Zheng and coworker [140] found enhanced equilibrium melting temperatures relative to that of the pure linear PCL. Both the overall crystallization and spherulitic growth rates of the POSS-end-capped PCL increased with the increase of POSS contents.

Our group has also reported that mono-POSS-end-capped PCL can form ICs with α - and γ -CDs, but not with β -CD. The PCL chain becomes included within the channel provided by the CDs to form a columnar crystalline structure [139]. A similar result was reported by Zheng and coworker [143], who found that the POSS-terminated PCL forms a channel-type crystalline structure with α -CD [143]. In addition, this POSS end-capped PCL, prepared through in situ polymerization with epoxy monomer, can obtain organic–inorganic hybrid nanocomposites after thermal curing [144].

Lee et al. [142] reported the preparation of double networks featuring the superposition of a covalent network with a physical network derived from a well-defined crystalline phase of strongly hydrophobic POSS moieties. Each covalent network chain features PCL or PLGA tethers on a single POSS moiety as a difunctional initiator for PCL or PLGA ring-opening polymerization. Inoue and coworkers [145] reported a PCL doubly end-capped with fullerene and POSS units. The aggregation of the fullerene moieties had much larger confinement effect on the crystallization of PCL than that of POSS. The successful incorporation of two nanosized objects into a PCL matrix may result in systems that display multi-functional properties [145].

4.5.2. Other polyester/POSS nanocomposites

Hana et al. [146] prepared bacterial poly(3-hydroxyalkanoate-co-3-hydroxyalkenoate), (PHAE)/POSS nanocomposites through free radical addition reactions of mercaptopropyl-isobutyl-POSS (SH-POSS) to the side-chain double bonds of the polymer. The appearance of the POSS-based PHAE changed from non-sticky and elastic to brittle and glass-like upon increasing the POSS contents; this system has potential application because it can be classified as non-toxic and suitable for food contact. In addition, PC/OPE-POSS nanocomposites have been produced through melting or solution blending [147–149]. Since PC/POSS nanocomposites can be classified as polymer chains containing non-bonded POSS moieties, the substituent groups of the POSS units play an important role determining the miscibility of PC and POSS. Yoon et al. [150] prepared the PET/POSS nanocomposites through melt blending and in situ polymerization method. PET/POSS composites prepared through melting blending with small amounts of POSS resulted in phase separation and poor mechanical properties. To obtain a homogeneous phase of the blend, they employed in situ polymerization using the reaction between the epoxy groups of a triepoxy-POSS derivative and the hydroxyl end groups of PET and resulted in improved bulk mechanical properties when compared with pure PET [150]. Zhou et al. [151] used a similar method to prepare PBT/POSS nanocomposite through reactions between the epoxy groups of POSS (octakis(epoxycyclohexyldimethylsilyl)-POSS, OEC-POSS) and the hydroxyl groups of PBT within a twin-screw extruder. The melt flow index of PBT decreased, while the elongation at break and tensile strength increased, after the addition of OEC-POSS. Kim et al. [152] used in situ polymerization to prepare poly(trimethylene terephthalate) (PTT)/POSS nanocomposites by incorporating 1,2-propanediolisobutyl-POSS (PDIB-POSS) with PTT monomer (dimethyl terephthalate (DMT) and 1,3-propanediol (PDO)). Increasing the POSS content caused the resultant PTT blends to exhibit decreased glass transition, cold crystallization and melting temperatures.

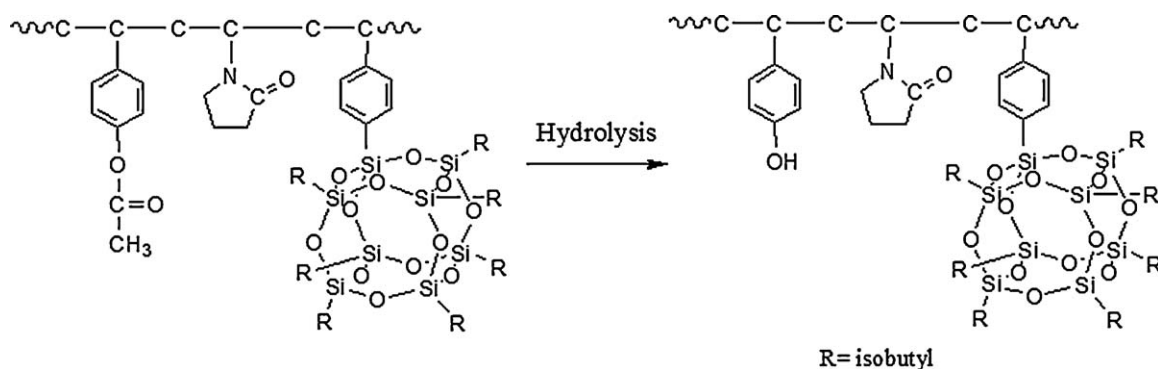


Fig. 24. The chemical structure of PVPh-co-PVP-co-POSS.

In addition, the initial modulus, breaking strength, and elongation at break all decreased upon increasing the POSS content.

4.6. Polyamide/POSS nanocomposites

4.6.1. Nylon/POSS nanocomposites

Ricco and coworkers [153,154] prepared polyamide 6/POSS nanocomposites through two different in situ polymerization mechanisms (hydrolytic and anionic) from 3-caprolactam (CL) in presence of AM-POSS. These Nylon 6/POSS nanocomposites featured a modified version of the polymeric crystal structure of Nylon 6, exhibiting decreases in their crystallinity and T_g . In addition, the octaepoxycyclohexyldimethylsilyl-POSS (OEC-POSS) has been used as a reactive compatibilizer in PPO/PA6 blends via melt-mixing [155]. The morphology of the composites transformed from a droplet/matrix to a co-continuous morphology upon increasing the OEC-POSS content from 2 to 4 phr. The PPO/PA6/POSS composites with a co-continuous morphology had better mechanical properties than those having the droplet/matrix morphology. Yu et al. [156] prepared Nylon 1010/POSS composites through melt blending with OV-POSS and OEC-POSS; these Nylon 1010/POSS composites exhibited higher decomposition temperatures and char yields. Wan et al. [157] prepared polyamide 12 (PA12)/POSS composites through melt blending and found that the presence of trisilanophenyl-POSS did not affect the crystalline structure of PA12, but it did enhance its tensile strength and thermal stability.

4.6.2. PNIPAM/POSS nanocomposites

Poly(*N*-isopropyl acrylamide) (PNIPAM) undergoes a sharp coil-globule transition in water at 32 °C, changing from a hydrophilic state below this temperature to a hydrophobic state above it [158–160]. The lower critical solution temperature (LCST) corresponds to the region in the phase diagram where the enthalpic contribution of water hydrogen-bonded to the polymer chain is less than the entropic gain of the system as a whole, it is largely dependent on the hydrogen-bonding capabilities of the constituent monomer units. Zheng and coworkers [161] reported that PNIPAM/POSS nanocomposites prepared through the chemical reaction between the N–H group of PNIPAM and the epoxy group of octa(propylglycidyl ether)-

POSS swelled in water and exhibited the characteristics of hydrogels. These POSS-containing hybrid hydrogels showed substantially faster swelling, de-swelling and re-swelling response rates than a control organic gel featuring a comparable degree of crosslinking. They also incorporated the POSS-end-capped PEO into the cross-linked PNIPAM to form a physically interpenetrating polymer network structure [162]. Acrylic-POSS, NIPAM monomer and *N,N*-methylenebisacrylamide have been used to prepare POSS-containing PNIPAM cross-linked networks [163]. These nanocomposite hydrogels displayed significantly faster response rates than those of the pure PNIPAM hydrogel in terms of swelling, de-swelling, and re-swelling. Zhang et al. [164] used the POSS-containing RAFT agent in the RAFT polymerization of NIPAM to form a POSS-end-capped PNIPAM hybrid, which assembled into well-defined core/shell nanostructured micelles in solvents, with the average diameter of the micelles increasing upon increasing the molecular weight of PNIPAM.

4.6.3. PVP/POSS nanocomposites

Eshel et al. [165] reported that the presence of small amounts of POSS within PVP hydrogels enhanced the storage modulus and the swelling ability relative to those for the pure PVP hydrogels. Due to its large surface area, only relatively small amounts of POSS was needed to cause significant changes. Our group prepared PVP/POSS nanocomposites with isobutyl-POSS (pendant type) through one-step free radical copolymerization. T_g of the PVP/POSS hybrid was influenced by three main factors: (1) the diluent role of the POSS units to reduce the self-association of the PVP; (2) strong interactions between the POSS siloxane and the PVP carbonyl groups; and (3) physical aggregation of the nanosized POSS units [166]. At a relatively low POSS content, the role as a diluent dominated and resulted in decreasing T_g . At a relatively high POSS content, the latter two factors dominated and resulted in increasing T_g for the PVP/POSS hybrid. Xu and coworkers [167] studied PVP/POSS networks containing OV-POSS with the POSS units in a junction structure, the change in T_g was primarily due to the effect of the crosslinking structure. Furthermore, a series of poly(vinylphenol-co-vinylpyrrolidone-co-isobutylstyryl-POSS) (PVPh-co-PVP-co-POSS) hybrid polymers incorporating various POSS contents have

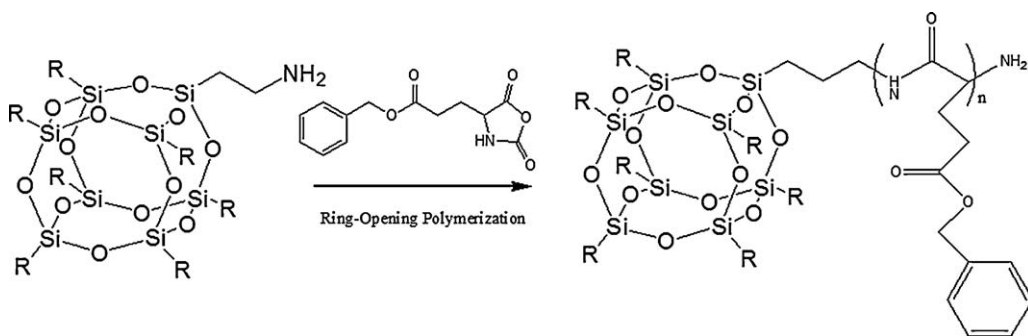


Fig. 25. Synthesis of POSS end-capped-PBLG copolymers.

been prepared through free radical copolymerization of acetoxystyrene, vinylpyrrolidone, and POSS, followed by selective removal of the acetyl protecting group (Fig. 24) [168,169]. The T_g of the PVPh-PVP-POSS hybrid increased substantially upon incorporating the POSS moieties [169]. The presence of the physically crosslinked (hydrogen bonded) POSS units in these hybrid polymers restricted the polymer chain motion, resulting in extremely high T_g . We also discussed the miscibility behavior and interaction mechanism of poly(methyl methacrylate-co-vinylpyrrolidone) (PMMA-co-PVP) with OP-POSS [170–172]. The VP units in PMMA acted as physical crosslinking points to increase the T_g of the PMMA-co-PVP copolymer; each of their DSC traces featured only a single glass transition temperature. Moreover, intermolecular hydrogen bonding became stronger than intramolecular hydrogen bonding after copolymerization with the VP, because the hydroxyl group preferred to interact with the VP segments. Furthermore, the presence of OP-POSS units in LiClO₄/OP-POSS/MMA61 ternary blends leads to enhance the ionic conductivity [171,172].

4.6.4. Other polyamide/POSS nanocomposites

Liu et al. [173] prepared POSS-tethered aromatic polyamide nanocomposites through Michael addition between maleimide-containing polyamides and AM-POSS. These polyamide-POSS nanocomposites showed good homogeneity and higher storage and Young's modulus, but slightly decreased their T_g s and significantly lowered dielectric constants. Through the reaction between NCO-POSS and NH₂-PAMAM, Dvornic et al. [174] prepared a core/shell system featuring a PAMAM dendrimer core and a POSS shell. Hybrid star-shaped polyoxazolines (POZ) with POSS cores have been prepared through ring-opening polymerization of 2-methyl-2-oxazoline using various octafunctional POSS derivatives as initiators [175,176]. The core-first method, using an active multifunctional core to initiate growth of polymer chains, allowed the synthesis of hybrid POSS-core star-shaped POZ. The thermal stability of this star shaped POZ/POSS nanocomposite was greater than that of the corresponding pure linear POZ. They also reported the preparation of POSS-end-capped POZ nanocomposites by ring-opening polymerization of 2-methyl-2-oxazoline initiated by a functionalized POSS derivative.

Similar to polyamide chains, the peptide chains possess distinct secondary structures that influence the well-defined tertiary structures of proteins. Poly(γ -benzyl-L-glutamate) (PBLG) is a synthetic polypeptide that forms α -helix and β -sheet secondary structures that are stabilized through intramolecular and intermolecular hydrogen bonds, respectively [177]. The α -helical form of PBLG exists as a rigid-rod structure in the solid state and in solution, providing PBLG with its unique bulk and solution properties, including thermotropic liquid crystalline ordering and thermo-reversible gelation [178–180]. POSS-PBLG helical polypeptide copolymers are macromolecular self-assembling building blocks that have been synthesized through ring-opening polymerization of γ -benzyl-L-glutamate N-carboxyanhydride (γ -Bn-Glu NCA) using AM-POSS as a macroinitiator (Fig. 25) [181].

The incorporation of POSS units at the chain ends of PBLG moieties has two important effects: (i) allowing intramolecular hydrogen bonding between the POSS and PBLG units to enhance the latter's α -helical conformations in the solid state and (ii) preventing the aggregation of nanoribbons through the POSS blocks' protrusion from the ribbons, leading to the formation of clear gels in solution. 2D IR correlation spectroscopy has been used to detect the presence of intramolecular hydrogen bonds between the POSS and PBLG units. Fig. 26(a) presents the synchronous 2D correlation map (from 800 to 2000 cm⁻¹) for the POSS-PBLG₁₈ sample; the bands at 1730, 1655, and 1550 cm⁻¹ correspond to the C=O, amide I, and amide II bands of the PBLG unit, respectively [181]. The band at 1087 cm⁻¹ represents Si-O-Si stretching of the POSS cage. These four absorptions exhibit many positive auto and cross peaks. A new auto-peak appeared at 1150 cm⁻¹ for the copolymer, indicating that hydrogen bonding occurred between the amide and carbonyl groups of the PBLG unit and the siloxane groups of the POSS moiety. In contrast, the corresponding asynchronous 2D correlation map (Fig. 26b) does not show any such auto or cross peaks over the same wavenumber range. Thus, the incorporation of a POSS moiety at the PBLG chain end leads to intramolecular hydrogen bonding between the POSS and PBLG units, such that the latter units form α -helices in the solid state.

Fig. 27(a) and (b) presents TEM images of fibrous structures formed from pure PBLG₅₃ and from the POSS-PBLG₅₆ copolymer. The turbid gel formed by the pure PBLG₅₃ featured a disordered and irregular fiber aggregation with

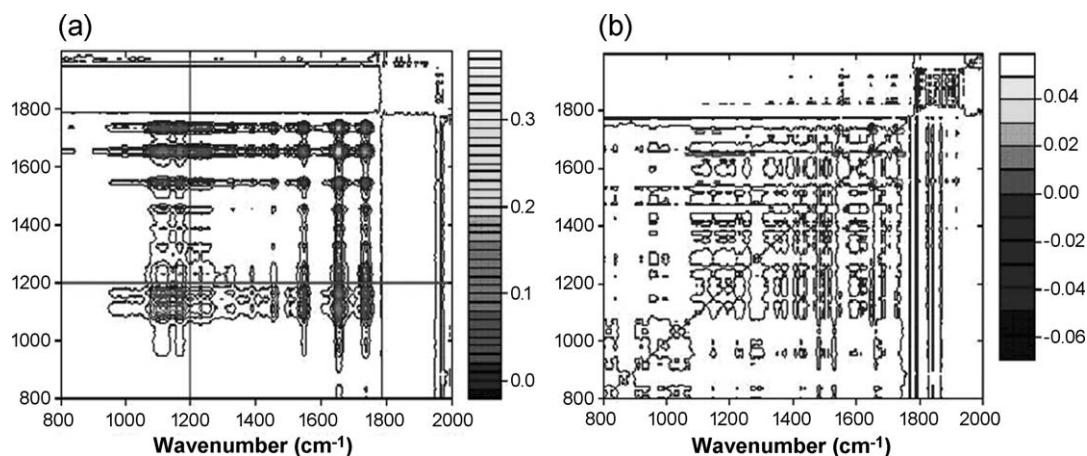


Fig. 26. 2D FTIR spectral (a) synchronous and (b) asynchronous maps of the POSS-*b*-PLBG₁₈ under temperature perturbation. Reprinted with permission from Ref. [181]. Copyright 2009, American Chemical Society, USA.

ranging from 500 to 1000 nm (Fig. 27(a)) [181]. Strong dipolar π - π interactions between the phenyl groups and PBLG rods stabilized the micro-fibers that were intertwined into an irregular 3D network structure. In contrast, the clear gels of the POSS-PBLG₅₆ copolymer featured bundles of ordered fibers, with the fiber units having a width of ca. 10 nm. AFM experiment revealed the fibers' lateral dimensions and height profile (Fig. 27(c)). In the AFM height

profile, these fiber units possessed an average height of ca. 2 nm and a lateral dimension of ca. 25 nm, implying that the fibrous structure were not cylindrical, but rather had a ribbon- or tape-like morphology formed by stacking of the POSS-PBLG copolymer chains, which contained PBLG helices (diameter: ca. 1.5 nm). SAXS measurements of the dried toluene gels of POSS-PBLG₅₆ suggested an individual fiber width of 11.8 nm, consistent with the TEM

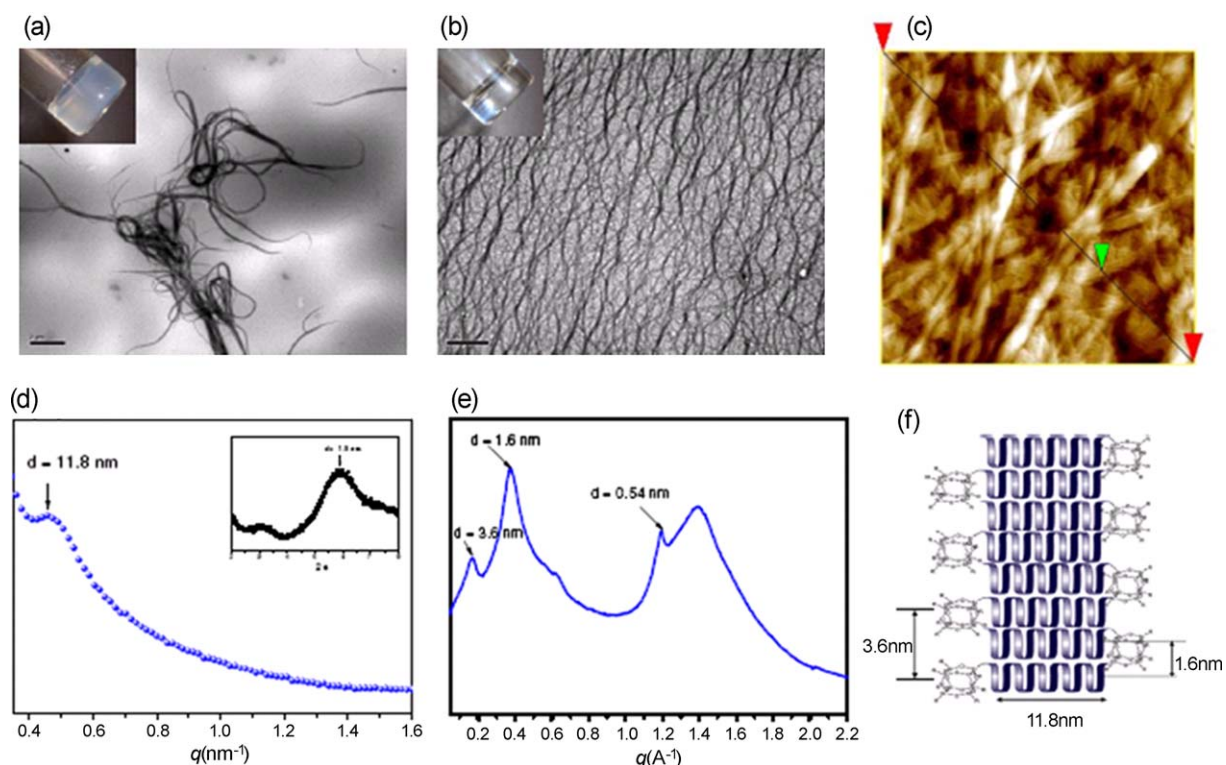


Fig. 27. TEM images of (a) pure PBLG₅₃ and (b) POSS-PBLG₅₆. (c) AFM height image and section analysis of POSS-PBLG₅₆ on a wafer substrate. (d) SAXS profile of POSS-PBLG₅₆. (e) WAXD profile of a dried POSS-PBLG₅₆ toluene gel at 0.2 wt%. (f) Schematic representation of a nanoribbon formed in the network structure of the toluene gel.

Reprinted with permission from Ref. [181]. Copyright 2009, American Chemical Society, USA.

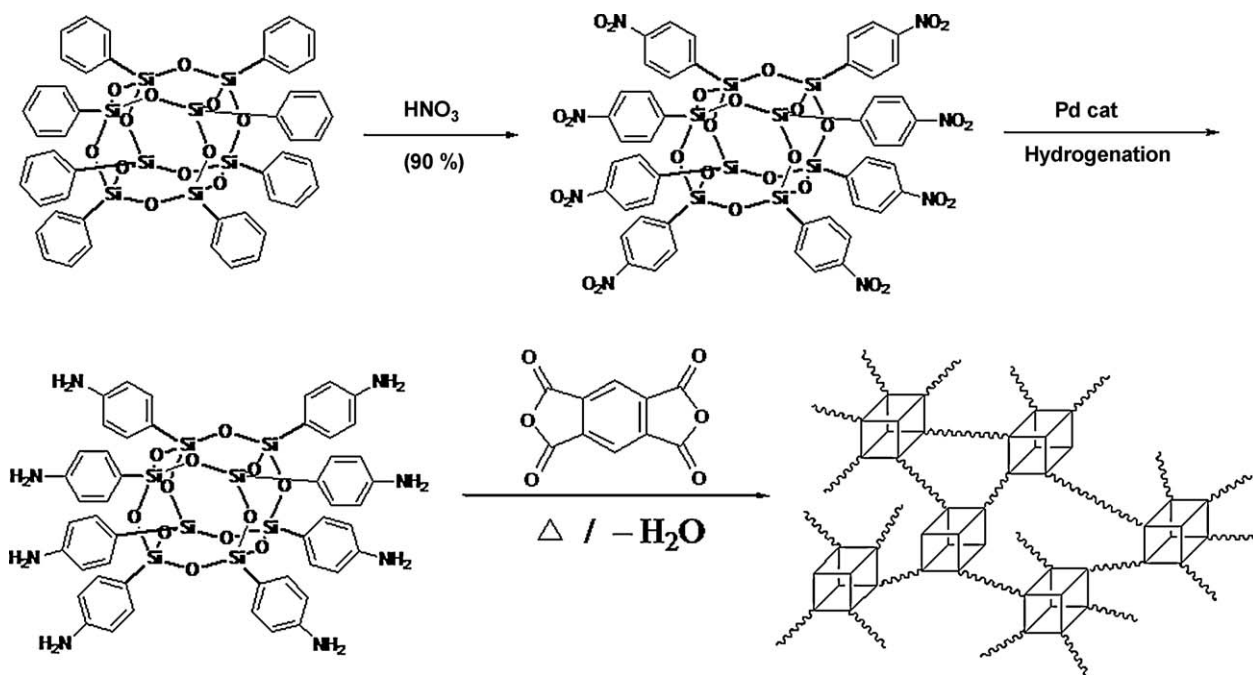


Fig. 28. The preparation of polyimide from octakis(aminophenyl)-POSS.

and AFM results. Observation of such a lateral dimension of the fiber through SAXS was not possible for the pure PBLG₅₃ gels because of the lack of order in their fibers. WAXD (Fig. 27(e)) profiles of the dried POSS–PBLG₅₆ gels showed three diffraction peaks at 3.6, 1.6 and 0.54 nm, corresponding to the distance between two neighboring POSS blocks, the distance between the α -helices of the PBLG units, and the pitch length of the α -helix, respectively. The POSS–PBLG copolymer can self-assemble in an anti-parallel manner to minimize steric hindrance between the POSS blocks, thereby forming an unfavorable orientation of the PBLG helical dipole moment in the nanoribbon structure (Fig. 27(f)) where the long axis of the PBLG helix is parallel to the plane of the ribbon. In an anti-parallel stacking mode, the distance between two neighboring POSS blocks is ca. 3.7 nm, a situation that cannot accommodate the bulky POSS units in the planar nanoribbon structures without changing the morphology. The POSS block protrudes outside of the ribbon due to high solubility in toluene, suppressing aggregation between the nanoribbons and forming clear gels.

4.7. Polyimide/POSS nanocomposites

Polyimides (PIs) are widely used in the microelectronics industry because of their excellent tensile strengths and modulus, good thermal stabilities and dielectric properties, and high resistance to organic solvents. Two routes are commonly employed to incorporate POSS units into a PI matrix. One method to achieve PI–POSS nanocomposites is to use a POSS derivative possessing eight functional groups (e.g., epoxy or amino groups) to serve as a cross-linking agent. Laine and coworkers [182] described the nitration of octa-phenyl POSS and subsequently produced

octakis(aminophenyl)-POSS (OAP-POSS) through Pd/C-catalyzed hydrogenation (Fig. 28). OAP-POSS was then employed in conjunction with dianhydrides to prepare extremely thermally resistant cross-linked PI networks [182]. He et al. [183] and our group [184] have both demonstrated that polyamic acid (PAA), a PI prepolymer, can react with OG-POSS (Fig. 29). Using these approaches, the dielectric constants of the PI nanocomposites can be reduced, and their thermal properties modified, upon increasing the POSS content. Excess 4,4'-oxydianiline diamine (ODA) was reacted initially with 4,4'-carbonyldipthalic anhydride (BTDA) and then the terminal amino groups of the PAA were reacted with OG-POSS. By varying the equivalent ratio of ODA and using PAAs of various molecular weights, nanocomposites possessing various morphologies have been obtained. The decrease in the dielectric constant of the PI–POSS hybrids results from nano-void volume of the POSS cores and from the free volume increase resulting from the presence of the rigid and large POSS units inducing a loose PI network [184]. He and coworkers [185] also reported the use of OH-POSS for the preparation of PI/POSS nanocomposites; high-performance low- k PI nanocomposites were obtained when PAA was cured with OH-POSS.

Our group has used a hybrid star PEO-POSS template to prepare nanoporous PI films (Fig. 21) [129]. These nanoporous foams were generated by blending PI as the major phase with a minor phase consisting of the thermally labile PEO-POSS NPs. During oxidative thermolysis, these labile PEO-POSS NPs released small molecules as byproducts diffusing out of the matrix, thereby leaving voids within the polymer matrix. Fig. 30 illustrates the storage modulus and $\tan \delta$ for pure and porous PIs containing 5 wt% PEO-POSS [129]. The pure PI has a modulus of ca. 2000 MPa at room temperature and a single T_g at 370 °C.

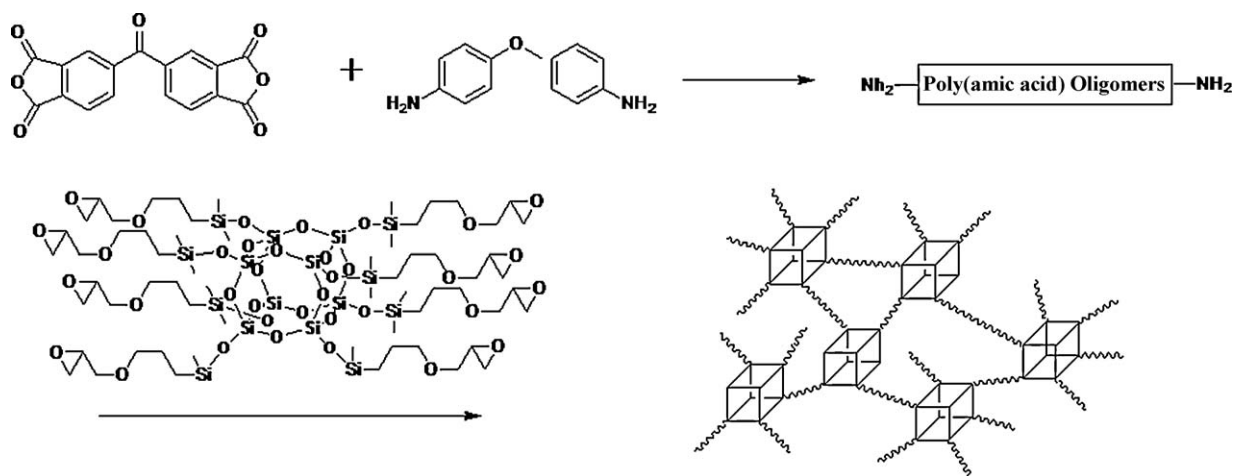


Fig. 29. The preparation of polyimide from OG-POSS.

In the case of the porous PI, two relaxations appear at ca. 360 and 385 °C, based on the $\tan \delta$ peaks. The relaxation at 360 °C is a typical microphase separation for a porous PI undergoing a sudden decrease in storage modulus. This transition (370 °C for the homopolymer) arose from the finite solubility of the PEO-POSS NPs in the matrix and from the microphase separation of the foams after curing. The overall modulus of the porous PI was lower than that of the pure PI due to its foam structure. At higher temperatures (>370 °C), these foams collapsed and the porous structure no longer existed. The higher value of T_g of the nanoporous system (385 °C, based on the maximum of the $\tan \delta$ peak) was probably due to the content of residual silica produced by PEO-POSS in the solid matrix. The resulting storage modulus and softening temperature decreased slightly with increasing content of nanofoam in the PI matrix. After post-curing, however, the foam structure collapsed and the storage modulus increased upon increasing the PEO-POSS content; in addition, the relaxation effect through the microphase separation of the nanofoams disappeared. The increased modulus in this nanocomposite may have arisen from (i) the SiO_2 particles derived from

the PEO-POSS being distributed evenly within the polymer matrix on the nanometer scale or (ii) the presence of physical bonds (e.g., hydrogen bonding) between the PI units and these rigid silica particles, hindering the mobility of the polymer chains and resulting in higher-than-expected values for the modulus and T_g . A significant reduction in dielectric constant (k , from 3.25 to 2.25) occurred for the porous PI hybrid films having pore sizes in the range from 10 to 40 nm.

The second common method for the preparation of PI/POSS derivatives featuring low dielectric constants and good thermal properties was accomplished by blending the PI precursor with a fluorinated POSS derivative (OF-POSS) [186,187]. The low polarizability of OF makes it compatible with PI matrices; therefore, it can improve the component dispersion and increase the free volume of the resulting composites, both of which are responsible for the observed lower dielectric constants of PI-OF nanocomposites. Yeh and coworkers [186] reported a high-performance and low- k PI nanocomposite from PAA cured with octakis(dimethylsilyloxyhexafluoro propylglycidyl ether)-POSS (OFG-POSS) [185,187]. This reactive POSS isomer has an average of four epoxy groups and four fluorine groups on the POSS cage; its epoxy group reacted with PAA to form a PI/POSS nanocomposite featuring a network framework (Fig. 31). The resulting PI/OFG-POSS nanocomposite had a high crosslinking density, high porosity, high hydrophobicity, and low polarizability.

A third method for the simultaneous and convenient production of high-performance PI with a low dielectric constant involves the introduction of an octa-acrylated POSS into a PI matrix to form PI semi-interpenetrating polymer network (semi-IPN) nanocomposites [186]. Analyses using DSC and FTIR spectroscopy revealed that the self-curing of methacrylated-POSS and the imidization of PAA occurred simultaneously. The semi-IPN structures of the [PI/POSS] nanocomposites featured aggregated POSS NPs (average size: ca. 50–60 nm) uniformly embedded within the matrix. At high POSS contents, the PI/POSS nanocomposites featuring interconnected POSS particles were highly crosslinked and, therefore, exhibited enhanced

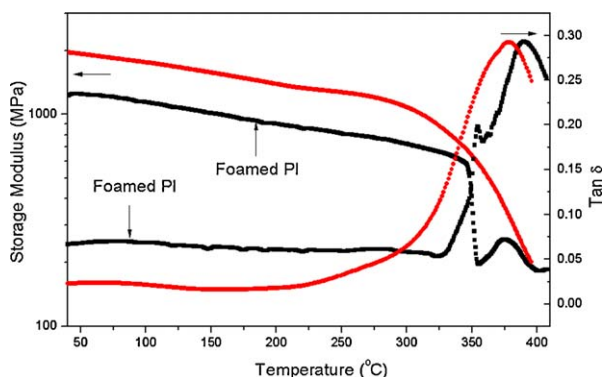


Fig. 30. DMA curves for the pure and porous polyimide (obtained from 10 wt% PEO-POSS) recorded at a heating rate of 2 °C/min. Reprinted with permission from Ref. [129]. Copyright 2005, Elsevier Science Ltd., UK.

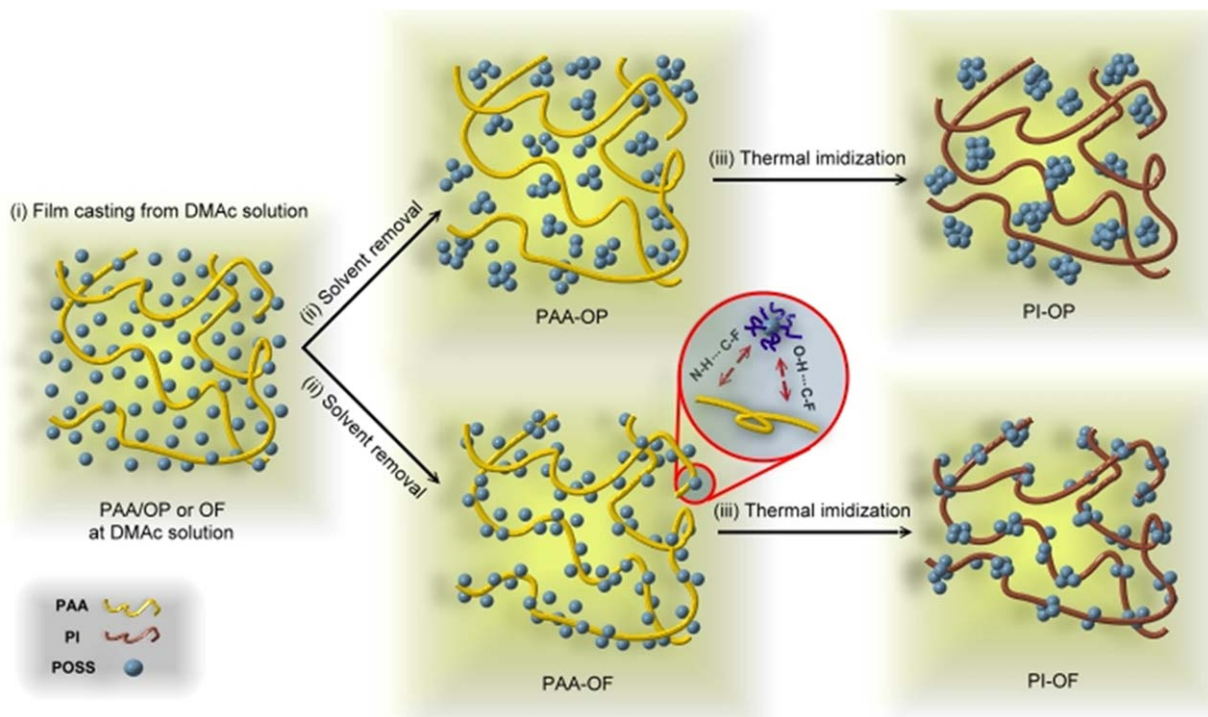


Fig. 31. Schematic draw of the deformation during the imidization process.

Reprinted with permission from Ref. [186]. Copyright 2008, Wiley-VCH, Germany.

glass transition temperatures. The high porosity of the PI/POSS nanocomposites resulting from the nanometer-scale porous structure of POSS markedly reduced the dielectric constant of PI. Similar methods have been employed by Chen and coworkers [188,189] to prepare the low dielectric-constant nanocomposites of PIs with grafted methacrylate side chains containing POSS units prepared through thermally initiated free-radical graft copolymerization of MA-POSS with ozone-preactivated PAA, followed by thermal imidization.

Wei and coworkers [190–192] reported the grafting of a POSS derivative to PI-tethered POSS nanocomposites possessing well-defined architectures. Relative to pure PI, these types of POSS nanocomposites have both lower and tunable dielectric constants, and controllable mechanical properties. The presence of these tethered POSS molecules in the amorphous PI resulted in a nanoporous crystalline structure and also in an additional ordered architecture through microphase separation. Using this approach, the dielectric constant of the film can be tuned by controlling the amount of added POSS [189,190]. Wright et al. [193] reported a series of end-capped and hydroxymethyl-functionalized PIs covalently attached to the AM-POSS polymer backbone; POSS loadings as high as 36 wt% could be obtained while maintaining excellent processability and optical clarity of resulting films. Seckin et al. [194] reported a similar method using octakis(aminopropyl)-POSS (OAM-POSS) for the molecular-level design of low dielectric-constant PI materials for use in the manufacture of integrated circuits. The presence of OAM-POSS units restricts chain rotation through multiple-point attachment

to the PI backbone, thereby creating additional free volume in the film to lower its dielectric constant. A process for synthesizing POSS-PI star nanocomposites has been reported [194] involving the formation of a porous-type POSS derivative and subsequent reaction with a PI precursor. Appropriate insertion of POSS units into a PI backbone can reduce its dielectric constant and also improve its mechanical and thermal properties. Wu and coworkers [195,196] reported a new method for preparing main chain PI-POSS hybrids from a double-decker shaped silsesquioxane diamine and various tetracarboxylic dianhydrides; these hybrids possessed good thermal stability, improved mechanical properties and low-dielectric constants.

4.8. Polyurethane/POSS nanocomposites

Hsiao and coworkers [197] prepared polyurethane (PU)/POSS nanocomposites through the reactions of POSS derivative featuring one corner group substituted by either a hydridomethylsiloxy group (hydrido-POSS) or a 3-(allylbisphenol-A) propyldimethylsiloxy groups (BPA-POSS). BPA-POSS compound is a diol used as a chain extender in PU synthesis. Turri and coworkers [198,199] synthesized a linear PU/POSS nanocomposite through a diol-functionalized POSS macromer; this nanocomposite exhibited significantly enhanced surface hydrophobicity and decreased surface energy relative to that of PU. These approaches have opened up new pathways for the development of high-performance nanostructured waterborne coatings. Mather and coworkers [200] prepared a PU system using an organic biodegradable PDLA soft block and an

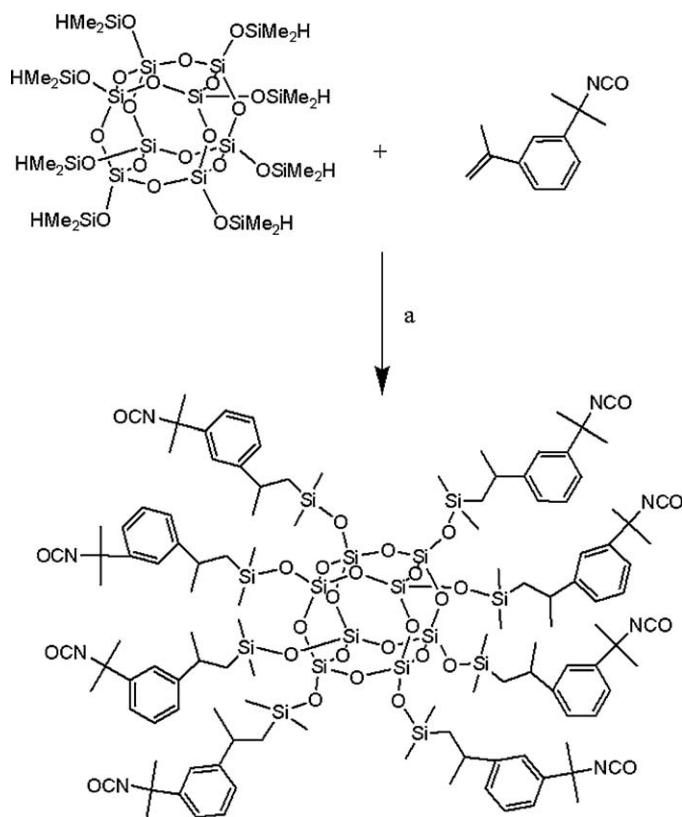


Fig. 32. Synthesis of TMI-POSS. Conditions: (a) THF, Karstedt's catalyst, reflux for 2 days.

inorganic diol-POSS hard block. Pieliowski and coworker [201] synthesized PU/POSS nanocomposites using MDI with polytetramethylene glycol, 1,4-butanediol, and diol-POSS; TGA revealed that the highest thermal stability occurred at POSS contents of 4 and 6 wt%. Neumann et al. [202] synthesized a POSS macromer with eight reactive isocyanate groups ((NCO)₈-POSS) through hydrosilylation of *m*-isopropenyl-*R,R*-dimethylbenzyl isocyanate (*m*-TMI) with Si-H bonds of Q₈M₈^H and resulted in quantitative yield only the α -addition product without any competing reaction of the isocyanate group (Fig. 32). This macromer has also been used to synthesize the first cross-linked PU featuring discrete POSS molecules dispersed within the polymer matrix [204]. He and coworkers [203] subjected the same (NCO)₈-POSS macromer to polyaddition reactions with (OH)₈-POSS; resulting hybrid films were relatively transparent. The incorporation of octafunctional POSS in PU films resulted in higher thermal stability and crosslink density. Nanda et al. [204] prepared aqueous PU dispersions with functionalized POSS through homogeneous solution polymerization. The use of acetone as the initial polymerization solvent allowed the facile incorporation of both diamine- and diol-functional POSS monomers. The storage modulus, glass transition temperature, complex viscosity, and surface hydrophobicity all increased upon increasing the POSS content, due to incorporation of the POSS moieties into the PU hard segment domains. They also discussed the viscoelastic behavior of PU-urea film prepared by varying the functionalized diamino-POSS contents and found

significant increases in the melt viscosity and zero shear viscosity resulted from the reaction between diamino-POSS and the hard segment of PU [205,206].

4.9. Phenolic/POSS nanocomposites

Our group has investigated phenolic/POSS nanocomposites, as described in Section 3, concerning the miscibility of phenolic resin with different functionalized POSS derivatives. Zhang et al. [207] also prepared a resole phenolic resin with trisilanophenyl-POSS nanocomposites through solution blending, where the thermal stability increased with the increase of POSS loading while the T_g of the nanocomposite was only slightly affected by the loading of POSS. Zhang et al. [208] used the OAP-POSS as a cross-linking agent for the phenolic resin because the OAP-POSS can form both covalent and hydrogen bonds with phenolic resin and POSS NPs. The storage modulus in both glassy and rubbery regions, the thermal stability and T_g of the POSS composites were improved in the presence of 1 wt% OAP-POSS. Zheng and coworkers [209] also used OG-POSS as a cross-linking agent for phenolic resin; T_g and thermal stability of the phenolic/POSS nanocomposites both increased upon increasing the POSS content. These phenolic/POSS nanocomposites also displayed significantly enhanced surface hydrophobicity as well as reduction in surface free energy which is consistent with our group's previous findings [40].

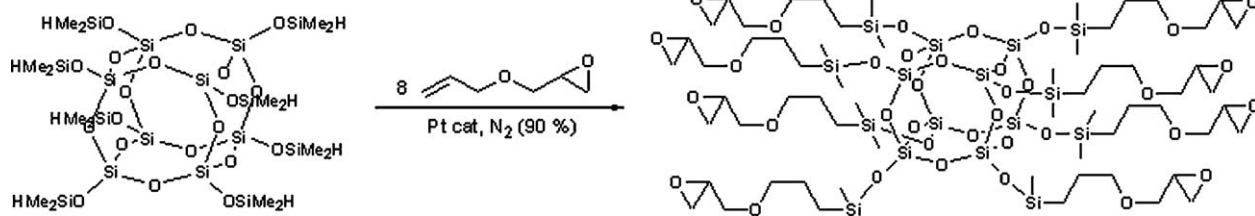


Fig. 33. The synthesis of OG-POSS.

4.10. Epoxy/POSS nanocomposites

Monofunctional POSS–epoxies have been incorporated into the backbones of epoxy resins to improve their thermal properties [210–217]. Multifunctional epoxy-substituted POSS monomers have been incorporated into an epoxy resin network composed of di- and tetra-functionalized epoxies. The presence of POSS units can increase the glass transition temperature of epoxy resin because the nanoscopic sizes and masses of the POSS cages enhance their ability to hinder the segmental motion of molecular chains and network junctions [218–239].

4.10.1. Multifunctional epoxy–POSS nanocomposites

Laine et al. prepared an epoxy–POSS macromer through the reaction of $Q_8M_8^H$ with 4 or 8 equiv of allyl glycidyl ether using Karstedt's catalyst [Pt(dvs)] (Fig. 33) [220]. The epoxy nanocomposites were prepared by reacting OG-POSS with 4,4'-diaminodiphenylmethane (DDM) at various compositional ratios.

DMA results and model reaction studies suggested that the maximum cross-linking density would be obtained

at an NH_2 -to-epoxy ratio (N) of 0.5, with the mechanical properties maximized at a value of N of 1.0 [219]. Mather and coworkers [220] reacted OG-POSS with 4,4'-diaminodiphenyl sulfone (DDS) to study the relationship between the thermal and rheological properties and the nanoscopic deformation property and, thereby, determine the toughening mechanism. DMA analysis showed that increasing the DDS concentration increased the storage modulus in both the glassy and rubbery states due to the increased crosslink density. The main toughening mechanism in the epoxy/POSS was void formation at nanoscale, possibly templated by limited POSS aggregation. He and coworkers [225] also reported the thermomechanical properties of OG-POSS modified epoxy resins. Lee et al. [226] reported the epoxy resin reacting with OG-POSS and DDM to form epoxy/POSS nanocomposites. DSC and DMA analyses showed that the T_g remained almost unchanged at POSS concentration (<30 wt%), whereas the nanocomposites containing POSS at greater than 40 wt% displayed values of T_g lower than that of the control epoxy. Xiao et al. [230] studied epoxy resin prepared from OG-POSS cured with 4,4-methylenebis(cyclohexylamine) and

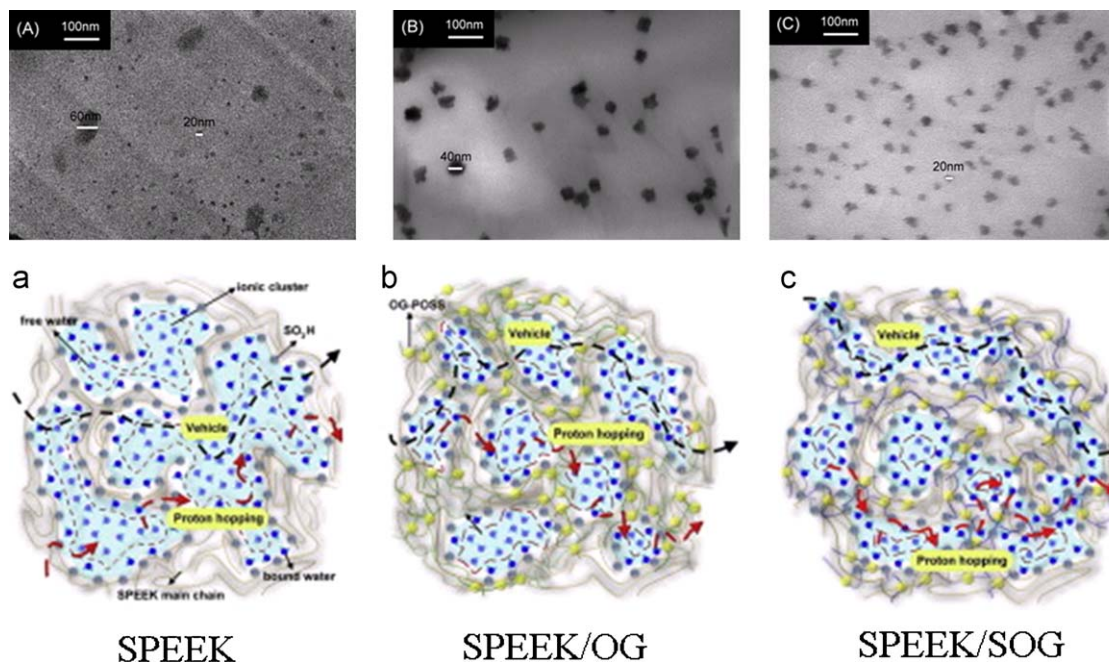


Fig. 34. TEM micrographs and proposed mechanisms of proton transfer within of the (a) sulfonated poly(ether ether ketone) (SPEEK), (b) SPEEK/OG10 (OG-POSS with 10 wt% ODA content), and (c) SPEEK/SOG10 (OG-POSS with 10 wt% ODADS) membranes.

Reprinted with permission from Ref. [243]. Copyright 2010, Elsevier Science Ltd., UK.

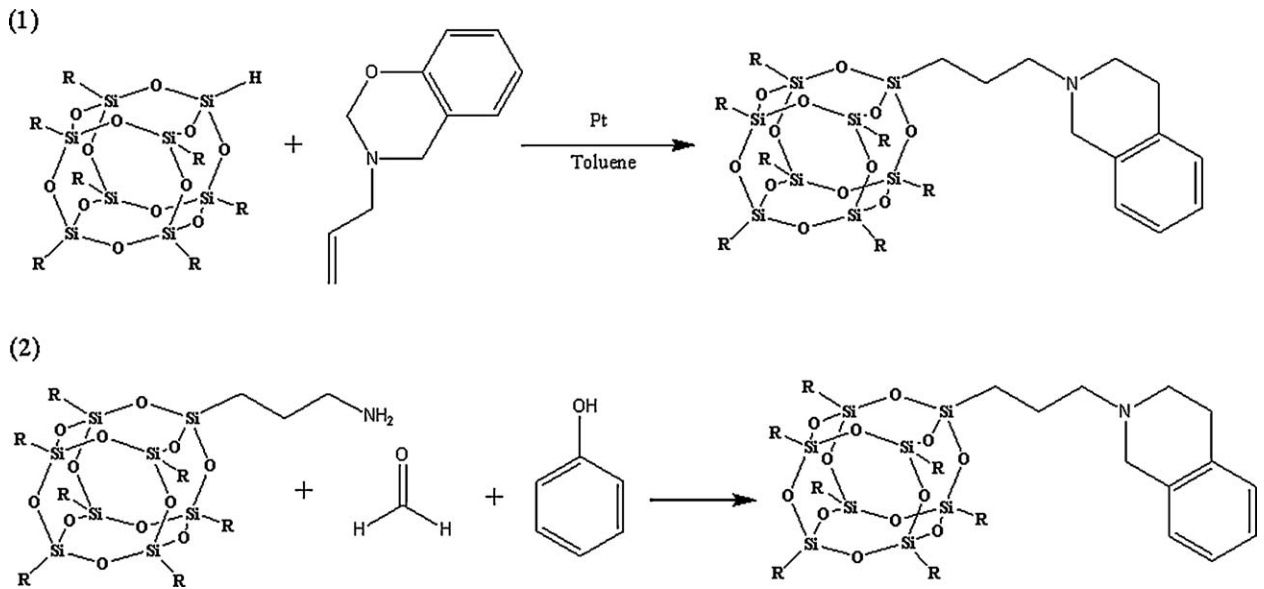


Fig. 35. The synthesis of benzoxazine-POSS through two different methods.

4-methylhexahydrophthalic anhydride to obtain highly crosslinked hybrid materials. FTIR spectroscopy revealed that the curing reactions of epoxy-POSS are more difficult than those of diglycidyl ether bisphenol A (DGEBA) resin because of steric hindrance. The resulting POSS composites did not exhibit glass transition behavior because of motion of the tethers between the POSS cores. Bian et al. [232] investigated the segmental dynamics in OG-POSS/poly(propylene oxide) nanocomposites. Pure poly(propylene oxide) exhibited two relaxation processes (normal and segmental modes). The OG-POSS undergoes a segmental process at lower frequency and a local relaxation at higher frequency. Teo et al. [233] prepared epoxy/POSS nanocomposites through copolymerization of OG-POSS, tetraglycidyl-4,4'-diaminodiphenyl methane (TGDDM), and hexahydrophthalic anhydride (HHPA). Kinetic studies revealed that the rate of curing of OG/HHPA was significantly higher than that for TGDDM/HHPA. By introducing 5 mol% OG-POSS into the networks, the hybrid underwent a large jump of 20 °C in its T_g and a slight improvement in T_d and storage modulus, compared with that of TGDDM/HHPA. Rico et al. [234] reported epoxy/OG-POSS nanocomposites in which OG-

POSS was used to partially replace the DGEBA resin while the curing agent was the aromatic diamine, 4,4-(1,3-phenylenediisopropylidene) bisaniline. They used three different methods, the differential of Kissinger, the integral of Flynn-Wall-Ozawa, and the phenomenological model of Kamal to obtain the kinetic parameters of the curing reaction. The presence of POSS accelerated the rate of opening of the glycidyl epoxy rings of DGEBA. The behavior of the mixture during the curing process could be explained in terms of an autocatalytic model, corrected for the contribution of the diffusion of the molecules during the course of the reaction. Our group has also reported a new nanomaterial based on OG-POSS and *meta*-phenylenediamine (mPDA) [240]. The activation energy in curing the OG-POSS/mPDA system was higher than that of the DGEBA/mPDA system, as determined using both the Kissinger and Flynn-Wall-Ozawa methods. In an isothermal kinetic study based on an autocatalytic system, the activation energy for the curing of OG-POSS/mPDA was also higher than that of the DGEBA/mPDA system [240]. The T_g of the cured OG-POSS/mPDA product was significantly higher than that of the DGEBA/mPDA material because the POSS cages effectively hindered the motion

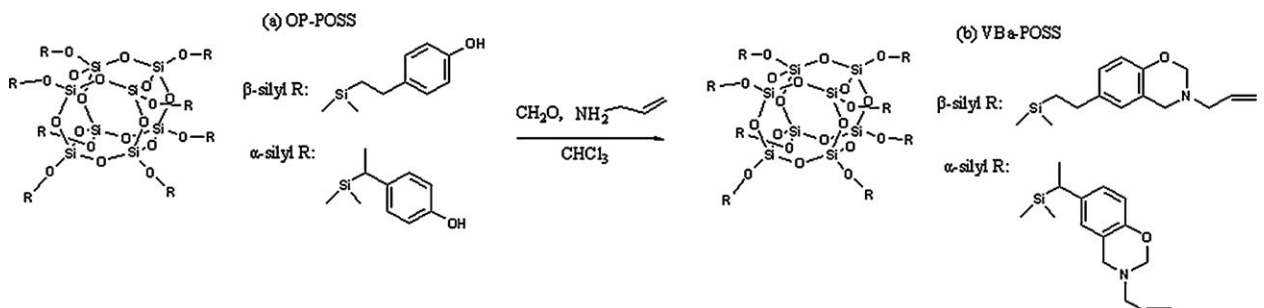


Fig. 36. The synthesis of VBa-POSS (b) through OP-POSS (a).

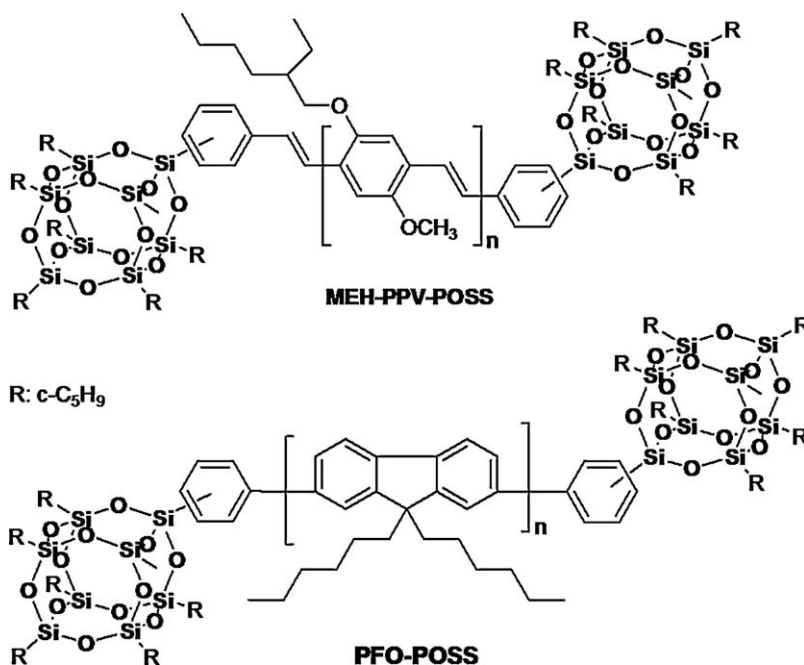


Fig. 37. Molecular structure of MEH-PPV-POSS and PFO-POSS.

of the network junctions. The cured OG-POSS/mPDA product possessed inherently higher thermal stability than that of the cured DGEBA/mPDA product, as evidenced by the higher maximum decomposition temperature and the higher char yield of the former system. The dielectric constant of the OG-POSS/mPDA material ($k=2.31$) was substantially lower than that of the DGEBA/mPDA system ($k=3.51$) because of the presence of the nanoporous POSS cubes in the epoxy matrix [240]. Our group has also prepared epoxy/POSS nanocomposites from OG-POSS and the small-molecule curing agents of diethylphosphite (DEP) and dicyandiamide (DICY), the nanocomposites possessing high OG-POSS contents exhibited good thermal stability, lower flammability, and high storage modulus [239]. We observed a disordered POSS aggregation structure in the DGEBA/OG-POSS nanocomposites, with an average particle size of 30–50 nm through photopolymerization; all of these nanocomposites exhibited enhanced storage modulus in the rubbery state due to the nano-reinforcement effect of the POSS cages and the additional degree of crosslinking formed through reactions between the DGEBA and OG-POSS units [241]. Epoxy/POSS nanocomposites have been prepared through the reaction of OF-POSS, possessing eight functional hexafluorine groups, with the UV-cured epoxy resin [242]. The 10 wt% OF-POSS containing epoxy had significantly lower dielectric constant ($k=2.65$) than that of the plain epoxy ($k=3.71$). The incorporation of fluorine-containing additives reduces the dielectric constant because of its lower polarizability and the presence of the bulky POSS units created additional free spaces or pores to further reduce the dielectric constant of the epoxy matrix. Our group has also incorporated OG-POSS into sulfonated poly(ether ether ketone) (SPEEK) to form a new cross-linked proton exchange membrane (PEM). The dis-

tribution of the OG-POSS-containing cross-linkers (with (ODADS) or without sulfonic acid groups (ODA)) dictated the water behavior and connectivity of the hydrophilic domains of the PEM (Fig. 34) [243]. In Fig. 34(a), the size of the hydrophilic domains of SPEEK varied different particles up to 100 nm, indicating that the SPEEK membrane hydrophilic domains were poorly distributed. Fig. 34(b) reveals that the hydrophilic domains were separated and that their size became more uniform in the OG10 membrane (OG-POSS with 10 wt% ODA content) relative to that of the SPEEK while all of these large hydrophilic domains disappeared. The presence of OG-POSS/ODA cross-linkers tends to reduce the connectivity of hydrophilic domains. Fig. 34(c) reveals that, relative to OG10, these hydrophilic domains within the SOG10 membrane (OG-POSS with ca. 10 wt% ODADS content) are relatively smaller (20 nm) and better dispersed. A PEM formed by incorporating 17.5 wt% of the cross-linker (containing OG-POSS macromer and ODADS) into SPEEK exhibited high proton conductivity (0.0153 S/cm), low methanol permeability ($1.34 \times 10^{-7}\text{ cm}^2/\text{s}$), and high selectivity ($1.14 \times 10^5\text{ Ss/cm}^3$). Xu et al. [227] prepared epoxy resins through reaction of diepoxyhexavinyll POSS with diamines of various chain lengths; the thermal stability was strongly related to the diamine's length, with the highest decomposition temperature being obtained with butanediamine (rather than porpanediamine or ethylenediamine).

4.10.2. Multifunctional NH_2 -POSS and OH-POSS nanocomposites

Zheng and coworkers [244] reported epoxy/POSS nanocomposites based on DGEBA and DDM in the presence of two POSS monomers containing aminophenyl and nitrophenyl groups. The morphologies of the resulted

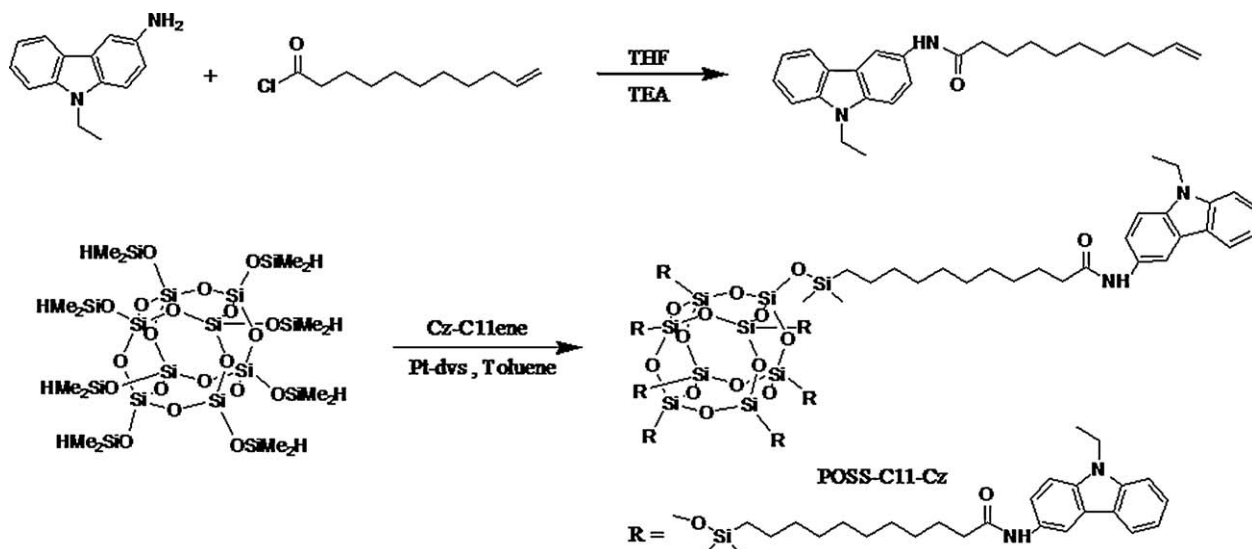


Fig. 38. Synthetic procedures used to obtain POSS-C11-Cz.

hybrids were dependent on the type of functional group in the POSS monomer. The OAP-POSS containing epoxy/POSS nanocomposites exhibited homogeneous morphologies. In contrast, phase separation induced by polymerization occurred in the hybrids containing octakis(nitrophenyl)-POSS, with spherical particles of the POSS-rich phase (average diameter: 0.5 μm) dispersed within the continuous epoxy matrix. They also prepared octamaleimidophenyl-POSS via the imidization reaction between octamaleimidophenyl-POSS and maleic anhydride [245]. Epoxy/POSS nanocomposites were obtained after in situ polymerization of DGEBA, DDM, and octamaleimidophenyl-POSS. The T_g of the epoxy/POSS nanocomposites increased with the increase of POSS content. Cho et al. [246] also reported a similar nanocomposite structure. Zhang and coworkers [247–249] prepared epoxy/POSS derivatives from DGEBA and OAM-POSS, the incorporation of POSS into the epoxy resin improved the thermal stabilities of the epoxy significantly. The average activation energies of thermodegradation of the

epoxy/POSS nanocomposites were calculated using the integral method by Flynn–Wall–Ozawa ($E = 105.01 \text{ kJ/mol}$) and the Coats–Redfern method ($E = 113.07 \text{ kJ/mol}$) [247]. The curing of the epoxy/OAM-POSS hybrid resin system using DDS as a curing agent, the reactivity of the epoxy/POSS system was slightly lower than that of the pure epoxy resin based on the Kissinger and Flynn–Wall–Ozawa methods [249]. Pellice et al. [250] reported epoxy/POSS nanocomposites through the reactions of OH-POSS with DGEBA in the presence of benzyldimethylamine. The elastic modulus and the yield stress both increased with the increase of POSS contents as a result of the increase in cohesive energy density caused by hydrogen bonding of the hydroxyl groups.

4.10.3. Monofunctional epoxy–POSS and NH_2 -POSS nanocomposites

Lee et al. [210] reacted DGEBA epoxy resin with monofunctional-epoxy–POSS and subsequently cured the system to obtain transparent nanoreinforced polymer

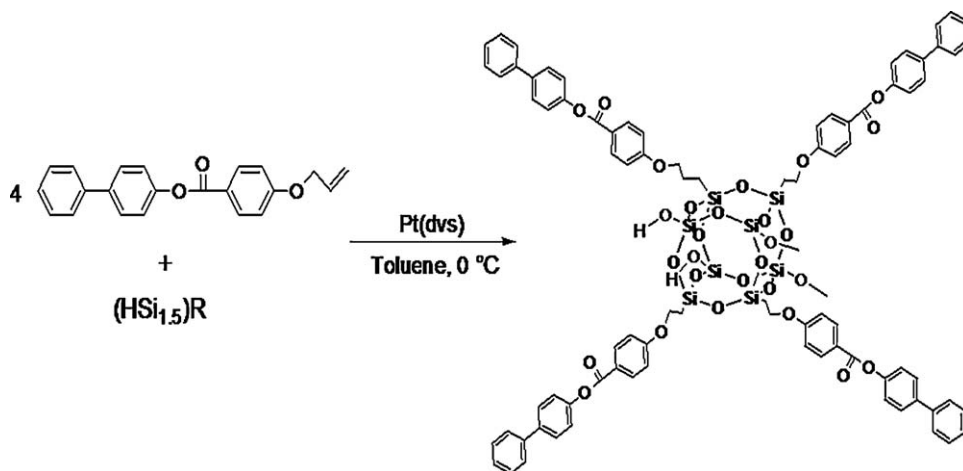


Fig. 39. Syntheses of LC-POSS.

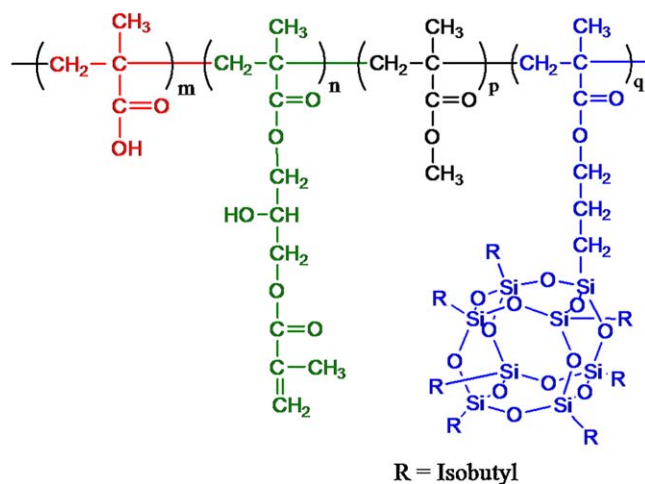


Fig. 41. Synthetic routes of POSS-containing photosensitive copolymers.

yses. The improved thermomechanical properties of this epoxy/POSS nanocomposite were ascribed to the nanodispersion of POSS moieties.

4.11. Polybenzoxazine/POSS nanocomposites

1,3-Benzoxazines are intriguing heterocyclic compounds that have attracted considerable attention for their use as cyclic monomers. These benzoxazine monomers are readily synthesized through the reaction of primary amines with phenol and formaldehyde. These monomers can be polymerized through ring-opening polymerization in the absence of a catalyst, without releasing any byproducts [255,256]. Wang et al. [257] reported that the strong intramolecular hydrogen bonds within polybenzoxazines (PBZs) make them a new class of non-fluorine/non-silicon low-surface-free-energy polymeric materials, which have wide-ranging applications as superhydrophobic surfaces [258,259], in lithographic patterning [260], and as mold-release materials in nanoimprint technology [261]. To improve the performance of PBZs, polymerizable alkynyl and allyl side groups have been introduced into the benzoxazine monomers. Another approach to improve the stability of PBZs is by blending with other polymers [262], such as PU and epoxy resin, or with inorganic silica-based materials, such as clay [263] and POSS [264–269]. Our group has synthesized a novel benzoxazine containing POSS monomer (BZ-POSS) through two routes (Fig. 35): (i) hydrosilylation of a vinyl-terminated benzoxazine with a hydrosilane-functionalized POSS derivative (H-POSS) and (ii) the reaction of a primary amine-containing POSS (AM-POSS) with phenol and formaldehyde [266]. The BZ-POSS monomer was then copolymerized with other benzoxazine monomers through ring-opening polymerization under conditions similar to those used to polymerize pure benzoxazines. The thermal properties of these POSS-containing organic/inorganic PBZ nanocomposites were improved relative to those of the pure PBZ. Our group has also blended a vinyl-terminated benzoxazine (VBa) with H-POSS through ring-opening polymerization [265]. For comparison, we also treated VBa with POSS derivative lack-

ing the hydrosilane group (OiBu-POSS). The glass transition temperature of the PVBa-POSS copolymer increased from 307 to 333 °C. The degradation temperature under N₂ also increased and the char yield was greater than 40 wt% at 600 °C, thus, modifying PBZ through the incorporation of POSS improved the thermal stabilities of these composite materials. We further prepared PBZ/POSS nanocomposites using a reactive multifunctional benzoxazine POSS (OBZ-POSS) and benzoxazine monomers at various compositional ratios [266]. We synthesized the OBZ-POSS curing agent containing eight organic benzoxazine tethers through hydrosilylation of VB-a with Q₈M₈^H using a Pt complex catalyst. Incorporation of the silsesquioxane core into the PBZ matrix significantly hindered the mobility of the polymer chains and enhanced the thermal stability of these hybrid materials. We also prepared poly(VB-a)/POSS hybrids through hydrosilylation of VB-a hydrosilylation with POSS, followed by thermal curing of the benzoxazine monomer to form poly(VB-a)/POSS hybrid nanocomposites. FTIR spectra indicated that not all of the Si–H groups had reacted with VB-a, presumably due to the steric bulk of the POSS cages. The addition of POSS to the poly(VB-a) network greatly increased the crosslinking density and improved the thermal properties [266].

Yu and coworkers [267] reported the reaction between OAP-POSS with 2,2(1,3-phenylene)-bis(4,5-dihydrooxazoles) (PBO) at various temperatures. They used OAP-POSS to modify benzoxazine in the presence of PBO. When only a small amount of OAP-POSS was incorporated into the system, both *T_g* and *T_d* of the resulting PBZ/POSS nanocomposites were substantially enhanced relative to those of the pure PBZ and PBZ-PBO resins, while the storage modulus was still maintained at higher temperatures. They prepared a multi-benzoxazinyl functionalized POSS derivative (OBZ-POSS) from OAP-POSS, p-cresol, and para-formaldehyde; BZ monomer and OBZ-POSS were copolymerized through ring-opening copolymerization [267]. DMA and TGA analyses showed that the thermal stability, cross-linking densities, and flame retardance of the PBZ/POSS nanocomposites all increased with the increase of OBZ-POSS contents. Yu and coworkers [268]

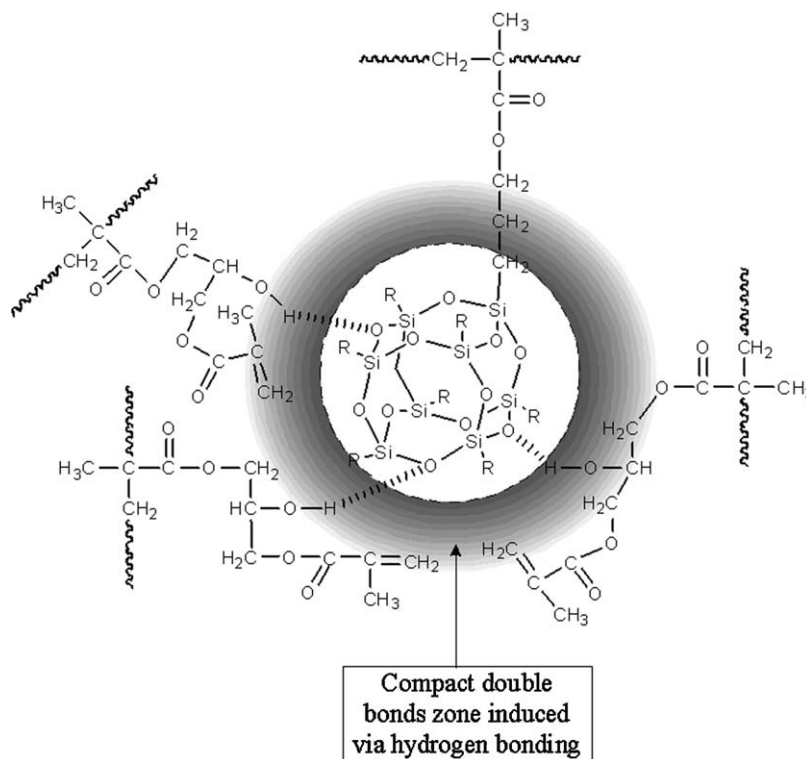


Fig. 42. The proposed microstructure via hydrogen bonding interaction of POSS.

also reported PBZ formed from the incomplete functionalized trisilanol-POSS, the thermal stability of the composite was greatly enhanced after the incorporation of the POSS units.

Zheng and coworker [269] prepared PBZ/POSS nanocomposites based on OG-POSS in which the crosslinking reactions divided into two steps: (1) ring-opening polymerization of benzoxazine and (2) reaction between the in situ formed phenolic hydroxyls of PBZ and the epoxide groups of OG-POSS. DSC and DMA analyses showed that the PBZ/POSS nanocomposites exhibited higher T_g than that of the pure PBZ. In the glassy state, the storage modulus increased when the nanocomposites contained less than 30 wt% of POSS. We also combined the advantageous properties of allyl-functionalized benzoxazine and POSS nanocomposites to improve both the thermal and mechanical properties of the resulting PBZ matrix [270]. We synthesized a multifunctional POSS bearing eight vinyl-terminated benzoxazine groups (VBa-POSS) through the reaction of OP-POSS with formaldehyde and allyl amine (Fig. 36) [270] and then copolymerized it with VBa benzoxazine monomers through ring opening polymerization. Since these PBZ/POSS hybrid materials incorporated large numbers of POSS units into their PBZs, they exhibited notably improved thermal and mechanical properties. We observed a gradual increase in the decomposition temperature of the PBZ/POSS nanocomposites upon increasing the VBa-POSS content. The char yield, another indicator of thermal stability, also increased upon increasing the POSS content in these hybrid materials. We also prepared a new class of polybenzoxazine-POSS

network nanocomposites by reacting the multifunctional benzoxazine POSS (OBZ-POSS), which was synthesized from octa-azido functionalized POSS (OVBN₃-POSS) with 3,4-dihydro-3-(prop-2-ynyl)-2H-benzoxazine (P-pa) via a click reaction [271]. Incorporation of the silsesquioxane core into the PBZ matrix significantly hindered the mobility of the polymer chains and thus enhanced the thermal stability of these hybrid materials.

5. POSS-containing functional materials

5.1. Polymer light emitting diodes (PLEDs) incorporating POSS hybrid polymers

Heeger and coworkers [272,273] reported the incorporation of POSS moieties into conjugated polymers by synthesizing semiconducting polymers, POSS-anchored poly(2-methoxy-5-(ethoxyloxy)-1,4-phenylenevinylene) (MEH-PPV-POSS) and POSS-anchored poly(9,9-dihexyfluorenyl-2,7-diyl) (PFO-POSS) (Fig. 37). Relative to the corresponding parent polymer, these POSS-anchored semiconducting polymers exhibited higher brightnesses and external quantum efficiency. It has been suggested that the presence of POSS reduces the formation of aggregates and/or excimers or lowers the concentration of conjugated defects. Shim and coworkers [274–277] prepared POSS-substituted polyfluorene polymers and found that the incorporation of POSS units inhibited interchain interactions and fluorenone formation, thereby leading to a reduction in undesired emission (>500 nm) of the poly(dialkylfluorene)s and improved thermal stability

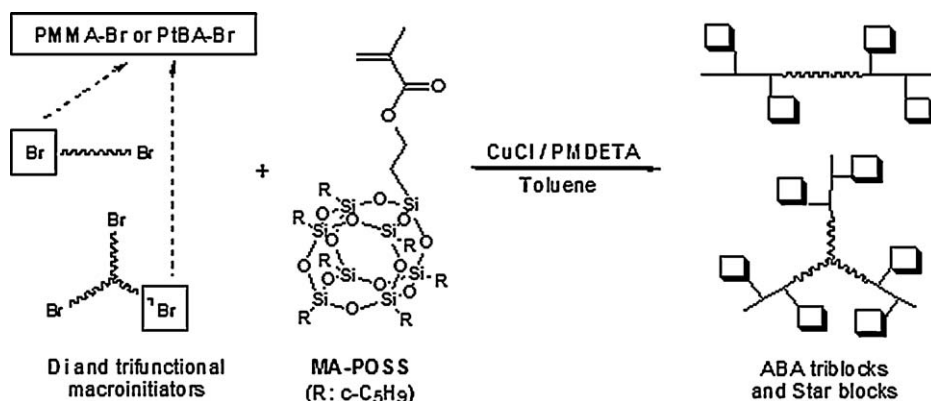


Fig. 43. Synthesis of triblock and star-block copolymers.

of the PFOPOSS systems. Devices incorporating PFOPOSS hybrids as emitting layers have exhibited very stable blue light emissions and high performance [277].

Hsu and coworkers [278] and Wei and coworkers [279,280] reported asymmetric conjugated polymers featuring POSS units attached to their side chains. An electroluminescent (EL) device prepared from MEH-PPV emitted a strong peak at 590 nm and a vibronic signal in the range 610–620 nm [278]. The introduction of bulky siloxane units into the PPV side chains presumably increased the inter-chain distance, thereby retarding interchain interactions and reducing the degree of exciton migration to defect sites. A star-like polyfluorene derivative, PFO-SQ, has been synthesized through the Ni(0)-catalyzed reaction of octa(2-(4-bromophenyl)ethyl)silsesquioxane (OBPE-SQ) and polydioctylfluorene (PFO) [281]. The incorporation of the silsesquioxane core into the polyfluorene significantly reduced the degree of aggregation and enhanced the thermal stability. The incorporation of inorganic silsesquioxane cores into polyfluorenes is a new method for preparing organic light-emitting diodes with improved thermal and optoelectronic characteristics [281]. Our group reported a POSS-based blue-light electroluminescent NP, octakis[*N*-(9-ethyl-9H-carbazol-3-yl)undecanamide-11-dimethylsiloxy] silsesquioxane (POSS-C11-Cz), possessing eight carbazole chromophore arms, that was synthesized through hydrosilylation of the terminal olefin with octakis(dimethylsiloxy)silsesquioxane (Fig. 38) [282]. The optical and photoluminescence (PL) spectra of POSS-C11-Cz in solution and in the solid state indicated reduced levels of aggregation and excimer formation because inter-chain interactions were prohibited in the presence of the bulky POSS cores. Moreover, PL spectra of the POSS-C11-Cz (3 wt%)/polyfluorene (97 wt%) blend revealed that its color was stable after heating at 200 °C for 5 h; in contrast, the pure polyfluorene exhibited a significant green emission at 530 nm after such treatment.

5.2. Liquid crystal polymers (LCPs) incorporating POSS hybrid polymers

With the goal of developing diverse building blocks for nanocomposite materials, Laine and coworkers [283]

synthesized liquid crystalline materials by appending mesogenic groups to cubic silsesquioxane cores via hydrosilylation of allyloxy-functionalized mesogens with $Q_8M_8^H$. Fig. 39 indicates that hydrosilylation led to each cube to possess an average of five appended LC groups. Despite the structural irregularity, three of the four penta-LC-cube derivatives exhibited LC transitions, with a tendency to form the SmA phase. One interesting observation was the redistribution of the diffuse liquid-like scattered intensity at 11–12 Å in the smectic phase upon alignment. These results provide the basis for future work on producing LC cubes as potential precursors to LC-ordered organic/inorganic nanocomposites. Although, the LC transition temperatures were reduced somewhat, they remained above those considered useful for biologically important applications [283]. Chujo and coworker [284] reported the preparation of a POSS macromonomer through radical copolymerization and LC hybrid copolymers incorporating various proportions of the synthesized LC monomer; the thermal stability of the hybrid polymers increased upon increasing the ratio of POSS moieties. Zhou and coworkers [285] prepared bent-core liquid crystals with different numbers of bent-core mesogens end-capped onto POSS cores through hydrosilylation (Fig. 40). A two-bilayer SmCAPA phase was observed when eight bent-core mesogens were end-attached to POSS. Monolayer SmCPA phases were obtained upon increasing the content or the size of the siloxane core.

5.3. Lithographic applications of POSS-containing photoresists

Several POSS-based photoresists have been reported including positive-tone systems. Wu and coworkers [286,287] reported that the incorporation of POSS units in methacrylate-based chemically amplified photoresists influenced their reactive ion etching (RIE) behavior. Whereas polymers incorporating low POSS concentrations exhibited little improvements in their RIE resistances, the presence of 20.5 wt% of POSS monomer in a methacrylate-based resist significantly improved the RIE resistance in O_2 plasma. High-resolution TEM revealed that the improved RIE resistance was due to the formation of rectangular

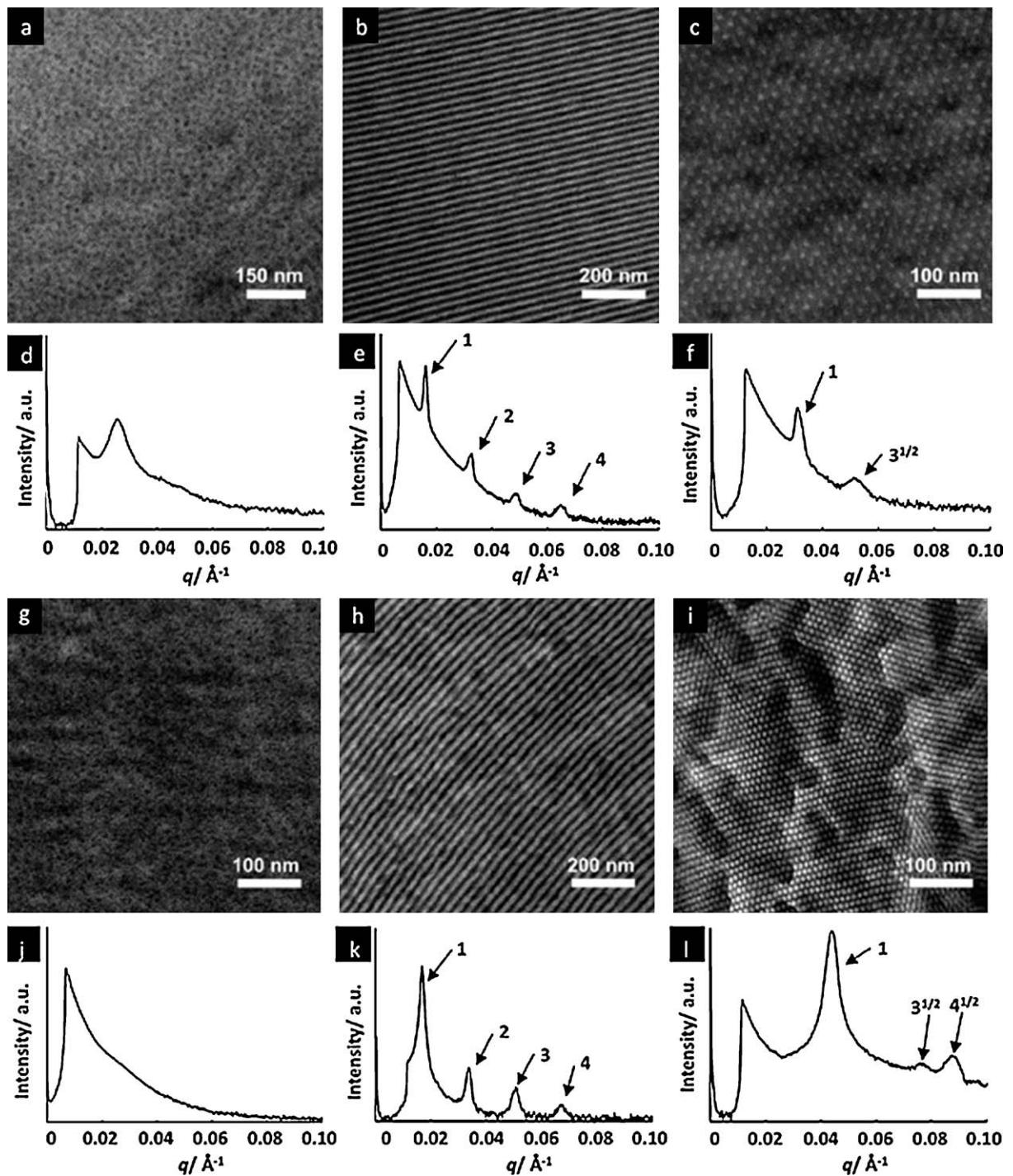


Fig. 44. TEM and SAXS profiles of (a, d) PMMA₄₅₀-*b*-PMAPOSS₇, (b, e) PMMA₂₆₂-*b*-PMAPOSS₂₃, (c, f) PMMA₅₂-*b*-PMAPOSS₁₈, (g, j) PS₂₆₆-*b*-PMAPOSS₂₀, and (i, l) PS₅₂-*b*-PMAPOSS₉. (d, j) lack long range order, (e, k) characteristic ratio of 1:2:3:4, indicating lamellar morphologies, (f, l) characteristic ratio of 1:3^{1/2}:4^{1/2}, indicating hexagonally packed cylinders.

Reprinted with permission from Ref. [315]. Copyright 2009, American Chemical Society, USA.

crystallite-constituting networks of the silica cages uniformly distributed within the polymer matrix [286,287]. Gonsalves and coworkers [288,289] characterized a series of POSS-containing positive-tone photoresists for use in both extreme ultraviolet lithography (EUVL) and electron

beam lithography. These photoresist systems exhibited the ideal combination of enhanced etch resistance and enhanced sensitivity required to satisfy both low- and high-voltage patterning applications. The photoresist sensitivity was enhanced after the direct incorporation of a photoacid-

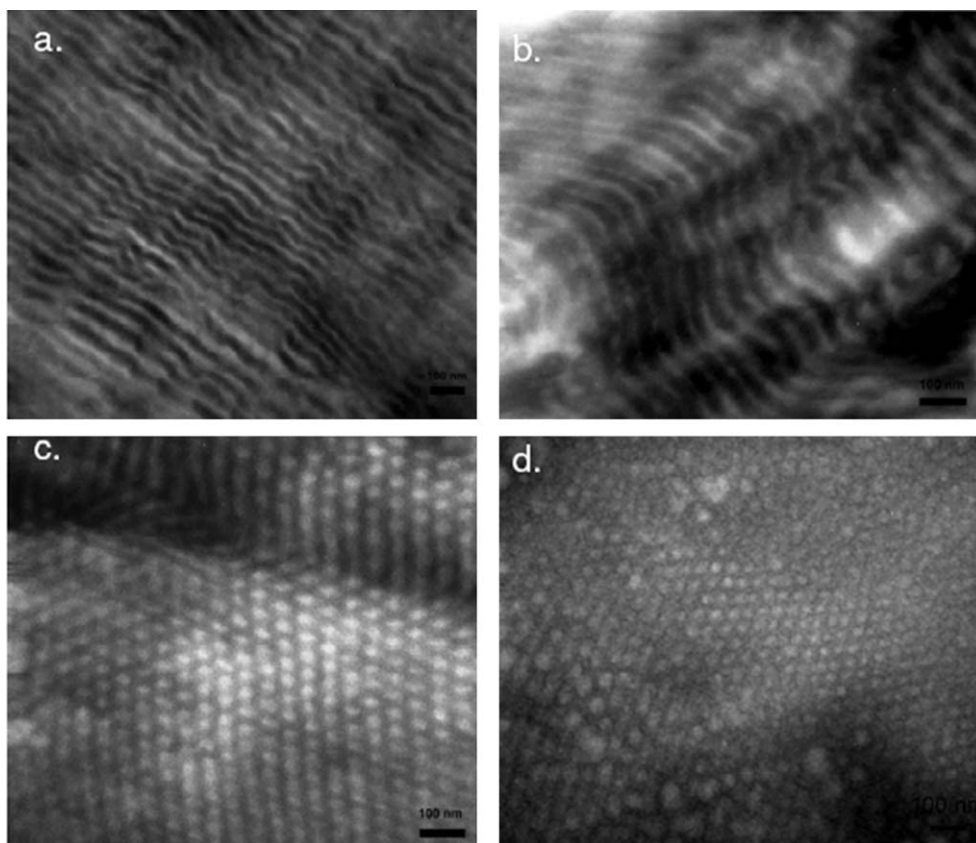


Fig. 45. TEM images of (a) pure PCL-*b*-P4VP diblock copolymer, stained by I_2 (b) pyridine/OH = 4/1, (c) pyridine/OH = 2/1, and (d) pyridine/OH = 4/3 without staining. P4VP domain appears as dark region and the PCL domain as bright region in the micrographs.

generating monomer into the resist polymer backbone, while the etch resistance of the material was improved after copolymerization with a POSS-containing monomer [288]. Argitis and coworkers [290–292] described the lithographic behavior and related material properties of chemically amplified, positive-tone, methacrylate-based photoresists incorporating POSS groups as the etch-resistant component. The POSS-containing photoresists for 157-nm lithographic applications exhibited high sensitivity ($<10 \text{ mJ/cm}^2$ under open field exposure), no silicon outgassing, and sub-100-nm resolution capabilities. Alternatively, an octavinylsilsesquioxane dry resist has been prepared, as a negative-tone resist exhibiting high sensitivity, for deep-UV, electron-beam, and X-ray lithography [293]. Furthermore, Zheng and coworker [294] synthesized a novel photosensitive octakis(cinnamoylamidophenyl)-POSS derivative (OcapPOSS) through the reaction of cinnamoyl chloride and OAP-POSS. The presence of the POSS cages restricted the mobility of the poly(vinyl cinnamate) macromolecular chains and, thus, hindered the formation of tetrabutane rings.

Recently, our group developed methacrylate-based, POSS derivative-containing photoresist materials for UV-lithography with enhanced sensitivity, higher contrast, and improved resolution taking advantage of the hydrogen bonding interactions between the siloxane units of the POSS moieties and the OH groups of methacrylate-

based polymers (Fig. 41) [295,296]. These copolymers exhibited acceptable transmittances (from 99 to 92.5%) at a wavelength of 365 nm. The sensitivity for the POSS-free photoresist 1 was 71.8 mJ/cm^2 while those POSS-containing photoresists were significantly lower, ranging from 20.0 to 10.8 mJ/cm^2 . The contrasts for the photoresists followed the same trend as the sensitivities. Thus, the presence of POSS units had an effect on the properties of the negative-type photoresist. The strong hydrogen bonding interactions drew the methacrylate double bonds toward the POSS moieties, resulting in a higher concentration of these methacrylate olefinic bonds around the POSS units, thereby, enhancing the rate of chemically crosslinking through photo-polymerization (Fig. 42) [295].

5.4. Low-*k* applications of POSS-containing materials

To decrease the dielectric constants of polymers, several research groups [297–301] have explored the possibility of incorporating various nanoforms into polymer matrixes to take advantage of the low dielectric constant of air ($k=1$). There are two typical routes employed for preparing materials with low dielectric constants: (i) nanopore formation through decomposition (e.g., thermal decomposition, photodegradation with UV irradiation, or solvent etching) of a dispersed phase within a material matrix and (ii) incorporation of a low-*k* moieties (e.g., fluorinated

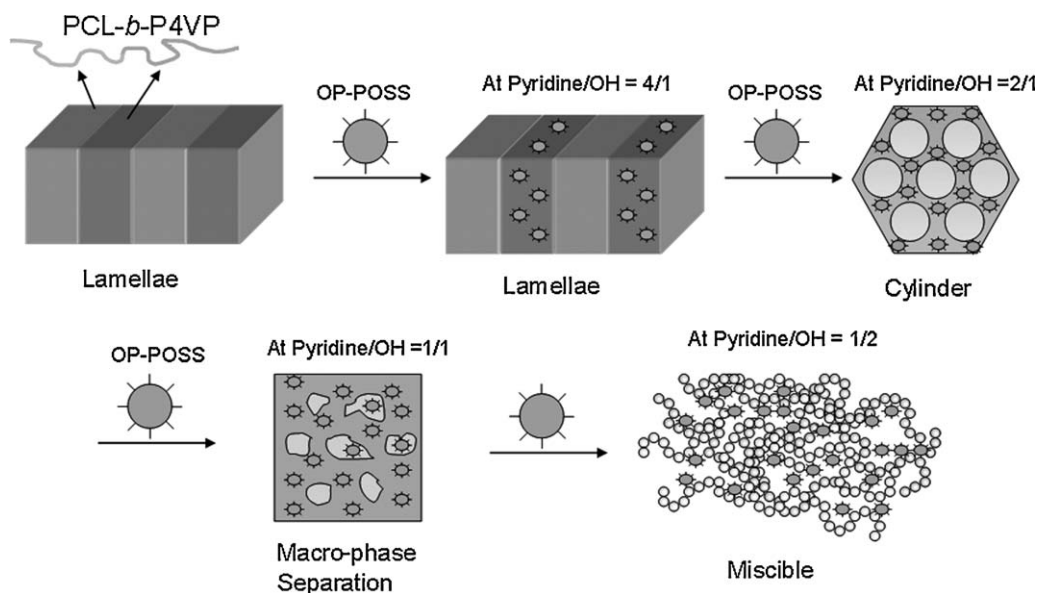


Fig. 46. Morphology change in PCL-*b*-P4VP/OP-POSS blends with the increase of OP-POSS contents.

units, supercritical fluids, or low-*k* particles) within a material matrix. Recently, several low dielectric constant materials have been prepared through dispersion of POSS-containing molecules into polymer matrices. Our group has prepared some POSS-containing low-*k* materials using both of the methods mentioned above, taking advantage of hydrogen bonding interactions between the POSS moieties and the OH groups of the matrix to achieve homogenous nanocomposites [128,301], in which the POSS moieties not only served as low-*k* materials but also contributed to the improved thermal and mechanical properties.

For the molecular-level design of low-*k* materials, Seckin et al. [194] studied star PIs incorporating OAM-POSS through in situ curing of PAA macromolecules. The presence of OAM-POSS, which imparted restricted rotation by multiple point attachment to the PI backbone, introduces free volume into the films, thereby lowering their dielectric constants. The process for synthesizing the POSS-PI star nanocomposites involved two steps: forming the porous-type POSS and then reacting it with the PI precursor. The POSS-containing PIs exhibited a number of desirable properties including low-water absorption and high thermal stability. Thus, insertion of POSS units into a PI backbone can reduce a material's dielectric constant while also improving its mechanical and thermal properties. Xu and coworker [302] prepared four novel organic/inorganic network hybrids via hydrosilylation of dienes with octahydro-silsesquioxanes (H₈-POSS). All of their POSS hybrid films exhibited high thermal stability and low dielectric constants. Interestingly, these properties were tunable by adjusting the length and structure of the linking chain between the POSS cages. Liu et al. [303] prepared ultralow *k* ($k = 1.47$) POSS nanocomposites from two liquid monomers using a spinning-on process; their low dielectric constants were attributed to the formation of lamellar POSS structures.

5.5. Self-assembly behavior of POSS-containing block copolymer materials

Self-organizing materials allow the development of “bottom-up” method, a relatively simple and low-cost process for fabrication of large-area periodic nanostructures from diblock copolymers or other materials (e.g., low molecular weight compounds) by controlling their self-assembly [304–306]. Pyun and Matyjaszewski and coworkers [307,308] used ATRP to synthesize an MA-POSS homopolymer and block copolymers from a cyclopentyl-substituted POSS monomer. They employed ATRP to prepare the block copolymer from MA-POSS and *n*-butyl acrylate, with 4-methylphenyl 2-bromoisobutyrate as the initiator and CuCl/PMDETA as the catalyst (Fig. 43) [307,308]. TEM characterization of the triblock copolymer thin film P(MA-POSS)₁₀-*b*-PBA₂₀₁-*b*-P(MA-POSS)₁₀ revealed the formation of PBA cylinders in a P(MA-POSS) matrix.

Liu and coworker [309] also prepared a well-defined diblock copolymer based on POSS through ATRP with POSS/PMMA-Cl as a macro-initiator; their AB diblock copolymer based on POSS formed tadpole-shaped structures, with the inorganic head of the POSS units and an organic tail of polymer. Lee and coworkers [310–312] used hydrosilylation to prepare an organic/inorganic triblock copolymer of SBS containing grafted POSS. Their POSS derivative was designed to contain a single silane functional group for grafting onto 1,2-butadiene units in the PB soft block. Since these POSS moieties were dispersed on the molecular scale, the SBS copolymer gradually lost its long-range ordering upon increasing the POSS content. SAXS analysis showed that the scattering of the cylindrical structure became diffuse with the lamellar structure and transformed into a perforated layer morphology. Zhu and coworkers [313] reported the self-assembly of a PEO-*b*-

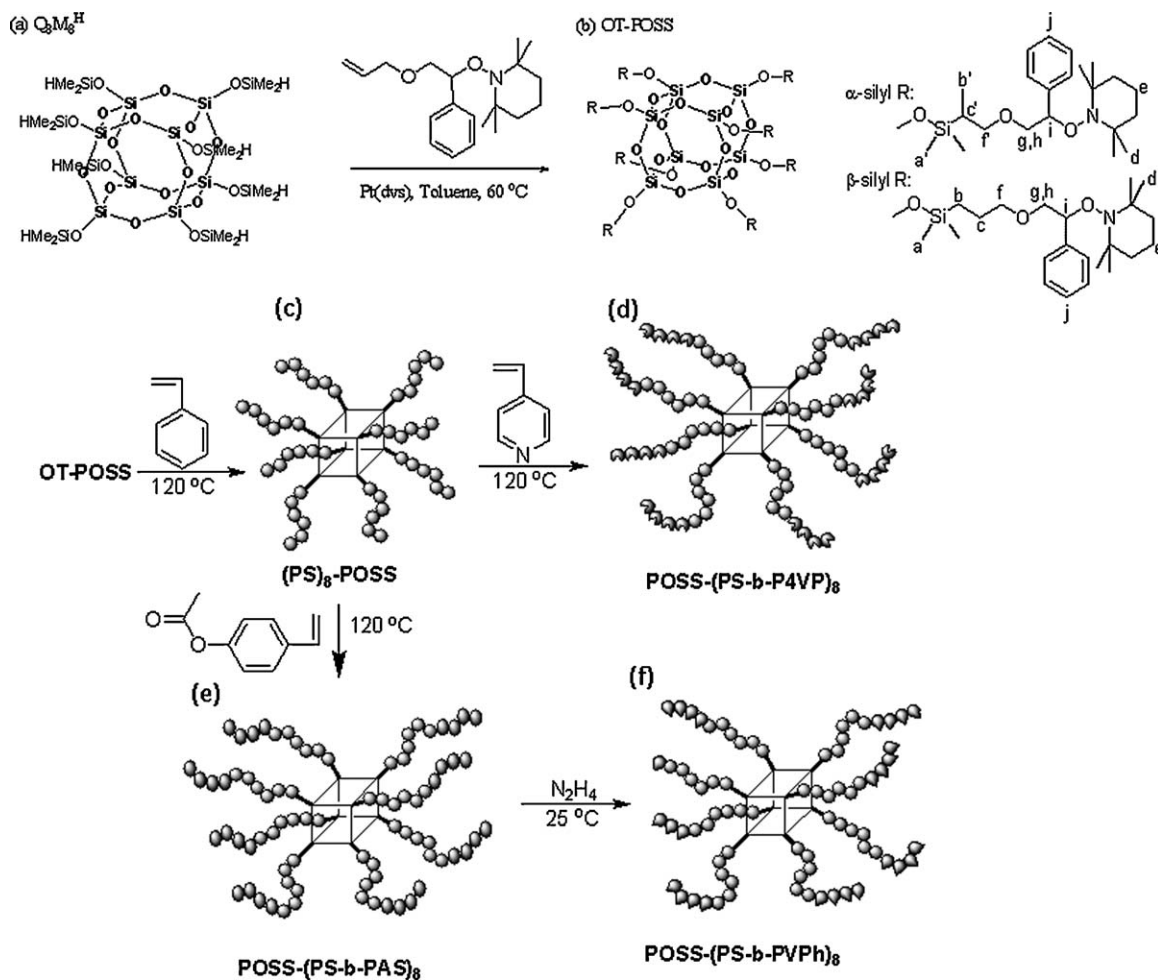


Fig. 47. Preparation of OT-POSS (b), $(PS)_8$ -POSS (c), $(PS-b-P4VP)_8$ -POSS (d), $(PS-b-PAS)_8$ -POSS (e), and $(PS-b-PVPh)_8$ -POSS (f).

PE-POSS triblock copolymer, in which the POSS molecules crystallized prior to crystallization of PE, forming a well-defined lamellar structure. Hirai and coworkers [314,315] prepared two kinds of POSS-containing block copolymers, PMMA-*b*-PMAPOSS and PS-*b*-PMAPOSS, through anionic living polymerization. These two kinds of diblock copolymers formed various self-assembled structures including spherical, cylindrical, and lamellar morphologies (Fig. 44) [315]. When applied in lithography processes, these diblock copolymers possessed narrow polydispersity and resulted in well-defined morphologies [316]. Using a POSS-PEO macroinitiator for the ATRP of styrene, Zhang et al. [317] synthesized PS-*b*-PEO diblock copolymer featuring a POSS moiety at the junction of the diblock copolymer between the two blocks. Self-assembly of this block copolymer led to the formation of vesicles in aqueous solution. Cheng and coworkers [318] used silyl-hydrid functionalized 1,1-diphenylethylene derivative (DPE-SiH) as an intermediate for the anionic synthesis of in-chain-functionalized polymers, where the reactive Si-H bond of the POSS cage at the junction was used for the preparation of PS-*b*-PDMS diblock copolymers.

Our group has reported the variation of self-assembled morphologies of the immiscible PCL-*b*-P4VP diblock copolymer upon increasing the OP-POSS content through competitive hydrogen bonding interactions [319]. TEM images revealed highly long-range ordered morphologies such as cylinder or sphere structures at relatively low OP-POSS contents and shifted to short-range ordered or even disordered structures at higher OP-POSS contents (Fig. 45) [319]. Fig. 46 presents a plot of the morphological transformations occurred upon increasing the OP-POSS content [319]. A long-range ordered nanostructure existed in PCL-*b*-P4VP/OP-POSS at lower OP-POSS contents pyridine/OH=4/1 (lamellae structure), pyridine/OH=2/1 (cylinder structure), short-range order nanostructure existed at relatively higher OP-POSS contents (pyridine/OH=4/3 to 1/1), and the disorder structure existed at the highest OP-POSS content (pyridine/OH=1/2). We also reported a series of star block copolymers through nitroxide-mediated radical polymerization (NMRP) from POSS NPs through core-first polymerization [320]. We first incorporated *N*-alkoxyamine groups onto the eight corners of a POSS cube through quanti-

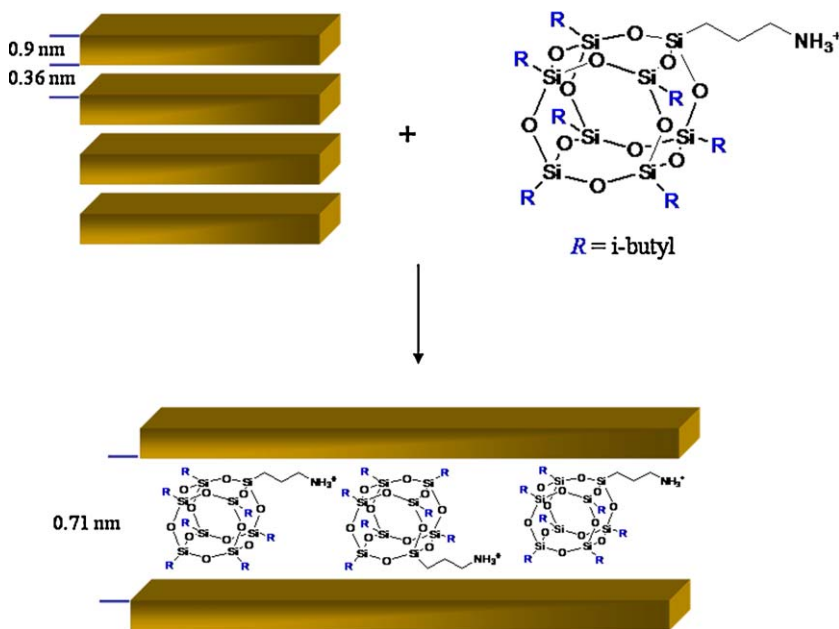


Fig. 48. Schematic drawing of the clay intercalated by the POSS.

tative hydrosilylation of 1-(2-(allyloxy)-1-phenylethoxy)-2,2,6,6-tetramethylpiperidine (allyl-TEMPO) with $Q_8M_8^H$ using Karstedt's agent as the catalyst. We then used the octakis(*N*-alkoxyamines)-POSS (OT-POSS) as a platform to synthesize star $(PS)_8$ -POSS homopolymers and the diblock copolymers $(PS\text{-}b\text{-}P4VP)_8$ -POSS and $(PS\text{-}b\text{-}PAS)_8$ -POSS through NMRP. Subsequent selective hydrolysis of the acetyl protective groups of $(PS\text{-}b\text{-}PAS)_8$ -POSS led to the formation of $(PS\text{-}b\text{-}PVPh)_8$ -POSS, featuring strongly hydrogen bonding groups (Fig. 47) [320].

5.6. Nanoparticle with POSS-containing materials

5.6.1. POSS modified clay nanocomposites

Nanoclay-filled polymeric systems offer the prospect of great improving many of the physical properties of polymers. Montmorillonite (MMT), an aluminosilicate mineral featuring sodium counterions between its layers, is the

most commonly used clay. The space between these clay layers is referred to as the clay gallery for these purposes. To make this inorganic clay compatible with organic polymers, the sodium counterions are usually ion-exchanged with an organic ammonium or phosphonium salt to convert the material into hydrophobic ammonium- or phosphonium-treated clays. Alkyl ammonium salts of low molecular weight are thermally unstable; therefore, their use greatly limits the processing of such materials, especially at elevated temperatures.

Our group first reported that ammonia-POSS could be used as a surfactant to modify the clay gallery. The major reason for choosing POSS molecules in this role is their thermal stability up to 300 °C, higher than the thermal degradation temperatures of most organic molecules. POSS derivatives containing amino functional groups can function as surfactants for the treatment of clay; enhanced thermal stability of the resulting nanocomposites can be

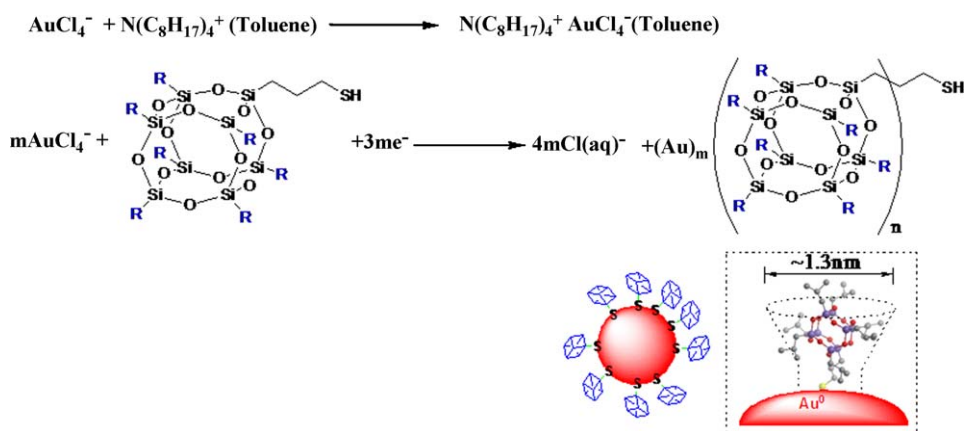


Fig. 49. Schematic drawing of the clay intercalated by the POSS.

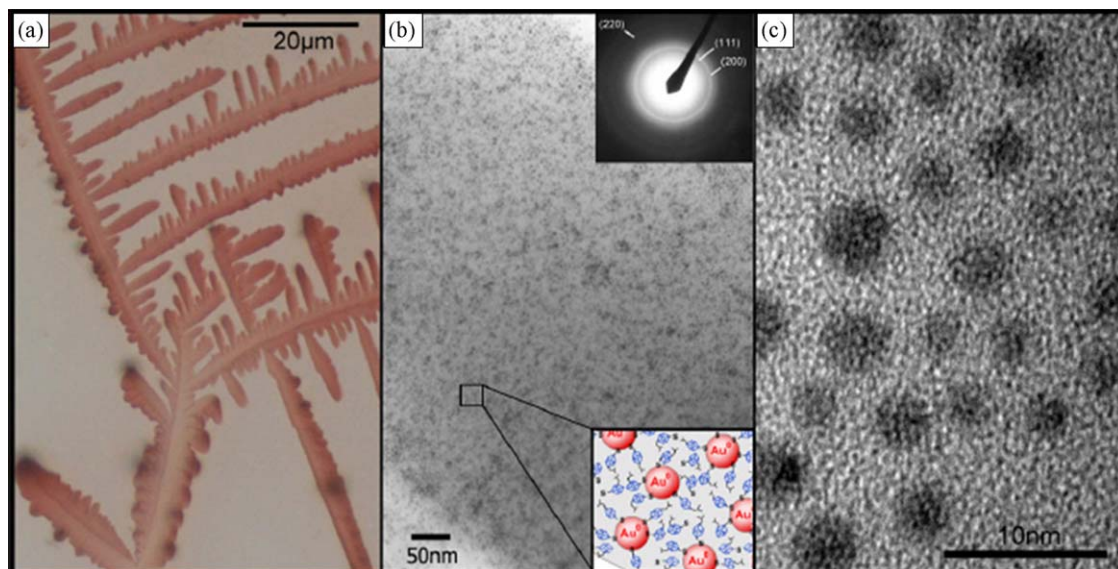


Fig. 50. Micrographs of Au-POSS aggregation on different scales by (a) optical microscopy (OM), (b) transmission electron microscopy (TEM) and (c) high resolution transmission electron microscopy (HRTEM). The insert in (b) shows an electron diffraction pattern of Au-POSS nanoparticles and an aggregation model corresponding to a micrograph of (b).

Reprinted with permission from Ref. [335]. Copyright 2009, Wiley-VCH, Germany.

expected. When the POSS surfactant was inserted between the galleries of the clay, the d spacing increased from 1.26 nm for the pristine clay to 1.61 nm, indicating that the POSS surfactant was indeed intercalated into the galleries of the clay. The POSS surfactant-intercalated clay composite (POSS/clay; Fig. 48) exhibited only one diffraction peak, no peak was detected from the aggregation of POSS [321]. Cariniato et al. [322] also reported the intercalation of bifunctional protonated titanium-containing aminopropyl isobutyl POSS (Ti-NH₃-POSS) within the interlayer space of a synthetic sodium saponite. The embedding of Ti-NH₃-POSS into this clay led to significant stabilization of the resulting hybrids. Our group has compared the effects of different chain lengths of NH₂-POSS as intercalated agents for organically modified clays [323,324]. For the NH₂-POSS/clay and C₂₀-POSS/clay, the value of 2θ shifted from 6.92° (1.28 nm) to 5.51° (1.61 nm) and 2.33° (3.80 nm), respectively, after ion exchange, indicating that the basal spacing was expanded as the sodium cations in the interlayer galleries were replaced by the intercalated agents of NH₂-POSS and C₂₀-POSS [323]. The increase basal spacings indicate that the clay can be efficiently intercalated by NH₂-POSS and C₂₀-POSS. The d -spacing of the C₂₀-POSS-modified clay was substantially greater than that of the NH₂-POSS modified clay, nevertheless, the NH₂-POSS clay was relatively more stable than the C₂₀-POSS-modified clay because long alkyl chains are inherently thermally unstable.

Zheng and coworkers [325] prepared the octakis(ammonium chloride) salt of OAPS-POSS as an intercalating agent to modify MMT. X-ray diffraction data indicated that MMT was successfully intercalated by this the ammonium salt of OAPS-POSS: the basal spacing of the MMT galleries was expanded from 1.3 to 1.7 nm. TEM imaging indicated a random dispersion of

intercalated/exfoliated aggregates in the epoxy matrix. TGA analysis showed that the incorporation of POSS-MMT into epoxy networks improved thermal stability; the char residue increased with increasing the concentration of POSS-MMT. Fox et al. [326] reported a POSS-imidazolium surfactant for use as an organic modifier for MMT and observed that the self-assembled crystalline POSS domains were present in the clay interlayer. The d -spacing of the exchanged clay was ca. 3.6 nm, sufficiently high to accommodate the bilayer structure of the POSS and the POSS/clay exhibited higher thermal stability than that of typical ammonium-exchanged MMT. Wan et al. [327] also reported an NH₂-POSS modified MMT that exhibited a large interlayer distance and large specific surface area. Their POSS-MMT hybrid was used as a catalyst support to initiate the ring-opening polymerization of cyclic butylenes terephthalate oligomer. TEM and XRD revealed an exfoliated structure, with no diffraction peaks detected through XRD analysis. The tensile properties of the resultant PBT/POSS-MMT composites were highly improved relative to those of the pristine PBT due to the homogeneous dispersion of POSS-MMT in the PBT matrix.

5.6.2. POSS modified gold nanoparticles

Self-assembly of NPs with controlled organization of NPs into ordered or hierarchical structures offers potential applications in optoelectronics, sensing, imaging, and biomedical applications. Schmid et al. [328] used 3-mercaptopropylcyclopentyl-POSS (SH-POSS) to quantitatively exchange the PPh₃ ligands in (PPh₃)₁₂Au₅₅Cl₆ in an attempt to obtain POSS-Au NPs stabilized through Au-S bonds. However, they obtained amorphous structures, demonstrating the dramatic influence of this POSS ligand on the cluster properties. Naka and coworkers [329] and Rotello and coworkers [330–332] prepared POSS-Au hybrid

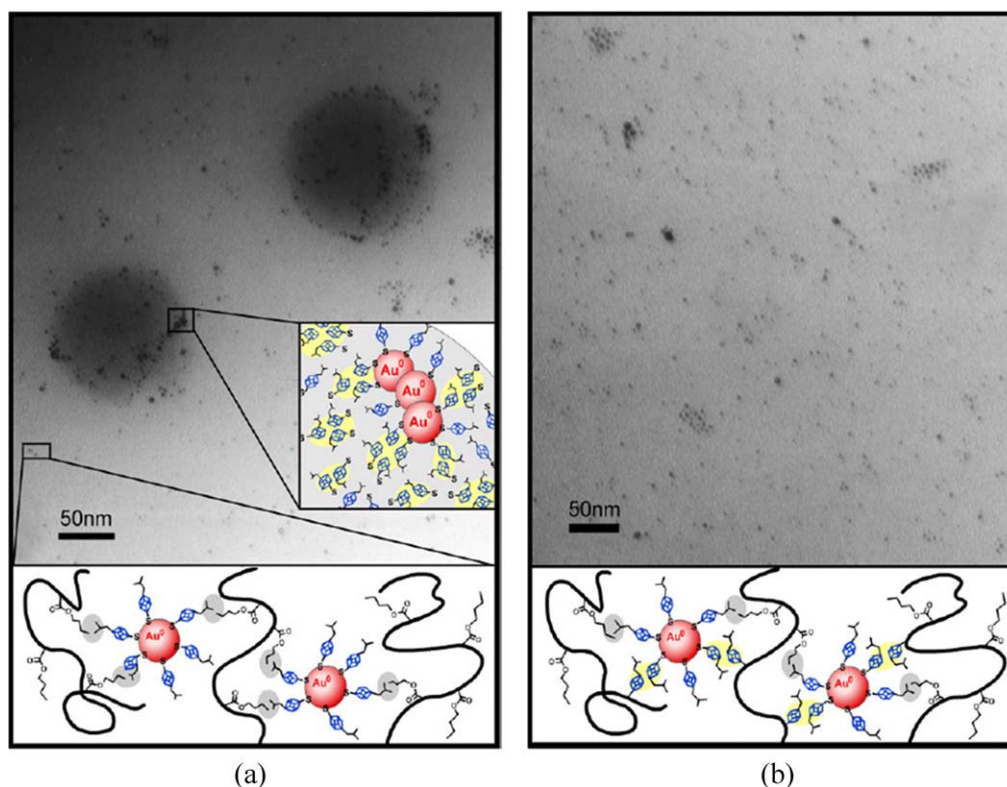


Fig. 51. TEM images of Au-POSS nanoparticles in a PnBMA homopolymer matrix (a) and PnBMA-*r*-PiBPPMA copolymer matrix (b). Reprinted with permission from Ref. [335]. Copyright 2009, Wiley-VCH, Germany.

NPs stabilized through electrostatic interaction with the HCl salts of OAPS-POSS or through hydrogen bonding with diaminopyridine-monofunctionalized octasilsesquioxane [330]. Such strong intermolecular interactions (i.e., electrostatic and hydrogen bonding interactions) suppressed the thin-film-forming characteristic of POSS during crystallization. Using this strategy, both the chemical and physical nature of the surface could be controlled through deposition of POSS-based surface modification agents. Rotello et al. [332] also used carboxylic acid-functionalized, mixed monolayer-protected Au clusters in conjunction with quaternary trimethylammonium-functionalized POSS units to produce well-ordered aggregates. TEM and SAXS analyses showed an increase in the average interparticle spacing upon self-assembly with POSS. This increase in spacing influenced the surface plasmon resonance band of the larger 6.8 nm Au NPs, as determined using UV-vis spectroscopy. Naka and coworkers [329] prepared microporous nanocomposites of Pd and Au NPs by taking advantage of the electrostatic attraction between oppositely charged Au NPs coated with carboxylate groups (Au-COO^-) and spherical aggregates of Pd NPs (Pd-NH_3^+), having a mean diameter of 20 nm and stabilized and cross-linked by OAPS-POSS (POSS-NH_3^+) [329]. Amide bonds were formed between the reactive ion couples to generate more stable nanocomposites with improved chemical and physical properties. They exhibited excellent catalytic properties because of their large surface areas and the synergistic effects of the Pd and Au NPs. They also prepared a colloidal

form of PdNPs@AuNPs by stirring the aggregates of Pd NPs protected by POSS-NH_3^+ with the colloidal Au NPs at room temperature [333].

Our group has used SH-POSS as a protective group for the preparation of POSS-protected Au NPs (POSS-Au NPs) as shown in Fig. 49 [334]. The organic/inorganic hybrid SH-POSS NPs exhibited an interesting platelike morphology arising from steric hindrance between the isobutyl groups of SH-POSS. Fig. 50(a) shows an optical microscopy (OM) image of the Au-POSS aggregates, displaying red ferny-like structures on the order of a few micrometers [334]. Fig. 50(b) displays a TEM image of the Au NPs dispersed within the ferny-like structure; these aggregates comprised individual Au NPs surrounded by SH-POSS units. The upper-right hand inset to Fig. 50(b) shows the selected-area electron diffraction (SAED) pattern of the Au NPs, revealing a face-centered cubic (FCC) structure corresponding to the (1 1 1), (2 0 0) and (2 2 0) Au crystalline facets, while many small particles have independent orientations. The TEM image of the POSS-functionalized Au NPs in Fig. 50(c) displays that the average diameter of the Au cores, calculated from Fig. 50(c), was ca. 5 nm. These Au-POSS NPs formed partial aggregates upon blending with poly(*n*-butyl methacrylate) (PnBMA) homopolymer, due to poor miscibility between Au-POSS and PnBMA polymer matrix [335]. The incorporation of POSS moieties into the PnBMA main chain to form a random copolymer matrix resulted in well-dispersed Au NPs because the POSS-POSS interactions enhanced the miscibility of the Au NPs in the

PnBMA-POSS copolymer matrix. Fig. 51(a) shows the morphology of the Au-POSS NPs incorporated into the PnBMA homopolymer matrix. Most of these Au-POSS NPs were located within the gray nano-sphere (average diameter: ca. 100 nm) of the SH-POSS domains, some portions were dispersed in the PnBMA polymer matrix as a result of hydrophobic interactions between the isobutyl groups of SH-POSS and the butyl groups of PnBMA (bottom inserted scheme, Fig. 51(a)). The gray nano-sphere composed of the SH-POSS macromer was formed as a result of strong POSS-POSS interactions between the SH-POSS units after desorption of Au-S covalent bond. Some of the Au NPs surrounded by SH-POSS units in the gray nano-sphere had connected together to form twinned particles after the desorption of the Au-S covalent bonds. To improve the miscibility in the Au-POSS/PnBMA nanocomposite, the PnBMA matrix was replaced by the random copolymer of PnBMA-*r*-PiBPPMA which was expected to be more compatible with Au-POSS through both POSS-POSS and hydrophobic butyl interactions (see inset scheme to Fig. 51(b)), demonstrating that the Au NPs were indeed more-evenly distributed within this random copolymer matrix than that in the PnBMA homopolymer matrix.

6. Conclusions

The POSS nanocomposites presented herein are composite materials reinforced with silica cages, ultrafine fillers of nanometer size, almost equal to the size of the polymer matrix. Even if the POSS content was as low as ca. 1–5 wt%, individual POSS particles could exist at distances as close as several nanometers apart. Therefore, these nanocomposites possessed microstructures that do not exist in conventional composites. For this reason, the field of POSS nanocomposite research has become extremely active in recent years [336]. In this review, we have discussed only those studies that have made major contributions to this research field, focusing on the preparation of such polymer-POSS nanocomposites as styryl-POSS, methacrylate-POSS, norbornyl-POSS, vinyl-POSS, epoxy-POSS, phenolic-POSS, benzoxazine-POSS, amine-POSS, and hydroxyl-POSS. Both monofunctional and multifunctional monomers of these types have been used to prepare commercial and/or high-performance thermoplastic and thermosetting polymers. We have also focused on discussing the corresponding thermal, dynamic mechanical, electrical, and surface properties of these materials.

Acknowledgments

This work was supported financially by the National Science Council, Taiwan, Republic of China, under contracts no. NSC 97-2221-E-110-013-MY3, NSC 99-2628-E-110-003, and NSC 99-2120-M-009-008.

References

- [1] Li G, Wang L, Ni H, Pittman Jr CU. Polyhedral oligomeric silsesquioxane (POSS) polymers and copolymers: a review. *J Inorg Organomet Polym* 2001;11:123–54.
- [2] Li G, Pittman Jr CU. Polyhedral oligomeric silsesquioxane (POSS) polymers, copolymers and resin nanocomposites. In: Abe-El-Aziz AS, Carraher Jr CE, Pittman Jr CU, Zeldin M, editors. *Macromolecules containing metal and metal-like elements*, vol. 4. Hoboken, NJ: John A Wiley & Sons; 2005. p. 79–132.
- [3] Scott DW. Thermal rearrangement of branched-chain methylpolysiloxanes. *J Am Chem Soc* 1946;68:356–8.
- [4] Baney RH, Itoh M, Sakakibara A, Suzuki T. Silsesquioxanes. *Chem Rev* 1995;95:1409–30.
- [5] Wu J, Mather PT. POSS polymers: physical properties and biomaterials applications. *Polym Rev* 2009;49:25–63.
- [6] Kawakami Y, Kakihana Y, Miyazato A, Tateyama S, Hoque MA. Polyhedral oligomeric silsesquioxanes with controlled structure: formation and application in new Si-based polymer systems. *Adv Polym Sci* 2010;55:1–44.
- [7] Voronkov MG, Lavrentyev VI. Polyhedral oligosilsesquioxanes and their homo derivatives. *Top Curr Chem* 1982;102:199–236.
- [8] Martynova TN, Chupakhina TI. Heterofunctional oligoorganosilsesquioxanes. *J Organometal Chem* 1988;345:10–8.
- [9] Shockey EG, Bolf AG, Jones PF, Schwab JJ, Chaffee KP, Haddad TS, Lichtenhan JD. Functionalized polyhedral oligosilsesquioxane (POSS) macromers: new graftable POSS hydride, POSS a-Olefin, POSS epoxy, and POSS chlorosilane macromers and POSS-siloxane triblocks. *Appl Organometal Chem* 1999;13:311–27.
- [10] Marcolli C, Calzaferri G. Review monosubstituted octasilsesquioxanes. *Appl Organometal Chem* 1999;13:213–26.
- [11] Agaskar PA. New synthetic route to the hydridospherosiloxanes Oh-H8Si8O12 and D5h-H10Si10O15. *Inorg Chem* 1991;30:2707.
- [12] Chalk AJ, Harrod JF. Homogeneous catalysis. II. The mechanism of the hydrosilylation of olefins catalyzed by group VIII metal complexes. *J Am Chem Soc* 1965;87:16–21.
- [13] Tsuchida A, Bolln C, Sernetz FG, Frey H, Mulhaupt R. Ethene and propene copolymers containing silsesquioxane side groups. *Macromolecules* 1997;30:2818–24.
- [14] Feher FJ. Polyhedral oligometallasilsesquioxanes (POMSS) as models for silica-supported transition-metal catalysts. Synthesis and characterization of (C5Me5)Zr[(SiO7)2](c-C6H11)7]. *J Am Chem Soc* 1986;108:3850–2.
- [15] Feher FJ, Weller KJ. Polyhedral aluminosilsesquioxanes as models for aluminosilicates: unique synthesis of anionic aluminum/silicon/oxygen frameworks. *Organometallics* 1990;9:2638–40.
- [16] Feher FJ, Weller KJ. Synthesis and characterization of labile spherosilicates: [(Me3SnO)8Si8O12] and [(Me4SbO)8Si8O12]. *Inorg Chem* 1991;30:880–2.
- [17] Feher FJ, Newman DA, Walzer JF. Silsesquioxanes as models for silica surfaces. *J Am Chem Soc* 1989;111:1741–8.
- [18] Ruffieux V, Schmid G, Braunstein P, Rose J. Oligosilsesquioxane8-OSS-ethylidiphenylphosphine: a new functional oligosilsesquioxane ligand. *Chem Eur J* 1997;3:900–3.
- [19] Murugavel R, Voigt A, Walawalkar MG, Roesky HW. Hetero- and metallasiloxanes derived from silanediols, disilanols, silanetriols, and trisilanols. *Chem Rev* 1996;96:2205–36.
- [20] Feher FJ, Budzichowski TA, Weller KJ. Polyhedral aluminosilsesquioxanes: soluble organic analogs of aluminosilicates. *J Am Chem Soc* 1989;111:7288–9.
- [21] Feher FJ, Budzichowski TA. Heterosilsesquioxanes: synthesis and characterization of group 15 containing polyhedral oligosilsesquioxanes. *Organometallics* 1991;10:812–5.
- [22] Frye CL, Collins WT. Oligomeric silsesquioxanes, (HSiO3/2)*n*. *J Am Chem Soc* 1970;92:5586–8.
- [23] Zhang C, Laine RM. Hydrosilylation of allyl alcohol with [HSiMe2OSiO1.5]8: octa(3-hydroxypropyldimethylsiloxy) octasilsesquioxane and its octamethacrylate derivative as potential precursors to hybrid nanocomposites. *J Am Chem Soc* 2000;122:6979–88.
- [24] Sellinger A, Laine RM. Silsesquioxanes as synthetic platforms. Thermally curable and photocurable inorganic/organic hybrids. *Macromolecules* 1996;29:2327–30.
- [25] Shenn YC, Lu CH, Huang CF, Kuo SW, Chang FC. Synthesis and characterization of amorphous octakis-functionalized polyhedral oligomeric silsesquioxanes for polymer nanocomposites. *Polymer* 2008;49:4017–24.
- [26] Painter PC, Coleman MC. Hydrogen bonded polymer blends. *Prog Polym Sci* 1995;20:1–59.
- [27] Lee YJ, Kuo SW, Huang WJ, Lee HY, Chang FC. Miscibility, specific interactions, and self-assembly behavior of phenolic/polyhedral oligomeric silsesquioxane hybrids. *J Polym Sci Part B: Polym Phys* 2004;42:1127–36.

- [28] Noda I. Two-dimensional infrared spectroscopy. *J Am Chem Soc* 1989;111:8116–8.
- [29] Noda I, Ozaki Y. Two-dimensional correlation spectroscopy: applications in vibrational and optical spectroscopy. Chichester, UK: John Wiley & Sons Inc.; 2004.
- [30] Coleman MM, Gref JF, Painter PC. Specific interactions and the miscibility of polymer blends. Lancaster, PA: Technomic Publishing; 1991.
- [31] Coleman MM, Painter PC. Miscible polymer blend-background and guide for calculations and design. Lancaster, PA: DEStech Publications Inc.; 2006.
- [32] Coggesthall ND, Saier EL. Infrared absorption study of hydrogen bonding equilibria. *J Am Chem Soc* 1951;73:5414–8.
- [33] Wu HD, Chu PP, Ma CCM, Chang FC. Effects of molecular structure of modifiers on the thermodynamics of phenolic blends: an entropic factor complementing PCAM. *Macromolecules* 1999;32:3097–105.
- [34] Kuo SW, Chang FC. Miscibility behavior and specific interaction of phenolic resin with poly(acetoxystyrene) blends. *Macromol Chem Phys* 2002;203:868–78.
- [35] Kuo SW, Lin HC, Huang WJ, Huang CF, Chang FC. Hydrogen bonding interaction between phenolic resin and octa(acetoxystyryl) polyhedral oligomeric silsesquioxane (AS-POSS) nanocomposites. *J Polym Sci Part B: Polym Phys* 2006;44:673–86.
- [36] Kuo SW, Chang FC. Effect of copolymer composition on the miscibility of poly(styrene-co-acetoxystyrene) with phenolic. *Polymer* 2001;42:9843–8.
- [37] Kuo SW, Liu WP, Chang FC. Effect of hydrolysis on the strength of hydrogen bonds and Tg of poly(vinyl phenol-co-acetoxystyrene). *Macromolecules* 2003;36:5168–73.
- [38] Kuo SW, Huang WJ, Huang CF, Chan SC, Chang FC. Miscibility, specific interactions, and spherulite growth rates of binary poly(acetoxystyrene)/poly(ethylene oxide) blends. *Macromolecules* 2004;37:4164–73.
- [39] Huang CF, Kuo SW, Lin HC, Chen JK, Chen YK, Xu H, Chang FC. Thermal properties, miscibility and specific interactions in comparison of linear and star poly(methyl methacrylate) blend with phenolic. *Polymer* 2004;45:5913–21.
- [40] Lin HC, Kuo SW, Huang CF, Chang FC. Syntheses, thermal property, and specific interaction of phenolic/octaphenol-POSS nanocomposites. *Macromol Rapid Commun* 2006;27:537–41.
- [41] Pan C. Polyhedral oligomeric silsesquioxane (POSS). In: Mark J, editor. *Physical properties of polymers handbook*, vol. 6. New York: Springer; 2007. p. 577–84.
- [42] Zheng L, Farris RJ, Coughlin EB. Synthesis of polyethylene hybrid copolymers containing polyhedral oligomeric silsesquioxane prepared with ring-opening metathesis copolymerization. *J Polym Sci Part A: Polym Chem* 2001;39:2920–8.
- [43] Waddon AJ, Zheng L, Farris RJ, Coughlin EB. Nanostructured polyethylene-POSS copolymers: control of crystallization and aggregation. *Nano Lett* 2002;2:1149–55.
- [44] Fu BX, Gelfer MY, Hsiao BS, Phillips S, Biers B, Blanski R, Ruth P. Physical gelation in ethylene-propylene copolymer melts induced by polyhedral oligomeric silsesquioxane (POSS) molecules. *Polymer* 2003;44:1499–506.
- [45] Joshi M, Butola BS. Studies on nonisothermal crystallization of HDPE/POSS nanocomposites. *Polymer* 2004;45:4953–68.
- [46] Capaldi FM, Rutledge GC, Boyce MC. Structure and dynamics of blends of polyhedral oligomeric silsesquioxanes and polyethylene by atomistic simulation. *Macromolecules* 2005;38:6700–9.
- [47] Joshi M, Butola BS, Simon G, Kukaleva N. Rheological and viscoelastic behavior of HDPE/octamethyl-POSS nanocomposites. *Macromolecules* 2006;39:1839–49.
- [48] He FA, Zhang LM. Using inorganic POSS-modified laponite clay to support a nickel α -diimine catalyst for in situ formation of high performance polyethylene nanocomposites. *Nanotechnology* 2006;17:5941–6.
- [49] Joshi M, Butola BS. Isothermal crystallization of HDPE/octamethyl polyhedral oligomeric silsesquioxane nanocomposites: role of POSS as a nanofiller. *J Appl Polym Sci* 2007;105:978–85.
- [50] Zhang HX, Jung MS, Shin YJ, Yoon KB, Lee DH. Preparation and properties of ethylene/POSS copolymer with rac-Et(Ind)₂ZrCl₂ catalyst. *J Appl Polym Sci* 2009;111:2697–702.
- [51] Zheng L, Hong S, Cardoen G, Burgaz E, Gido SP, Coughlin EB. Polymer nanocomposites through controlled self-assembly of cubic silsesquioxane scaffolds. *Macromolecules* 2004;37:8606–11.
- [52] Zheng L, Farris RJ, Coughlin EB. Novel polyolefin nanocomposites: synthesis and characterizations of metallocene-catalyzed polyolefin polyhedral oligomeric silsesquioxane copolymers. *Macromolecules* 2001;34:8034–9.
- [53] Mather PT, Jeon HG, Uribe AR. Mechanical relaxation and microstructure of poly(norbornyl-POSS) copolymers. *Macromolecules* 1999;32:1194–203.
- [54] Wang J, Ye Z, Joly H. Synthesis and characterization of hyperbranched polyethylenes tethered with polyhedral oligomeric silsesquioxane (POSS) nanoparticles by chain walking ethylene copolymerization with acryloisobutyl-POSS. *Macromolecules* 2007;40:6150–63.
- [55] Zhang HX, Shin YJ, Yoon KB, Lee DH. Preparation and properties of propylene/POSS copolymer with rac-Et(Ind)₂ZrCl₂ catalyst. *Eur Polym J* 2009;45:40–6.
- [56] Fu BX, Yang C, Somani RH, Zong SX, Hsiao BS, Phillips S, Blanski R, Ruth D. Crystallization studies of isotactic polypropylene containing nanostructured polyhedral oligomeric silsesquioxane molecules under quiescent and shear conditions. *J Polym Sci Part B: Polym Phys* 2001;39:2727–39.
- [57] Fina A, Tabuani D, Frache A, Camino G. Polypropylene-polyhedral oligomeric silsesquioxanes (POSS) nanocomposites. *Polymer* 2005;46:7855–66.
- [58] Pracella M, Chionna D, Fina A, Tabuani D, Frache A, Camino G. Polypropylene-POSS nanocomposites: morphology and crystallization behavior. *Macromol Symp* 2006;234:59–67.
- [59] Fina A, Abbenhuis HCL, Tabuani D, Camino G. Metal functionalized POSS as fire retardants in polypropylene. *Polym Degrad Stab* 2006;91:2275–81.
- [60] Baldi F, Bignotti F, Fina A, Tabuani D, Ricco T. Mechanical characterization of polyhedral oligomeric silsesquioxane/polypropylene blends. *J Appl Polym Sci* 2007;105:935–43.
- [61] Carniato F, Fina A, Tabuani D, Boccaleri E. Polypropylene containing Ti- and Al-polyhedral oligomeric silsesquioxanes: crystallization process and thermal properties. *Nanotechnology* 2008;19:475701/1–9.
- [62] Fina A, Tabuani D, Peijs T, Camino G. POSS grafting on PP-g-MA by one-step reactive blending. *Polymer* 2009;50:218–26.
- [63] Chen JH, Chiou YD. Crystallization behavior and morphological development of isotactic polypropylene blended with nanostructured polyhedral oligomeric silsesquioxane molecules. *J Polym Sci Part B: Polym Phys* 2006;44:2122–34.
- [64] Chen JH, Yao BX, Su WB, Yang YB. Isothermal crystallization behavior of isotactic polypropylene blended with small loading of polyhedral oligomeric silsesquioxane. *Polymer* 2007;48:1756–69.
- [65] Zhou Z, Cui L, Zhang Y, Zhang Y, Yin N. Isothermal crystallization kinetics of polypropylene/POSS composites. *J Polym Sci Part B: Polym Phys* 2008;46:1762–72.
- [66] Zhou Z, Zhang Y, Zeng Z, Zhang Y. Properties of POSS-filled polypropylene: comparison of physical blending and reactive blending. *J Appl Polym Sci* 2008;110:3745–51.
- [67] Zhou Z, Cui L, Zhang Y, Zhang Y, Yin N. Preparation and properties of POSS grafted polypropylene by reactive blending. *Eur Polym J* 2008;44:3057–66.
- [68] Zhou Z, Zhang Y, Zhang Y, Yin N. Rheological behavior of polypropylene/octavinyl polyhedral oligomeric silsesquioxane composites. *J Polym Sci Part B: Polym Phys* 2008;46:526–33.
- [69] Misra R, Fu BX, Morgan SE. Surface energetics, dispersion, and nanotribomechanical behavior of POSS/PP hybrid nanocomposites. *J Polym Sci Part B: Polym Phys* 2007;45:2441–55.
- [70] Tang Y, Lewin M. Migration and surface modification in polypropylene (PP)/polyhedral oligomeric silsesquioxane (POSS) nanocomposites. *Polymer Adv Technol* 2009;20:1–15.
- [71] Soong SY, Cohen RE, Boyce MC, Mulliken AD. Rate-dependent deformation behavior of POSS-filled and plasticized poly(vinyl chloride). *Macromolecules* 2006;39:2900–8.
- [72] Soong SY, Cohen RE, Boyce MC. Polyhedral oligomeric silsesquioxane as a novel plasticizer for poly(vinyl chloride). *Polymer* 2007;48:1410–8.
- [73] Zeng K, Liu Y, Zheng S. Poly(ethylene imine) hybrids containing polyhedral oligomeric silsesquioxanes: preparation, structure and properties. *Eur Polym J* 2008;44:3946–56.
- [74] Haddad TS, Lichtenhan JD. Hybrid organic-inorganic thermoplastics: styryl-based polyhedral oligomeric silsesquioxane polymers. *Macromolecules* 1996;29:7302–4.
- [75] Romo-Uribe A, Mather PT, Haddad TS, Lichtenhan JD. Viscoelastic and morphological behavior of hybrid styryl-based polyhedral oligomeric silsesquioxane (POSS) copolymers. *J Polym Sci Part B: Polym Phys* 1998;36:1857–72.
- [76] Wu J, Haddad TS, Kim GM, Mather PT. Rheological behavior of entangled polystyrene-polyhedral oligosilsesquioxane (POSS) copolymers. *Macromolecules* 2007;40:544–54.

- [77] Wu J, Haddad TS, Mather PT. Vertex group effects in entangled polystyrene–polyhedral oligosilsesquioxane (POSS) copolymers. *Macromolecules* 2009;42:1142–52.
- [78] Patel RR, Mohanraj R, Pittman Jr CU. Properties of polystyrene and polymethyl methacrylate copolymers of polyhedral oligomeric silsesquioxanes: a molecular dynamics study. *J Polym Sci Part B: Polym Phys* 2006;44:234–48.
- [79] Monticelli O, Fina A, Ullah A, Waghmare P. Preparation, characterization, and properties of novel PSMA–POSS systems by reactive blending. *Macromolecules* 2009;42:6614–23.
- [80] Cardoen G, Coughlin EB. Hemi-telechelic polystyrene–POSS copolymers as model systems for the study of well-defined inorganic/organic hybrid materials. *Macromolecules* 2004;37:5123–6.
- [81] Zheng W, Zhuang X, Li X, Lin Y, Bai J, Chen Y. Preparation and characterization of organic/inorganic hybrid polymers containing polyhedral oligomeric silsesquioxane via RAFT polymerization. *React Funct Polym* 2009;69:124–9.
- [82] Ge Z, Wang D, Zhou Y, Liu H, Liu S. Synthesis of organic/inorganic hybrid quatrefoil-shaped star-cyclic polymer containing a polyhedral oligomeric silsesquioxane core. *Macromolecules* 2009;42:2903–10.
- [83] Ning H, Martin B, Andreas S. Dielectric properties of nanocomposites based on polystyrene and polyhedral oligomeric phenethylsilsesquioxanes. *Macromolecules* 2007;40:9672–9.
- [84] Carroll JB, Waddon AJ, Nakade H, Rotello VM. “Plug and Play” polymers. Thermal and X-ray characterizations of noncovalently grafted polyhedral oligomeric silsesquioxane (POSS)–polystyrene nanocomposites. *Macromolecules* 2003;36:6289–91.
- [85] Zheng L, Kasi RM, Farris RJ, Coughlin EB. Synthesis and thermal properties of hybrid copolymers of syndiotactic polystyrene and polyhedral oligomeric silsesquioxane. *J Polym Sci Part A: Polym Chem* 2002;40:885–91.
- [86] Zhang HX, Lee HY, Shin YJ, Yoon KB, Noh SK, Lee DH. Preparation and characterization of styrene/styryl–polyhedral oligomeric silsesquioxane hybrid copolymers. *Polym Int* 2008;57:1351–6.
- [87] Xu H, Kuo SW, Huang CF, Chang FC. Poly(acetoxystyrene-co-isobutylstyryl POSS) nanocomposites: characterization and molecular interaction. *J Polym Res* 2002;9:239–44.
- [88] Xu H, Kuo SW, Lee JS, Chang FC. Preparations, thermal properties and T_g increase mechanism of inorganic/organic hybrid polymers based on polyhedral oligomeric silsesquioxanes. *Macromolecules* 2002;35:8788–93.
- [89] Xu H, Yang B, Wang J, Guang S, Li C. Preparation, thermal properties, and T_g increase mechanism of poly(acetoxystyrene-co-octavinyl-polyhedral oligomeric silsesquioxane) hybrid nanocomposites. *Macromolecules* 2005;38:10455–60.
- [90] Yang B, Xu H, Wang J, Gang S, Li C. Preparation and thermal property of hybrid nanocomposites by free radical copolymerization of styrene with octavinyl polyhedral oligomeric silsesquioxane. *J Appl Polym Sci* 2007;106:320–6.
- [91] Kuo SW, Kao HC, Chang FC. Thermal behavior, and specific interaction in high glass transition temperature PMMA copolymer. *Polymer* 2003;44:6873–82.
- [92] Chen JK, Kuo SW, Kao HC, Chang FC. Thermal property, specific interaction and surface energy in high glass transition temperature and low moisture absorption PMMA terpolymers. *Polymer* 2005;46:2354–64.
- [93] Kuo SW, Tsai ST. Complementary multiple hydrogen-bonding interactions increase the glass transition temperatures to PMMA copolymer mixtures. *Macromolecules* 2009;42:4701–11.
- [94] Kuo SW, Lin CT, Chang FC. Synthesis and thermal properties of PMMA terpolymers through mediated by hydrogen bonding. *Polymer* 2010;51:883–9.
- [95] Lichtenhan JD, Otonari YA, Carr MJ. Linear hybrid polymer building blocks: methacrylate-functionalized polyhedral oligomeric silsesquioxane monomers and polymers. *Macromolecules* 1995;28:8435–7.
- [96] Kopesky ET, Haddad TS, Cohen RE, McKinley GH. Thermomechanical properties of poly(methyl methacrylate)s containing tethered and untethered polyhedral oligomeric silsesquioxanes. *Macromolecules* 2004;37:8992–9004.
- [97] Li GZ, Cho H, Wang L, Toghiani H, Pittman JC. Synthesis and properties of poly(isobutyl methacrylate-co-butanediol dimethacrylate-co-methacryl polyhedral oligomeric silsesquioxane) nanocomposites. *J Polym Sci Part A: Polym Chem* 2005;43:355–72.
- [98] Bizet S, Galy J, Gerard JF. Structure–property relationships in organic–inorganic nanomaterials based on methacryl-POSS and dimethacrylate networks. *Macromolecules* 2006;39:2574–83.
- [99] Kopesky ET, McKinley GH, Cohen RE. Toughened poly(methyl methacrylate) nanocomposites by incorporating polyhedral oligomeric silsesquioxanes. *Polymer* 2006;47:299–309.
- [100] Castelvetro V, Ciardelli F, Vita CD, Puppo A. Hybrid nanocomposite films from mono- and multi-functional POSS copolyacrylates in miniemulsion. *Macromol Rapid Commun* 2006;27:619–25.
- [101] Escude NC, Chen EYX. Stereoregular methacrylate-POSS hybrid polymers: syntheses and nanostructured assemblies. *Chem Mater* 2009;21:5743–53.
- [102] Costa ROR, Vasconcelos WL, Tamaki R, Laine RM. Organic/inorganic nanocomposite star polymers via atom transfer radical polymerization of methyl methacrylate using octafunctional silsesquioxane cores. *Macromolecules* 2001;34:5398–407.
- [103] Ohno K, Sugiyama S, Koh K, Tsujii Y, Fukuda T, Yamahiro M, Oikawa H, Yamamoto Y, Ootake N, Watanabe K. Living radical polymerization by polyhedral oligomeric silsesquioxane-holding initiators: precision synthesis of tadpole-shaped organic/inorganic hybrid polymers. *Macromolecules* 2004;37:8517–22.
- [104] Koh K, Sugiyama S, Morinaga T, Ohno K, Tsujii Y, Fukuda T, Yamahiro M, Iijima T, Oikawa H, Watanabe K, Miyashita T. Precision synthesis of a fluorinated polyhedral oligomeric silsesquioxane-terminated polymer and surface characterization of its blend film with poly(methyl methacrylate). *Macromolecules* 2005;38:1264–70.
- [105] Huang CF, Kuo SW, Lin FJ, Huang WJ, Wang CF, Chen WY, Chang FC. Influence of PMMA-chain-end tethered polyhedral oligomeric silsesquioxanes (POSS) on the miscibility and specific interaction with phenolic blends. *Macromolecules* 2006;39:300–8.
- [106] Kotal A, Si S, Paira TK, Mandal TK. Synthesis of semitelechelic POSS–polymethacrylate hybrids by thiol-mediated controlled radical polymerization with unusual thermal behaviors. *J Polym Sci Part A: Polym Chem* 2008;46:1111–23.
- [107] Liu L, Wang W. Synthesis and characterization of poly(methyl methacrylate) using monofunctional polyhedral oligomeric silsesquioxane as an initiator. *Polym Bull* 2009;62:315–25.
- [108] Chen R, Feng W, Zhu S, Botton G, Ong B, Wu Y. Surface-initiated atom transfer radical polymerization of polyhedral oligomeric silsesquioxane (POSS) methacrylate from flat silicon wafer. *Polymer* 2006;47:1119–23.
- [109] Kopesky ET, Haddad TS, McKinley GH, Cohen RE. Miscibility and viscoelastic properties of acryl polyhedral oligomeric silsesquioxane–poly(methyl methacrylate) blends. *Polymer* 2005;46:4743–52.
- [110] Xu H, Yang B, Wang J, Guang S, Li C. Preparation, T_g improvement, and thermal stability enhancement mechanism of soluble poly(methyl methacrylate) nanocomposites by incorporating octavinyl polyhedral oligomeric silsesquioxanes. *J Polym Sci Part A: Polym Chem* 2007;45:5308–17.
- [111] Markovic E, Clarke S, Matison J, George P. Simon synthesis of POSS–methyl methacrylate-based cross-linked hybrid materials. *Macromolecules* 2008;41:1685–92.
- [112] Zhao C, Yang X, Wu X, Liu X, Wang X, Lu L. Preparation and characterization of poly(methyl methacrylate) nanocomposites containing octavinyl polyhedral oligomeric silsesquioxane. *Polym Bull* 2008;60:495–505.
- [113] Liu YL, Tseng MC, Chiang MH. Polymerization and nanocomposites properties of multifunctional methylmethacrylate POSS. *J Polym Sci Part A: Polym Chem* 2008;46:5157–66.
- [114] Zucchi IA, Galante MJ, Williams RJJ. Surface energies of linear and cross-linked polymers based on isobornyl methacrylate and methacryl-hepta-isobutyl POSS. *Eur Polym J* 2009;45:325–31.
- [115] Feng Y, Jia Y, Xu H. Preparation and thermal properties of hybrid nanocomposites of poly(methyl methacrylate)/octavinyl polyhedral oligomeric silsesquioxane blends. *J Appl Polym Sci* 2009;111:2684–90.
- [116] Seurer B, Coughlin EB. Fluoroelastomer copolymers incorporating polyhedral oligomeric silsesquioxane. *Macromol Chem Phys* 2008;209:2040–8.
- [117] Gungor E, Bilir C, Durmaz H, Hizal G, Tunca U. Star polymers with POSS via azide–alkyne click reaction. *J Polym Sci Part A: Polym Chem* 2009;47:5947–53.
- [118] Tanaka K, Adachi S, Chujo Y. Structure–property relationship of octa-substituted POSS in thermal and mechanical reinforcements of conventional polymers. *J Polym Sci Part A: Polym Chem* 2009;47:5690–7.
- [119] Chiu CY, Chen HW, Kuo SW, Huang CF, Chang FC. Investigation of miscibility effect on ionic conductivity based on LiClO₄/PEO/PCL ternary blends. *Macromolecules* 2004;37:8424–30.
- [120] Chiu CY, Hsu WH, Yen YJ, Kuo SW, Chang FC. Miscibility behavior and interaction mechanism of polymer electrolytes comprising

- LiClO₄ and MPEG-block-PCL copolymers. *Macromolecules* 2005;38:6640–7.
- [121] Yen YJ, Cheng CC, Kuo SW, Chang FC. A supramolecular solid state polymer electrolyte. *Macromolecules* 2010;43:2634–7.
- [122] Prithwiraj M, Stephanie L, Wunder SL. Oligomeric poly(ethylene oxide)-functionalized silsesquioxanes: interfacial effects on Tg, Tm, and ΔHm. *Chem Mater* 2002;14:4494–7.
- [123] Huang J, Li X, Lin T, He C, Mya KY, Xiao Y, Li J. Inclusion complex formation between α, γ-cyclodextrins and organic–inorganic star-shaped poly(ethylene glycol) from an octafunctional silsesquioxane core. *J Polym Sci Part B: Polym Phys* 2004;42:1173–80.
- [124] Prithwiraj M, Wunder SL. POSS based electrolytes for rechargeable lithium batteries. *Electrochem Solid-State Lett* 2004;7:A88–92.
- [125] Zhang H, Kulkarni S, Wunder SL. Polyethylene glycol functionalized polyoctahedral silsesquioxanes as electrolytes for lithium batteries. *J Electrochem Soc* 2006;153:A239–48.
- [126] Zhang H, Kulkarni S, Wunder SL. Blends of POSS-PEO(n)/4/8 and high molecular weight poly(ethylene oxide) as solid polymer electrolytes for lithium batteries. *J Phys Chem B* 2007;111:3583–90.
- [127] Markovic E, Ginic-Markovic M, Clarke S, Matison J, Hussain M, Simon GP. Poly(ethylene glycol)-octafunctionalized polyhedral oligomeric silsesquioxane: synthesis and thermal analysis. *Macromolecules* 2007;40:2694–701.
- [128] Lee YJ, Huang JM, Kuo SW, Chang FC. Low dielectric, nanoporous polyimide films prepared from PEO-POSS nanoparticles. *Polymer* 2005;46:10056–65.
- [129] Harada A, Li J, Kamachi M. Synthesis of a tubular polymer from threaded cyclodextrins. *Nature* 1993;364:516–8.
- [130] Harada A, Li J, Kamachi M. Double-stranded inclusion complexes of cyclodextrin threaded on poly(ethylene glycol). *Nature* 1994;370:126–8.
- [131] Zeng K, Zheng S. Synthesis and characterization of organic/inorganic polyrotaxanes from polyhedral oligomeric silsesquioxane and poly(ethylene oxide)/α-cyclodextrin polypseudorotaxanes via Click chemistry. *Macromol Chem Phys* 2009;210:783–91.
- [132] Mu J, Liu Y, Zheng S. Inorganic–organic interpenetrating polymer networks involving polyhedral oligomeric silsesquioxane and poly(ethylene oxide). *Polymer* 2007;48:1176–84.
- [133] Huang KW, Tsai LW, Kuo SW. Influence of octakis-functionalized groups on polyhedral oligomeric silsesquioxanes (POSS) for polymer nanocomposites. *Polymer* 2009;50:4876–87.
- [134] Kim BS, Mather PT. Amphiphilic telechelics incorporating polyhedral oligosilsesquioxane. 1. Synthesis and characterization. *Macromolecules* 2002;35:8378–84.
- [135] Kim BS, Mather PT. Amphiphilic telechelics with polyhedral oligosilsesquioxanes (POSS) end-groups: dilute solution viscometry. *Polymer* 2006;47:6202–7.
- [136] Lee W, Ni S, Deng J, Kim BS, Sattija SK, Mather PT, Esker AR. Telechelic poly(ethylene glycol)-POSS amphiphiles at the air/water interface. *Macromolecules* 2007;40:682–8.
- [137] Chan SC, Kuo SW, Chang FC. Synthesis of the organic–inorganic hybrid star polymers and their inclusion complexes with cyclodextrins. *Macromolecules* 2005;38:3099–107.
- [138] Liu YH, Yang XT, Zhang WA, Zheng SX. Star-shaped poly(3-caprolactone) with polyhedral oligomeric silsesquioxane core. *Polymer* 2006;47:6814–25.
- [139] Chan SC, Kuo SW, She HS, Lin HM, Lee HF, Chang FC. Supramolecular aggregations through inclusion complexation of cyclodextrins and polymers with bulky end group. *J Polym Sci Part A: Polym Chem* 2007;45:125–35.
- [140] Ni Y, Zheng S. Melting and crystallization behavior of polyhedral oligomeric silsesquioxane-capped poly(ε-caprolactone). *J Polym Sci Part B: Polym Phys* 2007;45:2201–14.
- [141] Goffin AL, Duquesne E, Moins S, Alexandre M, Dubois P. New organic–inorganic nanohybrids via ring opening polymerization of (di)lactones initiated by functionalized polyhedral oligomeric silsesquioxane. *Eur Polym J* 2007;43:4103–13.
- [142] Lee KM, Knight PT, Chung T, Mather PT. Polycaprolactone-POSS chemical/physical double networks. *Macromolecules* 2008;41:4730–8.
- [143] Ni Y, Zheng S. Supramolecular inclusion complexation of polyhedral oligomeric silsesquioxane capped poly(ε-caprolactone) with α-cyclodextrin. *J Polym Sci Part A: Polym Chem* 2007;45:1247–59.
- [144] Zeng K, Wang L, Zheng S, Qian X. Self-assembly behavior of hepta(3,3,3-trifluoropropyl) polyhedral oligomeric silsesquioxane-capped poly(3-caprolactone) in epoxy resin: nanostructures and surface properties. *Polymer* 2009;50:685–95.
- [145] Kai W, Hua L, Dong T, Pan P, Zhu B, Inoue Y. Polyhedral oligomeric silsesquioxane- and fullerene-end-capped poly(ε-caprolactone). *Macromol Chem Phys* 2008;209:1191–7.
- [146] Hana R, Hartmann R, Bohlen C, Brandenberger S, Kawada J, Lowe C, Zinn M, Witholt B, Robert H. Marchessault chemical synthesis and characterization of POSS-functionalized poly[3-hydroxyalkanoates]. *Polymer* 2005;46:5025–31.
- [147] Zhao Y, Schiraldi DA. Thermal and mechanical properties of polyhedral oligomeric silsesquioxane (POSS)/polycarbonate composites. *Polymer* 2005;46:11640–7.
- [148] Hao N, Bolning M, Coering H, Scholnhals A. Nanocomposites of polyhedral oligomeric phenethylsilsesquioxanes and poly(bisphenol A carbonate) as investigated by dielectric spectroscopy. *Macromolecules* 2007;40:2955–64.
- [149] Sanchez-Soto M, Schiraldi DA, Illescas S. Study of the morphology and properties of melt-mixed polycarbonate-POSS nanocomposites. *Eur Polym J* 2009;45:341–52.
- [150] Yoon KH, Polk MB, Park JH, Min BG, Schiraldi DA. Properties of poly(ethylene terephthalate) containing epoxy-functionalized polyhedral oligomeric silsesquioxane. *Polym Int* 2005;54:47–53.
- [151] Zhou Z, Yin N, Zhang Y, Zhang Y. Properties of poly(butylene terephthalate) chain-extended by epoxycyclohexyl polyhedral oligomeric silsesquioxane. *J Appl Polym Sci* 2008;107:825–30.
- [152] Kim KJ, Ramasundaram S, Soon LJ. Synthesis and characterization of poly(trimethylene terephthalate)/polyhedral oligomeric silsesquioxanes nanocomposites. *Polym Compos* 2008;29:894–901.
- [153] Ricco L, Russo S, Monticelli O, Bordo A, Bellucci F. 3-Caprolactam polymerization in presence of polyhedral oligomeric silsesquioxanes (POSS). *Polymer* 2005;46:6810–9.
- [154] Baldi F, Bignotti F, Ricco L, Monticelli O, Ricco T. Mechanical and structural characterization of POSS modified polyamide 6. *J Appl Polym Sci* 2006;100:3409–14.
- [155] Li B, Zhang Y, Wang S, Ji J. Effect of POSS on morphology and properties of poly(2,6-dimethyl-1,4-phenylene oxide)/polyamide 6 blends. *Eur Polym J* 2009;45:2202–10.
- [156] Yu H, Ren W, Zhang Y. Nonisothermal decomposition kinetics of nylon 1010/POSS composites. *J Appl Polym Sci* 2009;113:17–23.
- [157] Wan C, Zhao F, Bao X, Kandasubramanian B, Duggan M. Effect of POSS on crystalline transitions and physical properties of polyamide 12. *J Polym Sci Part B: Polym Phys* 2009;47:121–9.
- [158] Fu HK, Kuo SW, Huang CF, Chang FC, Lin HC. Synthesis and characterization the stimuli-responsive ZnS/PNIPAM hollow spheres. *Polymer* 2009;50:1246–50.
- [159] Huang CJ, Chang FC. Using click chemistry to fabricate ultrathin thermoresponsive microcapsules through direct covalent layer-by-layer assembly. *Macromolecules* 2009;42:5155–66.
- [160] Huang CJ, Chang FC. Polypeptide diblock copolymers: syntheses and properties of poly(N-isopropylacrylamide)-b-polylysine. *Macromolecules* 2008;41:7041–52.
- [161] Mu J, Zheng S. Poly(N-isopropylacrylamide) nanocrosslinked by polyhedral oligomeric silsesquioxane: temperature-responsive behavior of hydrogels. *J Colloid Interface Sci* 2007;307:377–85.
- [162] Zeng K, Wang L, Zheng S. Rapid deswelling and reswelling response of poly(N-isopropylacrylamide) hydrogels via formation of interpenetrating polymer networks with polyhedral oligomeric silsesquioxane-capped poly(ethylene oxide) amphiphilic telechelics. *J Phys Chem B* 2009;113:11831–40.
- [163] Zeng K, Fang Y, Zheng S. Organic–inorganic hybrid hydrogels involving poly(N-isopropylacrylamide) and polyhedral oligomeric silsesquioxane: preparation and rapid thermoresponsive properties. *J Polym Sci Part B: Polym Phys* 2009;47:504–16.
- [164] Zhang W, Liu L, Zhuang X, Li X, Bai J, Chen YU. Synthesis and self-assembly of tadpole-shaped organic/inorganic hybrid poly(N-isopropylacrylamide) containing polyhedral oligomeric silsesquioxane via RAFT polymerization. *J Polym Sci Part A: Polym Chem* 2008;46:7049–61.
- [165] Eshel H, Dahan L, Dotan A, Dodiuk H, Kenig S. Nanotailoring of nanocomposite hydrogels containing POSS. *Polym Bull* 2008;61:257–65.
- [166] Xu H, Kuo SW, Huang CF, Chang FC. Characterization of poly(vinyl pyrrolidone-co-isobutylstyryl) polyhedral oligomeric silsesquioxane) nanocomposites. *J Appl Polym Sci* 2004;91:2208–15.
- [167] Yang B, Li J, Wang J, Xu H, Guang S, Li C. Poly(vinyl pyrrolidone-co-octavinyl) polyhedral oligomeric silsesquioxane) hybrid nanocomposites: preparation, thermal properties, and Tg improvement mechanism. *J Appl Polym Sci* 2008;111:2963–9.
- [168] Xu H, Kuo SW, Chang FC. Significant glass transition temperature increase based on polyhedral oligomeric silsesquioxane

- (POSS) copolymer through hydrogen bonding. *Polym Bull* 2002;48:469–74.
- [169] Xu H, Kuo SW, Lee JS, Chang FC. Glass transition temperatures of poly(hydroxystyrene-co-vinylpyrrolidone-co-isobutylstyryl polyhedral oligosilsesquioxanes). *Polymer* 2002;43:5117–24.
- [170] Chiu CY, Yen YJ, Kuo SW, Chen HW, Chang FC. Complicated phase behavior and ionic conductivities of PVP-co-PMMA-based polymer electrolytes. *Polymer* 2007;48:1329–42.
- [171] Yen YJ, Kuo SW, Huang CF, Chen JK, Chang FC. Miscibility and hydrogen bonding behavior in organic/inorganic polymer hybrids containing octaphenol polyhedral oligomeric silsesquioxane. *J Phys Chem B* 2008;112:10821–9.
- [172] Yen YC, Ye YS, Cheng CC, Chen HM, Sheu HS, Chang FC. Effect of LiClO₄ on the thermal and morphological properties of organic/inorganic polymer hybrids. *Polymer* 2008;49:3625–8.
- [173] Liu YL, Lee HC. Preparation and properties of polyhedral oligosilsesquioxane tethered aromatic polyamide nanocomposites through Michael addition between maleimide-containing polyamides and an amino-functionalized polyhedral oligosilsesquioxane. *J Polym Sci Part A: Polym Chem* 2006;44:4632–43.
- [174] Dvornic PR, Claire HP, Keinath SE, Hill EJ. Organic-inorganic polyamidoamine (PAMAM) dendrimer-polyhedral oligosilsesquioxane (POSS) nanohybrids. *Macromolecules* 2004;37:7818–31.
- [175] Kim KM, Ouchi Y, Chujo Y. Synthesis of organic-inorganic star-shaped polyoxazolines using octafunctional silsesquioxane as an initiator. *Polym Bull* 2003;49:341–8.
- [176] Kim KM, Keum DK, Chujo Y. Organic-inorganic polymer hybrids using polyoxazoline initiated by functionalized silsesquioxane. *Macromolecules* 2003;36:867–75.
- [177] Klok HA, Lecommandoux S. Supramolecular materials via block copolymer self-assembly. *Adv Mater* 2001;13:1217–29.
- [178] Kim KT, Park C, Vandermeulen GWM, Rider DA, Kim C, Winnik MA, Manners I. Gelation of helical polypeptide-random coil diblock copolymers by a nanoribbon mechanism. *Angew Chem Int Ed* 2005;44:7964–8.
- [179] Kim KT, Vandermeulen GWM, Winnik MA, Manners I. Organometallic-polypeptide block copolymers: synthesis and properties of poly(ferrocenyldimethylsilane)-*b*-poly(γ -benzyl-L-glutamate). *Macromolecules* 2005;38:4958–61.
- [180] Kuo SW, Lee HF, Huang CF, Huang CJ, Chang FC. Synthesis and self-assembly of helical polypeptide – random coil amphiphilic diblock copolymer. *J Polym Sci Part A: Polym Chem* 2008;46:3108–19.
- [181] Kuo SW, Lee HF, Huang WJ, Jeong KU, Chang FC. Solid state and solution self-assembly of helical polypeptides tethered to polyhedral oligomeric silsesquioxanes. *Macromolecules* 2009;42:1619–26.
- [182] Tamaki R, Choi J, Laine RM. A polyimide nanocomposite from octa(aminophenyl)silsesquioxane. *Chem Mater* 2003;15:793–7.
- [183] Huang J, Xiao Y, Mya KY, Liu X, He C, Dai J, Siow YP. Thermomechanical properties of polyimide-epoxy nanocomposites from cubic silsesquioxane epoxides. *J Mater Chem* 2004;14:2858–63.
- [184] Lee YJ, Huang JM, Kuo SW, Lu JS, Chang FC. Polyimide and polyhedral oligomeric silsesquioxane nanocomposites for low-dielectric applications. *Polymer* 2005;46:173–81.
- [185] Wahab MA, Mya KY, He C. Synthesis, morphology, and properties of hydroxyl terminated-POSS/polyimide low-k nanocomposite films. *J Polym Sci Part A: Polym Chem* 2008;46:5887–96.
- [186] Ye YS, Yen YC, Chen WY, Cheng CC, Chang FC. A simple approach toward low-dielectric polyimide nanocomposites: blending the polyimide precursor with a fluorinated polyhedral oligomeric silsesquioxane. *J Polym Sci Part A: Polym Chem* 2008;46:6296–304.
- [187] Ye YS, Chen WY, Wang YZ. Synthesis and properties of low-dielectric-constant polyimides with introduced reactive fluorine polyhedral oligomeric silsesquioxanes. *J Polym Sci Part A: Polym Chem* 2006;44:5391–402.
- [188] Chen YI, Kang ET. New approach to nanocomposites of polyimides containing polyhedral oligomeric silsesquioxane for dielectric applications. *Mater Lett* 2004;58:3716–9.
- [189] Chen YI, Chen L, Nie H, Kang ET. Low-k nanocomposite films based on polyimides with grafted polyhedral oligomeric silsesquioxane. *J Appl Polym Sci* 2006;99:2226–32.
- [190] Leu CM, Chang YT, Wei KH. Synthesis and dielectric properties of polyimide-tethered polyhedral oligomeric silsesquioxane (POSS) nanocomposites via POSS-diamine. *Macromolecules* 2003;36:9122–7.
- [191] Leu CM, Reddy GM, Wei KH, Shu CF. Synthesis and dielectric properties of polyimide-chain-end tethered polyhedral oligomeric silsesquioxane nanocomposites. *Chem Mater* 2003;15:2261–5.
- [192] Leu CM, Chang YT, Wei KH. Polyimide-side-chain tethered polyhedral oligomeric silsesquioxane nanocomposites for low-dielectric film applications. *Chem Mater* 2003;15:3721–7.
- [193] Wright ME, Petteys BJ, Guenther AJ, Fallis S, Yandek GR, Tomczak SJ, Minton TK, Brunsvold A. Chemical modification of fluorinated polyimides: new thermally curing hybrid polymers with POSS. *Macromolecules* 2006;39:4710–8.
- [194] Seckin T, Koytepe KS, Adigel HI. Molecular design of POSS core star polyimides as a route to low-k dielectric materials. *Mater Chem Phys* 2008;112:1040–6.
- [195] Wu S, Hayakawa T, Kikuchi R, Grunzinger SJ, Kakimoto MA. Synthesis and characterization of semiaromatic polyimides containing POSS in main chain derived from double-decker-shaped silsesquioxane. *Macromolecules* 2007;40:5698–705.
- [196] Wu S, Hayakawa T, Kakimoto MA, Oikawa H. Synthesis and characterization of organosoluble aromatic polyimides containing POSS in main chain derived from double-decker-shaped silsesquioxane. *Macromolecules* 2008;41:3481–7.
- [197] Fu BX, Hsiao BS, Pagola S, Stephens P, White H, Rafailovich M, Sokolov J, Mather PT, Jeon HG, Phillips S, Lichtenhan J, Schwab J. Structural development during deformation of polyurethane containing polyhedral oligomeric silsesquioxanes (POSS) molecules. *Polymer* 2001;42:599–611.
- [198] Turri S, Levi M. Structure, dynamic properties, and surface behavior of nanostructured inorganic polyurethanes from reactive polyhedral oligomeric silsesquioxanes. *Macromolecules* 2005;38:5569–74.
- [199] Turri S, Levi M. Wettability of polyhedral oligomeric silsesquioxane nanostructured polymer surfaces. *Macromol Rapid Commun* 2005;26:1233–6.
- [200] Knight PT, Lee KM, Qin H, Mather PT. Biodegradable thermoplastic polyurethanes incorporating polyhedral oligosilsesquioxane. *Biomacromolecules* 2008;9:2458–67.
- [201] Janowski B, Pielichowski K. Thermo(oxidative) stability of novel polyurethane/POSS nanohybrid elastomers. *Thermochim Acta* 2008;478:51–3.
- [202] Neumann D, Fisher M, Tran L, Matisons JG. Synthesis and characterization of an isocyanate functionalized polyhedral oligosilsesquioxane and the subsequent formation of an organic-inorganic hybrid polyurethane. *J Am Chem Soc* 2002;124:13998–9.
- [203] Mya KY, Wang Y, Shen L, Xu JW, Wu YL, Lu XH, He CB. Star-like polyurethane hybrids with functional cubic silsesquioxanes: preparation, morphology, and thermomechanical properties. *J Polym Sci Part A: Polym Chem* 2009;47:4602–16.
- [204] Nanda AK, Wicks DA, Madbouly SA, Otaigbe JU. Nanostructured polyurethane/POSS hybrid aqueous dispersions prepared by homogeneous solution polymerization. *Macromolecules* 2006;39:7037–43.
- [205] Madbouly SA, Otaigbe JU, Nanda AK, Wicks DA. Rheological behavior of POSS/polyurethane-urea nanocomposite films prepared by homogeneous solution polymerization in aqueous dispersions. *Macromolecules* 2007;40:4982–91.
- [206] Madbouly SA, Otaigbe JU. Recent advances in synthesis, characterization and rheological properties of polyurethanes and POSS/polyurethane nanocomposites dispersions and films. *Prog Polym Sci* 2009;34:1283–332.
- [207] Zhang Y, Lee SH, Mitra Y, Kaiwen L, Pittman Jr CU. Phenolic resin-trisilanophenyl polyhedral oligomeric silsesquioxane POSS hybrid nanocomposites: structure and properties. *Polymer* 2006;47:2984–96.
- [208] Zhang Y, Lee SH, Mitra Y, Hossein T, Pittman Jr CU. Phenolic resin/octa(aminophenyl)-T8-polyhedral oligomeric silsesquioxane (POSS) hybrid nanocomposites: synthesis, morphology, thermal and mechanical properties. *J Inorg Organomet Polym Mater* 2007;17:159–71.
- [209] Liu YH, Zeng K, Zheng S. Organic-inorganic hybrid nanocomposites involving novolac resin and polyhedral oligomeric silsesquioxane. *React Funct Polym* 2007;67:627–35.
- [210] Lee A, Lichtenhan JD. Viscoelastic responses of polyhedral oligosilsesquioxane reinforced epoxy systems. *Macromolecules* 1998;31:4970–4.
- [211] Lee A, Lichtenhan JD. Thermal and viscoelastic property of epoxy-clay and hybrid inorganic-organic epoxy nanocomposites. *J Appl Polym Sci* 1999;73:1993–2001.
- [212] Li GZ, Wang LC, Toghiani H, Daulton TL, Koyama K, Pittman Jr CU. Viscoelastic and mechanical properties of epoxy/multifunctional polyhedral oligomeric silsesquioxane nanocomposites and epoxy/ladderlike polyphenylsilsesquioxane blends. *Macromolecules* 2001;34:8686–93.

- [213] Abad MJ, Barral L, Fasce DP, Williams RJ. Epoxy networks containing large mass fractions of a monofunctional polyhedral oligomeric silsesquioxane (POSS). *Macromolecules* 2003;36:3128–35.
- [214] Barral L, Diez FJ, Garcia-Garabal S, Lopez J, Montero B, Montes R, Ramirez C, Rico M. Thermodegradation kinetics of a hybrid inorganic–organic epoxy system. *Eur Polym J* 2005;41:1662–6.
- [215] Zucchi IA, Galante MJ, Williams RJ, Franchini E, Galy J, Gerard JF. Monofunctional epoxy–POSS dispersed in epoxy–amine networks: effect of a prereaction on the morphology and crystallinity of POSS domains. *Macromolecules* 2007;40:1274–82.
- [216] Strachota A, Whelan P, Kriz J, Brus J, Urbanova M, Sylouf M, Matejka L. Formation of nanostructured epoxy networks containing polyhedral oligomeric silsesquioxane (POSS) blocks. *Polymer* 2007;48:3041–58.
- [217] Rashid ESA, Ariffin K, Kooi CC, Akil HM. Preparation and properties of POSS/epoxy composites for electronic packaging applications. *Mater Des* 2009;30:1–8.
- [218] Liu YL, Chang GP. Novel approach to preparing epoxy/polyhedral oligomeric silsesquioxane hybrid materials possessing high mass fractions of polyhedral oligomeric silsesquioxane and good homogeneity. *J Polym Sci Part A: Polym Chem* 2006;44:1869–76.
- [219] Choi J, Harcup J, Yee AF, Zhu Q, Laine RM. Organic/inorganic hybrid composites from cubic silsesquioxanes. *J Am Chem Soc* 2001;123:11420–30.
- [220] Kim GM, Qin H, Fang X, Sun FC, Mather PT. Hybrid epoxy-based thermosets based on polyhedral oligosilsesquioxane: cure behavior and toughening mechanisms. *J Polym Sci Part B: Polym Phys* 2003;41:3299–313.
- [221] Mya KY, He C, Huang U, Xiao Y, Dai J, Siow YP. Preparation and thermomechanical properties of epoxy resins modified by octafunctional cubic silsesquioxane epoxides. *J Polym Sci Part A: Polym Chem* 2004;42:3490–503.
- [222] Matejka L, Strachota A, Plestil J, Whelan P, Steinhart M, Sylouf M. Epoxy networks reinforced with polyhedral oligomeric silsesquioxanes (POSS). Structure and morphology. *Macromolecules* 2004;37:9449–56.
- [223] Strachota A, Kroutilova I, Kovarova J, Matejka L. Epoxy networks reinforced with polyhedral oligomeric silsesquioxanes (POSS) thermomechanical properties. *Macromolecules* 2004;37:9457–64.
- [224] Liu YH, Zheng S, Nie KM. Epoxy nanocomposites with octa(propylglycidyl ether) polyhedral oligomeric silsesquioxane. *Polymer* 2005;46:12016–25.
- [225] Huang JC, He C, Liu XM, Xu JW, Tay CCS, Chow SY. Organic–inorganic nanocomposites from cubic silsesquioxane epoxides: direct characterization of interphase, and thermomechanical properties. *Polymer* 2005;46:7018–27.
- [226] Lee LH, Chen WC. Organic–inorganic hybrid materials from a new octa(2,3-epoxypropyl)silsesquioxane with diamines. *Polymer* 2005;46:2163–74.
- [227] Xu HY, Yang BH, Gao XY, Li C, Guang SY. Synthesis and characterization of organic–inorganic hybrid polymers with a well-defined structure from diamines and epoxy-functionalized polyhedral oligomeric silsesquioxanes. *J Appl Polym Sci* 2006;101:3730–5.
- [228] Lu T, Liang G, Guo Z. Preparation and characterization of organic–inorganic hybrid composites based on multi-epoxy silsesquioxane and cyanate resin. *J Appl Polym Sci* 2006;101:3652–8.
- [229] Liu YL, Chang GP, Hsu KY, Chang FC. Epoxy/polyhedral oligomeric silsesquioxane nanocomposites from octakis(glycidyl dimethylsiloxy)octasilsesquioxane and small-molecule curing agents. *J Polym Sci Part A: Polym Chem* 2006;44:3825–35.
- [230] Xiao F, Sun YY, Xiu YH, Wong CP. Preparation, thermal and mechanical properties of POSS epoxy hybrid composites. *J Appl Polym Sci* 2007;104:2113–21.
- [231] Wang YZ, Tsai HS, Ji ZY, Chen WY. Controlling POSS dispersion in epoxy in nanocomposite by introducing multi-epoxy POSS groups. *J Mater Sci* 2007;42:7611–6.
- [232] Bian Y, Pejanovic S, Kenny J, Mijovic J. Dynamics of multifunctional polyhedral oligomeric silsesquioxane/poly(propylene oxide) nanocomposites as studied by dielectric relaxation spectroscopy and dynamic mechanical spectroscopy. *Macromolecules* 2007;40:6239–48.
- [233] Teo JK, Teo KC, Pan B, Xiao Y, Lu X. Epoxy/polyhedral oligomeric silsesquioxane (POSS) hybrid networks cured with an anhydride: cure kinetics and thermal properties. *Polymer* 2007;48:5671–80.
- [234] Rico CRM, Torres A, Barral L, Lopez J, Montero B. Epoxy/POSS organic–inorganic hybrids: ATR-FTIR and DSC studies. *Eur Polym J* 2008;44:3035–45.
- [235] Gao J, Kong D, Li S. Preparation of BPA epoxy resin/POSS nanocomposites and nonisothermal co-curing kinetics with MeTHPA. *Int J Polym Mater* 2008;57:940–56.
- [236] Li Q, Hutcheson SA, McKenna GB, Simon SL. Viscoelastic properties and residual stresses in polyhedral oligomeric silsesquioxane-reinforced epoxy matrices. *J Polym Sci Part B: Polym Phys* 2008;46:2719–32.
- [237] Bian Y, Mijovic J. Nanonetworks of multifunctional polyhedral oligomeric silsesquioxane and polypropylene oxide. *Macromolecules* 2008;41:7122–30.
- [238] Bian Y, Mijovic J. Effect of side chain architecture on dielectric relaxation in polyhedral oligomeric silsesquioxane/polypropylene oxide nanocomposites. *Polymer* 2009;50:1541–7.
- [239] Yang CC, Chang FC, Wang YZ, Chan CM, Lin CL, Chen WY. Novel nanocomposite of epoxy resin by introduced reactive and nanoporous material. *J Polym Res* 2007;14:431–9.
- [240] Chen WY, Wang YZ, Kuo SW, Huang CF, Tung PH, Chang FC. Thermal and curing kinetics of nanomaterials formed from POSS–epoxy and meta-phenylenediamine. *Polymer* 2004;45:6897–908.
- [241] Huang JM, Huang HJ, Wang YX, Chen WY, Chang FC. Preparation and characterization of epoxy/polyhedral oligomeric silsesquioxane hybrid nanocomposites. *J Polym Sci Part B: Polym Phys* 2009;47:1927–34.
- [242] Wang YZ, Chen WY, Yang CC, Lin CL, Chang FC. Novel epoxy nanocomposite of low Dk introduced fluorine-containing POSS structure. *J Polym Sci Part B: Polym Phys* 2007;45:502–10.
- [243] Yen YC, Ye YS, Cheng CC, Lu CH, Tsai LD, Huang JM, Chang FC. The effect of sulfonic acid groups within a polyhedral oligomeric silsesquioxane containing cross-linked proton exchange membrane. *Polymer* 2010;51:84–91.
- [244] Nia Y, Zheng S, Nie KM. Morphology and thermal properties of inorganic–organic hybrids involving epoxy resin and polyhedral oligomeric silsesquioxanes. *Polymer* 2004;45:5557–68.
- [245] Ni Y, Zheng S. Epoxy resin containing octamaleimidophenyl polyhedral oligomeric silsesquioxane. *Macromol Chem Phys* 2005;206:2075–83.
- [246] Cho HS, Liang KW, Chatterjee S, Pittman Jr CU. Synthesis, morphology, and viscoelastic properties of polyhedral oligomeric silsesquioxane nanocomposites with epoxy and cyanate ester matrices. *J Inorg Organomet Polym Mater* 2005;15:541–53.
- [247] Zhang ZP, Liang G, Wang X. The effect of POSS on the thermal properties of epoxy. *Polym Bull* 2007;58:1013–20.
- [248] Zhang ZP, Liang G, Ren P, Wang J. Thermodegradation kinetics of epoxy/DDS/POSS System. *Polym Compos* 2007:755–61.
- [249] Zhang ZP, Liang G, Ren P, Wang J. Curing behavior of epoxy/POSS/DDS hybrid systems. *Polym Compos* 2008:77–83.
- [250] Pellice SA, Fasce DP, Williams RJ. Properties of epoxy networks derived from the reaction of diglycidyl ether of bisphenol A with polyhedral oligomeric silsesquioxanes bearing OH-functionalized organic substituents. *J Polym Sci Part B: Polym Phys* 2003;41:1451–61.
- [251] Zeng K, Zheng S. Nanostructures and surface dewettability of epoxy thermosets containing hepta(3,3,3-trifluoropropyl) polyhedral oligomeric silsesquioxane-capped poly(ethylene oxide). *J Phys Chem B* 2007;111:13919–28.
- [252] Ni Y, Zheng S. Nanostructured thermosets from epoxy resin and an organic–inorganic amphiphile. *Macromolecules* 2007;40:7009–18.
- [253] Fu BX, Namani M, Lee A. Influence of phenyl-trisilanol polyhedral silsesquioxane on properties of epoxy network glasses. *Polymer* 2003;44:7739–47.
- [254] Liu HZ, Zheng S, Nie KM. Morphology and thermomechanical properties of organic–inorganic hybrid composites involving epoxy resin and an incompletely condensed polyhedral oligomeric silsesquioxane. *Macromolecules* 2005;38:5088–97.
- [255] Nair CPR. Advances in addition-cure phenolic resins. *Prog Polym Sci* 2004;29:401–98.
- [256] Ghosh NN, Kiskan B, Yagci Y. Polybenzoxazines—new high performance thermosetting resins: synthesis and properties. *Prog Polym Sci* 2007;32:1344–491.
- [257] Wang CF, Su YC, Kuo SW, Huang CF, Sheen YC, Chang FC. Low-surface-free-energy materials based on polybenzoxazines. *Angew Chem Int Ed* 2006;45:2248–51.
- [258] Wang CF, Wang YT, Tung PH, Kuo SW, Lin CH, Sheen YC, Chang FC. Stable superhydrophobic polybenzoxazine surfaces over a wide pH range. *Langmuir* 2006;22:8289–92.
- [259] Liao CS, Wang CF, Lin HC, Chou HY, Chang FC. Fabrication of patterned superhydrophobic polybenzoxazine hybrid surfaces. *Langmuir* 2009;25:3359.

- [260] Liao CS, Wang CF, Li HC, Chou HY, Chang FC. Tuning the surface free energy of polybenzoxazine thin films. *J Phys Chem C* 2008;112:16189.
- [261] Wang CF, Chiou SF, Ko FH, Chen JK, Chou CT, Huang CF, Kuo SW, Chang FC. Polybenzoxazine as a mold-release agent for nanoimprint lithography. *Langmuir* 2007;23:5868–71.
- [262] Su YC, Kuo SW, Yei DR, Xu HY, Chang FC. Thermal property and hydrogen bonding in polymer blend of polybenzoxazine/poly(*N*-vinyl-2-pyrrolidone). *Polymer* 2003;44:2187–91.
- [263] Fu HK, Huang CF, Kuo SW, Lin HC, Yei DR, Chang FC. Effect of the organically modified nanoclay on low-surface-energy materials of polybenzoxazine. *Macromol Rapid Commun* 2008;29:1216–20.
- [264] Lee YJ, Kuo SW, Su YC, Chen JK, Tu CW, Chang FC. Syntheses, thermal properties, and phase morphologies of novel benzoxazines functionalized with polyhedral oligomeric silsesquioxane (POSS) nanocomposites. *Polymer* 2004;45:6321–31.
- [265] Lee YJ, Huang JM, Kuo SW, Chen JK, Chang FC. Synthesis and characterizations of a vinyl-terminated benzoxazine monomer and its blending with polyhedral oligomeric silsesquioxane (POSS). *Polymer* 2005;46:2320–30.
- [266] Lee YJ, Kuo SW, Huang CF, Chang FC. Synthesis and characterization of polybenzoxazine networks containing multifunctional polyhedral oligomeric silsesquioxane (POSS). *Polymer* 2006;47:4378–86.
- [267] Chen Q, Xu RW, Zhang J, Yu DS. Polyhedral oligomeric silsesquioxane (POSS) nanoscale reinforcement of thermosetting resin from benzoxazine and bisoxazoline. *Macromol Rapid Commun* 2005;26:1878–82.
- [268] Zhang J, Xu RW, Yu DS. A novel poly-benzoxazinyl functionalized polyhedral oligomeric silsesquioxane and its nanocomposite with polybenzoxazine. *Eur Polym J* 2007;43:743–52.
- [269] Liu YH, Zheng S. Inorganic–organic nanocomposites of polybenzoxazine with octa(propylglycidyl ether) polyhedral oligomeric silsesquioxane. *J Polym Sci Part A: Polym Chem* 2006;44:1168–81.
- [270] Kuo SW, Huang KW. High-performance polybenzoxazine nanocomposites containing multifunctional polyhedral oligomeric silsesquioxane cores presenting vinyl-terminated benzoxazine group. *Macromol Chem Phys* 2010;211:2301–11.
- [271] Wu YC, Kuo SW. Synthesis and characterization of polyhedral oligomeric silsesquioxane (POSS) with multifunctional benzoxazine groups through click chemistry. *Polymer* 2010;51:3948–55.
- [272] Xiao S, Nguyen M, Gong X, Cao Y, Wu H, Moses D, Heeger AJ. Stabilization of semiconducting polymers with silsesquioxane. *Adv Funct Mater* 2003;13:25–9.
- [273] Gong X, Soci C, Yang CY, Heeger AJ, Xiao S. Enhanced electron injection in polymer light-emitting diodes: polyhedral oligomeric silsesquioxanes as dilute additives. *J Phys D* 2006;39:2048–52.
- [274] Lee J, Cho H, Jung B, Cho N, Shim H. Stabilized blue luminescent polyfluorenes: introducing polyhedral oligomeric silsesquioxane. *Macromolecules* 2004;37:8523–9.
- [275] Cho HJ, Hwang DH, Lee JI, Yung YK, Park JH, Lee J, Lee SK, Shim HK. Electroluminescent polyhedral oligomeric silsesquioxane-based nanoparticle. *Chem Mater* 2006;18:3780–7.
- [276] Lee J, Cho HJ, Cho NS, Hwang DH, Kang JM, Lim E, Lee JI, Shim KH. Enhanced efficiency of polyfluorene derivatives: organic–inorganic hybrid polymer light-emitting diodes. *J Polym Sci Part A: Polym Chem* 2006;44:2943–54.
- [277] Kang JM, Cho HJ, Lee J, Lee JI, Lee SK, Cho NS, Hwang DH, Shim HK. Highly bright and efficient electroluminescence of new PPV derivatives containing polyhedral oligomeric silsesquioxanes (POSSs) and their blends. *Macromolecules* 2006;39:4999–5008.
- [278] Chen KB, Chen HY, Yang SH, Hsu CS. Synthesis and opto-electrical properties of stellar polyfluorene derivatives containing polyhedral oligomeric silsesquioxanes as the center core. *J Polym Res* 2006;13:237–45.
- [279] Chou CH, Hsu SL, Yeh SW, Wang HS, Wei KH. Enhanced luminance and thermal properties of poly(phenylenevinylene) copolymer presenting side-chain-tethered silsesquioxane units. *Macromolecules* 2005;38:9117–23.
- [280] Chou CH, Hsu SL, Dinakaran K, Chiu MY, Wei KH. Synthesis and characterization of luminescent polyfluorenes incorporating side-chain-tethered polyhedral oligomeric silsesquioxane units. *Macromolecules* 2005;38:745–51.
- [281] Lin WJ, Chen WC, Wu WC, Niu YH, Jen AKJ. Synthesis and optoelectronic properties of starlike polyfluorenes with a silsesquioxane core. *Macromolecules* 2004;37:2335–41.
- [282] Cheng CC, Chien CH, Yen YC, Ye YS, Kob FH, Lin CH, Chang FC. A new organic/inorganic electroluminescent material with a silsesquioxane core. *Acta Mater* 2009;57:1938–46.
- [283] Zhang CX, Bunning TJ, Laine RM. Synthesis and characterization of liquid crystalline silsesquioxanes. *Chem Mater* 2001;13:3653–62.
- [284] Kim KM, Chujo Y. Liquid-crystalline organic–inorganic hybrid polymers with functionalized silsesquioxanes. *J Polym Sci Part A: Polym Chem* 2001;39:4035–43.
- [285] Pan QW, Chen XF, Fan XH, Shen ZH, Zhou QF. Organic–inorganic hybrid bent-core liquid crystals with cubic silsesquioxane cores. *J Mater Chem* 2008;18:3481–8.
- [286] Wu H, Hu Y, Gonsalves KE, Yacaman MJ. Incorporation of polyhedral oligosilsesquioxane in chemically amplified resists to improve their reactive ion etching resistance. *J Vac Sci Technol B* 2001;19:851–5.
- [287] Wu H, Gonsalves KE. Novel positive-tone chemically amplified resists with photoacid generator in the polymer chains. *Adv Mater* 2001;13:670–2.
- [288] Ali MA, Gonsalves KE, Golovkina V, Cerrina F. High sensitivity nanocomposite resists for EUV lithography. *Microelectron Eng* 2003;65:454–62.
- [289] Ali MA, Gonsalves KE, Agrawal A, Jeyakumar A, Henderson CL. A new nanocomposite resist for low and high voltage electron beam lithography. *Microelectron Eng* 2003;70:19–29.
- [290] Bellas V, Tegou E, Raptis I, Gogolides E, Argitis P, Iatrou H, Hadjichristidis N, Sarantopoulou E, Cefalas AC. Evaluation of siloxane and polyhedral silsesquioxane copolymers for 157 nm lithography. *J Vac Sci Technol B* 2002;20:2902–8.
- [291] Tegou E, Bellas V, Gogolides E, Argitis P, Eon D, Cartry G, Cardinaud C. Polyhedral oligomeric silsesquioxane (POSS) based resists: material design challenges and lithographic evaluation at 157 nm. *Chem Mater* 2004;16:2567–77.
- [292] Tegou E, Bellas V, Gogolides E, Argitis P. Polyhedral oligomeric silsesquioxane (POSS) acrylate copolymers for microfabrication: properties and formulation of resist materials. *Microelectron Eng* 2004;73:238–43.
- [293] Schmidt A, Babin S, Koops HWP. Comparative study of the characteristics of octavinylsilsesquioxane dry resist in ultraviolet-, electron-beam and X-ray exposure. *Microelectron Eng* 1997;35:129–32.
- [294] Ni Y, Zheng S. A novel photocrosslinkable polyhedral oligomeric silsesquioxane and its nanocomposites with poly(vinyl cinnamate). *Chem Mater* 2004;16:5141–8.
- [295] Lin HM, Wu SY, Huang PY, Huang CF, Kuo SW, Chang FC. Polyhedral oligomeric silsesquioxane containing copolymers for negative-type photoresists. *Macromol Rapid Commun* 2006;27:1550–5.
- [296] Lin HM, Hseih KH, Chang FC. Characterization of negative-type photoresists containing polyhedral oligomeric silsesquioxane methacrylate. *Microelectron Eng* 2008;85:1624–8.
- [297] Carter KR, McGrath JE. Polyimide nanoforms based on ordered polyimides derived from poly(amic alkyl esters): PMDA/4-BDAF. *Chem Mater* 1997;9:105–18.
- [298] Carter KR, DiPietro RA, Sanchez MI, Swanson SA. Nanoporous polyimides derived from highly fluorinated polyimide/poly(propylene oxide) copolymers. *Chem Mater* 2001;13:213–21.
- [299] Krause BR, Mettinkhof NF. Microcellular foaming of amorphous high-T_g polymers using carbon dioxide. *Macromolecules* 2001;34:874–84.
- [300] Krause BR, Mettinkhof NF. Ultralow-k dielectrics made by supercritical foaming of thin polymer films. *Adv Mater* 2002;14:1041–6.
- [301] Chen WY, Ho KS, Hsieh TH, Chang FC, Wang YZ. Simultaneous preparation of PI/POSS semi-IPN nanocomposite. *Macromol Rapid Commun* 2006;27:452–7.
- [302] Yang BH, Xu HY, Yang ZZ, Liu XY. Design and architecture of low-dielectric-constant organic–inorganic hybrids from octahydrodisilsesquioxanes. *J Mater Chem* 2009;19:9038–44.
- [303] Liu YL, Fangchiang MH. Polyhedral oligomeric silsesquioxane nanocomposites exhibiting ultra-low dielectric constants through POSS orientation into lamellar structures. *J Mater Chem* 2009;19:3643–7.
- [304] Chen WC, Kuo SW, Lu CH, Chang FC. Specific interactions and self-assembly structures through competitive interactions of crystalline-amorphous diblock copolymer/homopolymer blends: poly(*ε*-caprolactone)-*b*-poly(4-vinyl pyridine)/poly(vinyl phenol). *Macromolecules* 2009;42:3580–90.
- [305] Chen SC, Kuo SW, Jeng US, Chang FC. Investigated of phase behavior of A-*b*-B/C blend systems possessing different hydrogen-bonding strength. *Macromolecules* 2010;43:1083–92.
- [306] Chen WC, Kuo SW, Jeng US, Chang FC. Self-assembly through competitive interactions of miscible diblock copolymer/homopolymer blends: poly(vinyl phenol)-*b*-methyl methacrylate/poly(vinyl pyrrolidone) blend. *Macromolecules* 2008;41:1401–10.

- [307] Pyun J, Matyjaszewski K. The synthesis of hybrid polymers using atom transfer radical polymerization: homopolymers and block copolymers from polyhedral oligomeric silsesquioxane monomers. *Macromolecules* 2000;33:217–20.
- [308] Pyun J, Matyjaszewski K, Wu J, Kim GM, Chun SB, Mather PT. ABA triblock copolymers containing polyhedral oligomeric silsesquioxane pendant groups: synthesis and unique properties. *Polymer* 2003;44:2739–50.
- [309] Fei M, Jin BK, Wang WP, Liu L. Synthesis and characterization of AB block copolymers based on polyhedral oligomeric silsesquioxane. *J Polym Res* 2010;17:19–23.
- [310] Fu BX, Lee A, Haddad TS. Styrene-butadiene-styrene triblock copolymers modified with polyhedral oligomeric silsesquioxanes. *Macromolecules* 2004;37:5211–8.
- [311] Drazkowski DB, Lee A, Haddad TS, Cookson DJ. Chemical substituent effects on morphological transitions in styrene-butadiene-styrene triblock copolymer grafted with polyhedral oligomeric silsesquioxanes. *Macromolecules* 2006;39:1854–63.
- [312] Drazkowski DB, Lee A, Haddad TS. Morphology and phase transitions in styrene-butadiene-styrene triblock copolymer grafted with isobutyl-substituted polyhedral oligomeric silsesquioxanes. *Macromolecules* 2007;40:2798–805.
- [313] Miao JJ, Cui L, Lau HP, Mather PT, Zhu L. Self-assembly and chain-folding in hybrid coil-coil-cube triblock oligomers of polyethylene-*b*-poly(ethylene oxide)-*b*-polyhedral oligomeric silsesquioxane. *Macromolecules* 2007;40:5460–70.
- [314] Hirai T, Leolukman M, Hayakawa T, Kamimoto M, Gopalan P. Hierarchical nanostructures of organosilicate nanosheets within self-organized block copolymer films. *Macromolecules* 2008;41:4558–60.
- [315] Hirai T, Leolukman M, Jin S, Goseki R, Ishida Y, Kakimoto M, Hayakawa T, Ree M, Gopalan P. Hierarchical self-assembled structures from POSS-containing block copolymers synthesized by living anionic polymerization. *Macromolecules* 2009;42:8835–43.
- [316] Hirai T, Leolukman M, Liu CC, Han E, Kim YJ, Ishida Y, Hayakawa T, Kakimoto MA, Nealey PF, Gopalan P. One-step direct-patterning template utilizing self-assembly of POSS-containing block copolymers. *Adv Mater* 2009;21:1–5.
- [317] Zhang L, Lu D, Tao K, Bai R. Synthesis, characterization and self-assembly of novel amphiphilic block copolymers with a polyhedral oligomeric silsesquioxanes moiety attached at the junction of the two blocks. *Macromol Rapid Commun* 2009;30:1015–20.
- [318] Zhang WB, Sun B, Li H, Ren X, Janoski J, Sahoo S, Dabney DE, Wesdemiotis C, Quirk RP, Cheng SZD. Synthesis of in-chain-functionalized polystyrene-block-poly(dimethylsiloxane) diblock copolymers by anionic polymerization and hydrosilylation using dimethyl-[4-(1-phenylvinyl)phenyl]silane. *Macromolecules* 2009;42:7258–62.
- [319] Lu CH, Kuo SW, Chang FC. Self-assembly structure transformation of PCL-*b*-P4VP diblock copolymer through mediated by competitive interaction with octaphenol polyhedral oligomeric silsesquioxane. *Macromol Rapid Commun* 2009;30:2121–7.
- [320] Lu CH, Chang FC, Kuo SW. Syntheses and characterizations of star polymers and star block copolymers from polyhedral oligomeric silsesquioxane core through nitroxide-mediated radical polymerization. *Macromol Chem Phys* 2010;211:1339–47.
- [321] Yei DR, Kuo SW, Su YC, Chang FC. Enhanced thermal properties of PS nanocomposites formed from inorganic POSS-treated montmorillonite. *Polymer* 2004;45:2633–40.
- [322] Carniato F, Bisio C, Gatti G, Boccaleri E, Bertinetti L, Coluccia S, Monticelli O, Marchese L. Titanosilsesquioxanes embedded in synthetic clay as a hybrid material for polymer science. *Angew Chem Int Ed* 2009;48:6059–61.
- [323] Fu HK, Kuo SW, Yeh DR, Chang FC. Properties enhancement of PS nanocomposites through the POSS surfactants. *J Nanomater* 2008;2008, 739613/1–7.
- [324] Fu HK, Huang CF, Huang JM, Chang FC. Studies on thermal properties of PS nanocomposites for the effect of intercalated agent with side groups. *Polymer* 2008;49:1305–11.
- [325] Liu HZ, Zhang W, Zheng S. Montmorillonite intercalated by ammonium of octaminopropyl polyhedral oligomeric silsesquioxane and its nanocomposites with epoxy resin. *Polymer* 2005;46:157–65.
- [326] Fox DM, Maupin PH, Harris Jr RH, Gilman JW, Eldred DV, Katsoulis D, Trulove PC, De HC. Long use of a polyhedral oligomeric silsesquioxane (POSS)-imidazolium cation as an organic modifier for montmorillonite. *Langmuir* 2007;23:7707–14.
- [327] Wan C, Zhao F, Bao X, Kandasubramanian B, Duggan M. Surface characteristics of polyhedral oligomeric silsesquioxane modified clay and its application in polymerization of macrocyclic polyester oligomers. *J Phys Chem B* 2008;112:11915–22.
- [328] Schmid G, Pugina R, Malmb JO, Bovinb JO. Silsesquioxanes as ligands for gold clusters. *Eur J Inorg Chem* 1998;1998:813–7.
- [329] Wang X, Naka K, Zhu M, Itoh H, Chujo Y. Microporous nanocomposites of Pd and Au nanoparticles via hierarchical self-assembly. *Langmuir* 2005;21:12395–8.
- [330] Carroll JB, Frankamp BL, Rotello VM. Self-assembly of gold nanoparticles through tandem hydrogen bonding and poly-oligosilsesquioxane (POSS)-POSS recognition processes. *Chem Commun* 2002:1892–3.
- [331] Jeoung E, Carroll JB, Rotello VM. Surface modification via 'lock and key' specific self-assembly of polyhedral oligomeric silsesquioxane (POSS) derivatives to modified gold surfaces. *Chem Commun* 2002:1510–1.
- [332] Carroll JB, Frankamp BL, Srivastava S, Rotello VM. Electrostatic self-assembly of structured gold nanoparticle/polyhedral oligomeric silsesquioxane (POSS) nanocomposites. *J Mater Chem* 2004;14:690–4.
- [333] Naka K, Sato M, Chujo Y. Stabilized spherical aggregate of palladium nanoparticles prepared by reduction of palladium acetate in octa(3-aminopropyl)octasilsesquioxane as a rigid template. *Langmuir* 2008;24:2719–26.
- [334] Lu CH, Kuo SW, Huang CF, Chang FC. Self-assembled fernlike microstructures of POSS/gold nanoparticle hybrids. *J Phys Chem C* 2009;113:3517–24.
- [335] Kuo SW, Wu YC, Lu CH, Chang FC. Surface modification of gold nanoparticles with polyhedral oligomeric silsesquioxane (POSS) and incorporation within polymer matrices. *J Polym Sci Part B: Polym Phys* 2009;47:811–9.
- [336] Kuo SW, Huang CF, Chang FC. Nanocomposites based on POSS. In: Thomas S, Zaikov G, Valsaraj SV, editors. *Recent advances in polymer nanocomposites*. Boston: Brill Academic Publishers; 2010. p. 155–91.